Intercollegiate Faculty of Biotechnology
University of Gdańsk & Medical University of Gdańsk

mgr Wiktoria Sztangierska

Role of yeast nucleotide exchange factor (Sse1) in functioning of Hsp70 chaperone system in protein disaggregation

Wpływ drożdżowego czynnika wymiany nukleotydów (Sse1) na funkcjonowanie systemu Hsp70 w dezagregacji białek

A Ph. D. dissertation in the field of Natural Sciences specialization Biotechnology presented to The Scientific Council of Biotechnology University of Gdańsk

Promoter: prof. dr hab. Krzysztof Liberek

Auxiliary Promoter: dr Agnieszka Kłosowska

Laboratory of Protein Biochemistry

Gdańsk, 2024

This project was supported by Polish National Science Centre Grant 2019/35/B/NZ1/01475

I would like to express my gratitude to Professor Krzysztof Liberek for providing me with the opportunity to develop scientifically, whose guidance and support have been invaluable throughout my academic journey.

I would also like to thank dr Agnieszka Kłosowska for the numerous enlightening discussions and advices given throughout my study.

My sincere thanks to my colleagues of the former Molecular and Cellular Biology Department for creating a friendly and development-supporting environment. Special thanks to Hubert Wyszkowski for sharing his knowledge, which has been important in advancing my skills in protein work and to Klaudia Kochanowicz for her support, and for the many tears and laughs we shared, making tough days easier.

I am grateful to my parents, who have supported every decision I've made, providing me with the freedom and backing to pursue my passions and ambitions.

Lastly, I owe a special thanks to my partner Damian for being my rock during this journey. Your presence and encouragement have helped me persevere through the most challenging moments.

Table of contents

1. Streszczenie

Komórka nieustannie narażona jest na działanie czynników stresowych, które mogą prowadzić do nieprawidłowego fałdowania białek i tworzenia agregatów białkowych. W celu zapobiegania takim zjawiskom komórki wykształciły system kontroli jakości białek. Jedną z jego strategii jest uwolnienie białek uwięzionych w agregatach i przywrócenie ich konformacji natywnej, w czym kluczową rolę odgrywa system Hsp70-Hsp100. Aktywność Hsp70 regulowana jest przez czynnik wymiany nukleotydów (ang. nucleotide exchange factor - NEF) i białka posiadające domeną J (ang. J-domain proteins - JDP). Białka JDP należą do klasy A lub B. Obecność różnych klas tych białek determinuje odmienny mechanizm interakcji Hsp70 z substratem białkowym, co ma decydujący wpływ na efektywność dezagregacji. Aby lepiej zrozumieć funkcjonalne oddziaływanie między Hsp70, jego pomocniczymi białkami opiekuńczymi i substratami białkowymi, zbadałam w jaki sposób cytoplazmatyczny NEF z rodziny Hsp110, Sse1, wpływa na aktywność Hsp70 w obecności białek JDP klasy A lub klasy B.

W mojej pracy doktorskiej użyłam oczyszczonych białek z organizmu modelowego *Saccharomyces cerevisiae*. Wykorzystując techniki biochemiczne, zbadałam wpływ Sse1 na aktywność drożdżowego Hsp70 (Ssa1) na różnych etapach dezagregacji w obecności białka JDP należącego do klasy A (Ydj1) lub klasy B (Sis1). Zaobserwowałam, że Sse1 ma istotny wpływ na początkowym etapie dezagregacji, natomiast nie bierze udziału w końcowym fałdowaniu substratów białkowych. Sse1 znacząco stymuluje aktywność dezagregacyjną Hsp70, jak również jego wiązanie do agregatów, jednak ten pozytywny efekt jest obserwowany tylko w obecności JDP klasy B. Korzystny wpływ Sse1 jest związany z modyfikacją agregatów, prowadzącą do ich zmniejszenia. Zmiana wielkości agregatów białkowych prawdopodobnie wynika ze zwiększonej ilości Hsp70 związanego z powierzchnią agregatu, na skutek działania Sse1. Kluczowe dla obserwowanych zjawisk jest charakterystyczne dla białek JDP klasy B dodatkowe miejsce wiązania z Hsp70, pomiędzy C-terminalną domeną JDP, a motywem EEVD obecnym w Hsp70. Zaburzenie tego oddziaływania znosi stymulację przez Sse1.

Z doniesień literaturowych wynika, że wpływ Sse1 na aktywność Hsp70 zależy od jego ilościowego stosunku do Hsp70. Wykazano, że Sse1 stymuluje

dezagregację białek tylko przy bardzo niskim stężeniu w stosunku do Hsp70, natomiast powyżej tego substechiometrycznego optimum obserwowana jest inhibicja. W mojej pracy doktorskiej analizowałam efekt hamujący Sse1 i pokazałam, że w zależności od tego czy obecna jest klasa A czy klasa B JDP, wrażliwość systemu Hsp70 na wysokie stężenie Sse1 różni się. Moje obserwacje wskazują również na istnienie dodatkowego mechanizmu inhibicji przez Sse1 w obecności białek JDP klasy B, w którym hamowanie wynika z konkurencji pomiędzy Sse1 a Sis1 o wiązanie do Hsp70.

Z uwagi na to, iż Metazoa nie posiadają białka Hsp100 i polegają w dezagregacji białek jedynie na Hsp70, chciałam również zbadać, jak ludzki Hsp110 wpływa na aktywność ludzkiego systemu Hsp70. Zaobserwowałam podobne trendy, jak w przypadku systemu drożdżowego, z tą różnicą, że ludzki system Hsp70 jest bardziej zależny od Hsp110 i mniej wrażliwy na działanie wysokiego stężenia Hsp110. Obserwowane wyniki stanowią podstawę do dalszych badań nad rolą NEF w funkcjonowaniu systemu Hsp70 u ludzi i innych eukariontów.

2. Abstract

Hsp70 plays a major role in maintaining protein homeostasis, which is constantly endangered by stress-induced protein misfolding and aggregation. In response, one of cellular pathways developed by a cell is protein recovery from aggregates by molecular chaperones. To cope with aggregation, Hsp70 collaborates with a disaggregase from the Hsp100 family. The activity of Hsp70 is regulated by nucleotide exchange factors (NEFs) and J-domain proteins (JDPs). Different JDP classes, namely class A or class B, determine the mechanism of the Hsp70 interaction with misfolded protein substrates and the total disaggregation efficacy. To gain more insight into the interplay between Hsp70, its co-chaperones and protein substrates, I addressed how Hsp110, the most abundant cytosolic NEF, impacts Hsp70 activity in the context of different JDP classes.

By using a reconstituted yeast chaperone system, I investigated the impact of Sse1, a NEF belonging to Hsp110 family, at individual stages of protein disaggregation by Hsp70 (Ssa1), when paired with either class A (Ydj1) or class B (Sis1) JDPs. It appears that Sse1 acts at early stages of protein disaggregation rather than during the final folding of protein substrates. Sse1 improves both the disaggregation capacity and binding to aggregates by Hsp70, however the stimulation occurs particularly with class B JDPs. The significantly enhanced protein disaggregation is achieved through the Sse1-mediated more abundant recruitment of Hsp70 to the aggregate, leading to its modification observed as an emergence of aggregate species smaller in size. My results imply that class B-specific interaction between the C-terminal domain of Sis1 and the C-terminal motif EEVD of Ssa1 is vital for these processes.

In accordance with the reported concentration-dependent impact of Hsp110 on Hsp70, I elucidated the basis of Hsp70 inhibition by the NEF. Based on my results, I propose a novel mechanism of inhibition by Sse1 of Hsp70 with class B JDPs, involving competition between these co-chaperones for binding to Hsp70.

Since Metazoa lack an Hsp100 disaggregase and rely solely on Hsp70, I wanted to dissect how the disaggregation activity of the human Hsp70 system is affected by Hsp110. Similarly as in yeasts, the human Hsp110 potentiates the disaggregation activity and recruitment of the Hsp70 system to the aggregate.

These effects are more pronounced for class B JDPs. Together, my results shed light on the mechanisms, by which Hsp110 regulates activity of Hsp70 chaperone machinery and provide a basis for further research on the role of NEF in the functioning of the Hsp70 system in humans and other eukaryotes.

3. Abbreviations

AAA+ ─ ATPases Associated with various cellular Activities

ATP ─ Adenosine Triphosphate

ADP – Adenosine Diphosphate

ATPase ─ Enzyme which hydrolyses ATP

BLI ─ Bio-Layer Interferometry

CTD – C-Terminal Domain

DLS – Dynamic Light Scattering

DTT ─ Dithiothreitol

ER – Endoplasmic Reticulum

E. coli ─ *Escherichia coli*

EDTA ─ Ethylenediaminetetraacetic acid

JDP – J-Domain Protein

GFP – Green Fluorescent Protein

HSP ─ Heat Shock Protein

HEPES - N-2-hydroxyethylpiperazine-N-2-ethane sulfonic acid

IPTG ─ Isopropyl β-D-1-thiogalactopyranoside

LB ─ Luria broth

LA – Luria Agar

Luc ─ Luciferase

NBD ─ Nucleotide-Binding Domain

NEF ─ Nucleotide Exchange Factor

PSIG ─ Pounds per Square Inch Gauge

RPM ─ Rotations Per Minute

S. cerevisiae – *Saccharomyces cerevisiae*

SBD ─ Substrate-Binding Domain

SDS ─ Sodium Dodecyl Sulphate

SDS-PAGE ─ SDS Polyacrylamide Gel Electrophoresis

TRIS ─ Tris(hydroxymethyl)aminomethane

ZFLR – zinc-finger like region

4. Introduction

Proteins are fundamental components of cells, essential for the functioning of all living organisms. Their ability to perform multiple tasks is determined by tertiary structure of a protein, which we refer to as three-dimensional conformation. This arrangement is achieved by folding of the polypeptide chains into defined structures stabilized by intramolecular interactions.

It is essential to control the balance within proteome to ensure the cellular and organismal well-being. The maintenance of proteome integrity is defined as proteostasis. It is accomplished by coordinated processes at different stages of a protein's lifetime, starting from protein synthesis, through folding, trafficking and finishing with eliminating the unwanted proteins by degradation. However, these processes are error-prone and constantly at high risk of exposure to stress conditions, leading to protein misfolding and aggregation.

4.1 Mechanism underlying protein aggregation

Proteins are polypeptides composed of amino acid residues, precise order of which determines the proper fold, defined as the native structure, which can be attained spontaneously or with an assistance of auxiliary proteins. The native conformation of a protein typically assumes its lowest energy state that defines the stability of the protein and the ability to endure destabilizing conditions. During folding, proteins move across energy landscape by transitioning through folding intermediates, as which they can be kinetically trapped (Fig. 1). These non-native structures with exposed hydrophobic amino acid residues that are normally buried within the folded structure are at high risk of interacting with each other due to the crowded cellular environment. These challenging circumstances, as well as an exposure to severe environmental conditions such as pH imbalance, heavy metal ions, presence of ethanol, oxidative stress or elevated temperature predispose polypeptides to misfolding and formation of stable protein assemblies, termed amorphous aggregates (Munson *et al*, 1996; Ellis & Minton, 2006). Alternatively, polypeptides can assemble into highly ordered amyloid fibrils, where β-sheets run perpendicular to the long fibril axis, forming cross-β-sheet supersecondary structures (Fig.1) (Landreh *et al*, 2016).

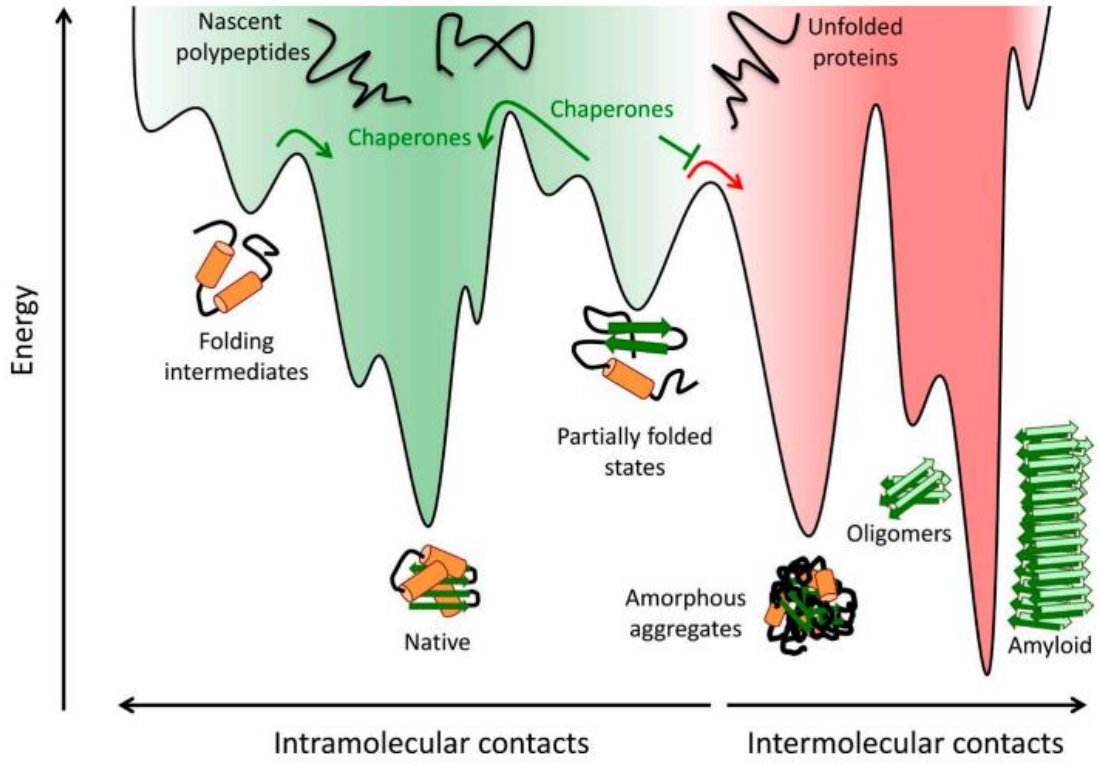

Figure 1. ***The energy landscape of protein folding and aggregation.*** *Nascent polypeptides fold into an energetically favorable native state by travelling downhill the energy landscape through different conformations promoted by intramolecular interactions (green part). Partially folded intermediates can be kinetically trapped and prone to intermolecular interactions, forming amorphous aggregates, oligomers and amyloid fibrils (red part). Chaperones act to prevent the intermolecular interactions, thereby mediating the correct folding into the native state. Adapted from (Klaips* et al*, 2018).*

Both amorphous aggregates and amyloid fibrils can exhibit cytotoxic effects, contributing to pathogenesis of various diseases, particularly neurodegenerative disorders. Parkinson's disease is related with accumulation of α-synuclein fibrils in Lewy bodies, amyloid-β (Aβ) plagues have been attributed to Alzheimer's disease and huntingtin protein with expanded polyglutamine tract leads to the aggregation linked to Huntington disease (Morimoto, 2011; Hipp *et al*, 2019). Understanding cytotoxicity and molecular pathways associated with protein aggregation is important to develop therapeutic strategies for diseases linked with protein misfolding and aggregation.

4.2 Chaperone network in encountering proteostasis collapse

Living cells have developed mechanisms to address toxic effects of protein misfolding and aggregation, which rely on molecular chaperones. They

counteract these events through mediating proper folding of newly synthesized polypeptides, solubilizing aggregated proteins and cooperating with degradation machineries. One of the strategies is protein disaggregation, where proteins trapped in aggregates are rescued by chaperones. The effectiveness of this process requires collaboration of a heat shock protein 70 (Hsp70) with a disaggregase from the heat shock protein 100 (Hsp100) family. The activity of Hsp70 is regulated by its co-chaperones, including a nucleotide exchange factor (NEF) and a J-domain protein (JDP), (Goloubinoff *et al*, 1999).

4.3 Hsp100

Disaggregase from the Hsp100 family binds to a protein substrate and, through its ATPase activity, forcefully disentangles the substrate from an aggregate. Hsp100 (ClpB from *E. coli* and Hsp104 from *S. cerevisiae)* assembles into hexamers featuring a central pore, wherein loop segments with aromatic residues are positioned for substrate interaction (Fig. 2). Monomer of ClpB/Hsp104 comprises an amino-terminal domain (N-domain) followed by two AAA+ domains, namely nucleotide-binding domain 1 (NBD1) and nucleotide-binding domain 2 (NBD2), and a middle domain (M-domain) embedded within NBD1, featuring four alpha-helices forming a coiled-coil structure (Fig. 2) (Schirmer *et al*, 1996; Lee *et al*, 2003).

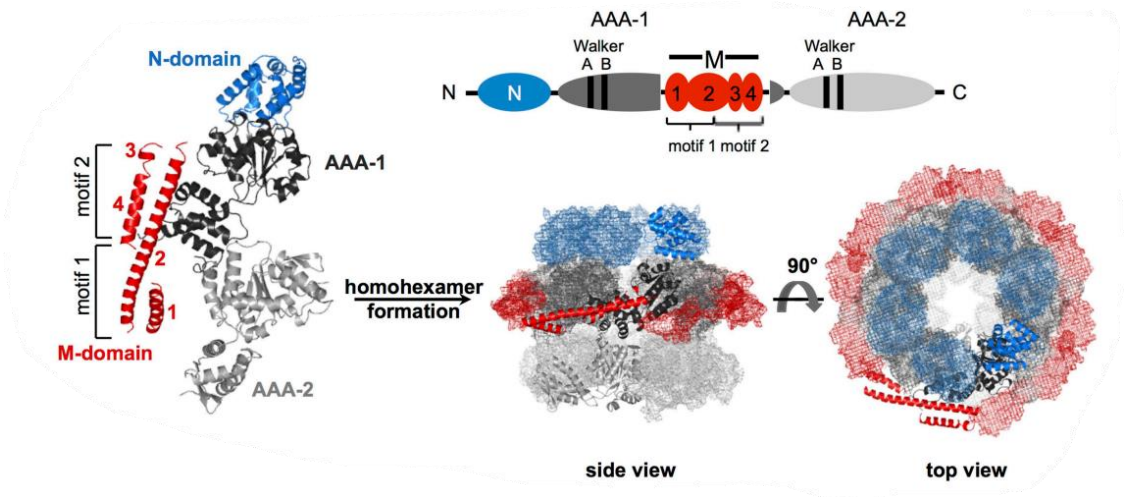

Figure 2. ***Structure of ClpB/Hsp104 disaggregase.*** *Domain organization, structure, and hexameric model of ClpB/Hsp104. Monomer of ClpB/Hsp104 comprises N-terminal (N) domain, two AAA domains (AAA-1, AAA-2) containing conserved Walker A and B motifs with an inserted coiled-coil middle (M) domain encompassing four α-helices. One monomer assemblies into hexamer featured by three rings formed by N-domains, AAA-1/M-domains, and AAA-2 domains. Adapted from (Mogk* et al*, 2015).*

Once a protein substrate is bound, ATP hydrolysis fuels conformational changes within the hexamer. Stepwise movement of the AAA+ domains drives threading of a polypeptide through the central channel in a mechanism resembling rope climbing (Mogk *et al*, 2003; Schlieker *et al*, 2004; Deville *et al*, 2019). The effectiveness of Hsp100 strictly depends on the cooperation with Hsp70. Assisted by its cochaperones, Hsp70 not only directs protein substrates towards Hsp100, but also plays a crucial role in its allosteric regulation (Glover & Lindquist, 1998; Ziętkiewicz *et al*, 2004; Lee *et al*, 2013; Rosenzweig *et al*, 2013; Zeymer *et al*, 2014; Chamera *et al*, 2019). When the M-domain is in a repressed state, ClpB/Hsp104 exhibits diminished ATPase activity. Upon coupling with Hsp70, the M-domain undergoes repositioning against NBD1, transitioning into a derepressed state characterized by elevated ATPase activity (Fig. 2). This regulatory mechanism through the M-domain is important for cell viability, as a hyperactive mutant of Hsp100 exhibiting the derepressed state leads to growth impediments (Haslberger *et al*, 2007; Oguchi *et al*, 2012; Lipińska *et al*, 2013). Once a polypeptide is released, it may attempt to refold into its native state spontaneously or with the assistance of chaperones.

Metazoans lack disaggregase from the Hsp100 family, and instead have developed a chaperone machinery comprising Hsp70/JDP/NEF to combat protein aggregation (Rampelt *et al*, 2012; Nillegoda *et al*, 2015).

4.4 Hsp70

The 70-kDa protein is a versatile and essential molecular chaperone that acts as a central hub in various cellular processes. It plays a pivotal role in folding of newly synthetized polypeptides (Bukau *et al*, 2000), translocating them to the dedicated organelles (Schatz & Dobberstein, 1996), targeting protein substrates to degradation (Shiber & Ravid, 2014), assembly and disassembly of protein complexes (Liberek *et al*, 1988) and disaggregation of protein aggregates (Ben-Zvi & Goloubinoff, 2001).

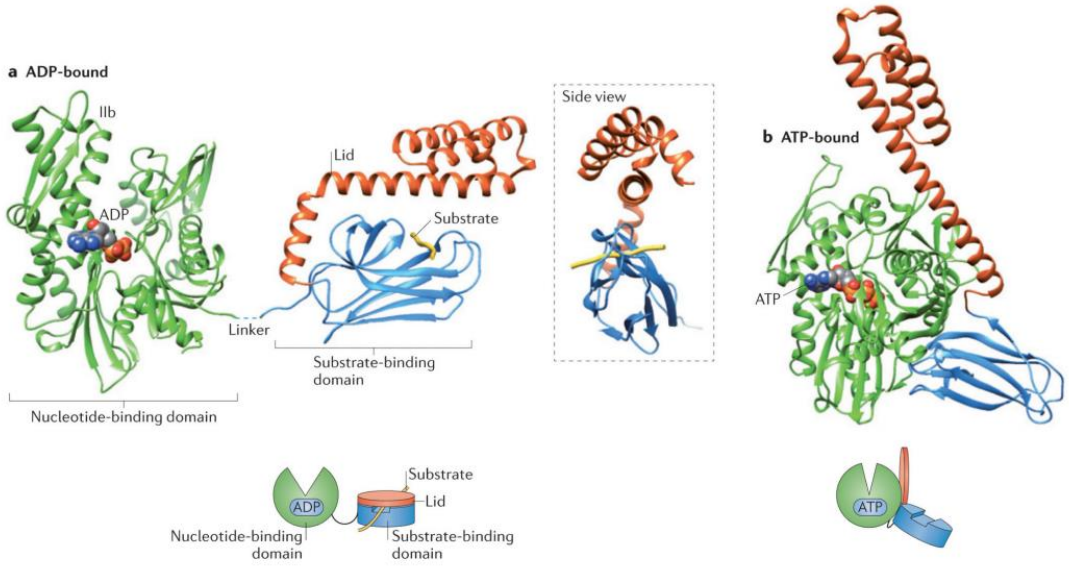

Figure 3. ***Structure and conformational states of Hsp70.*** *In the ADP-state (left), the nucleotide-binding domain (green; PDB code: 3HSC) is connected with the substrate-binding domain (blue; PDB code: 1DKZ) by a flexible linker. The C-terminal α-helical subdomain forms a lid (orange) over the β-sandwich subdomain (blue) and locks peptide substrate (yellow) in the binding pocket. In the ATP-state, peptide substrate is released by opening the lid. NBD and SBD remain closely associated, resulting in the widely an open conformation (PDB code: 4B9Q). Adapted from (Saibil, 2013)*

Hsp70s exhibit high sequence and structure similarity across diverse living organisms. The structure is organized into distinct domains, namely the substrate-binding domain (SBD), nucleotide-binding domain (NBD), and a flexible linker that serves as an allosteric regulator (Flaherty *et al*, 1990; Morshauser *et al*, 1995; Jiang *et al*, 2005). SBD is situated at the C-terminus and has two subdomains known as SBDβ and SBDα. SBDβ is comprised of two four-stranded beta sheets. Within this framework, a polypeptide-binding cleft is formed, featuring a deep pocket tailored specifically for a single hydrophobic amino acid side chain. Over this pocket lies a mobile α-helical lid, serving to cap and restrict access to the substrate binding cleft (Fig. 3) (Zhu *et al*, 1996; Rüdiger *et al*, 1997). In eukaryotic cytosolic and nuclear Hsp70s, the disordered tail frequently ends with a conserved charged motif: Glu-Glu-Val-Asp (EEVD), serving as an additional regulatory interface (Li *et al*, 2006).

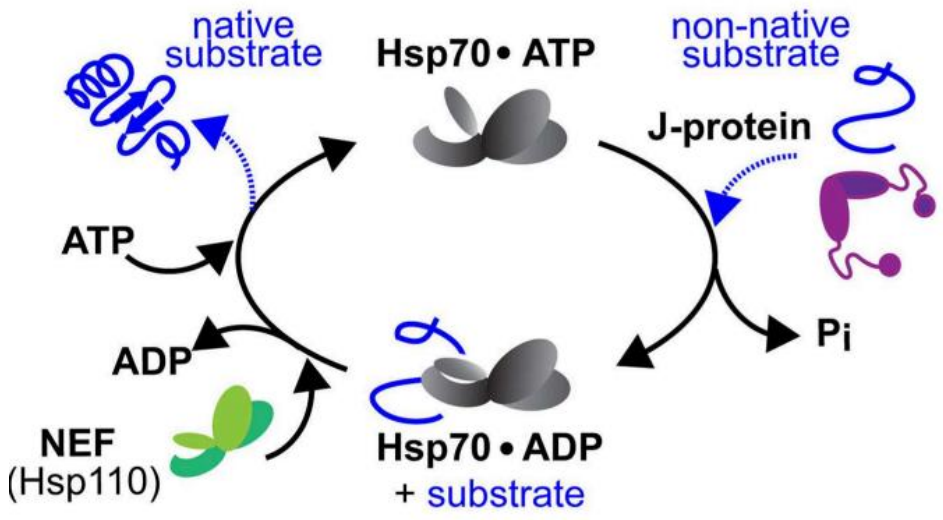

Figure 4. ***Functional cycle of Hsp70.*** *J-domain protein mediates recruitment of a protein substrate to Hsp70, triggering ATP hydrolysis and thereby stabilizing the interaction between Hsp70 and the substrate. Subsequent binding of NEF (nucleotide exchange factor) facilitates ADP dissociation and allows for ATP rebinding. This promotes the release of the substrate, completing the cycle. Adapted from (Nillegoda & Bukau, 2015).*

The chaperone activity of Hsp70 hinges on the swift association and timely release of a protein substrate in an ATP-dependent manner (Fig. 4). In the presence of ATP, Hsp70 adopts an open conformation characterized by low affinity for a polypeptide and high association and dissociation rates. This conformation uncovers a substrate-binding cleft in SBD, coupled with an open lid, allowing substrate binding. Binding of the exposed hydrophobic regions on substrates, promotes ATP hydrolysis in the NBD domain, thereby initiating conformational changes. Subsequently, the lid of SBD closes over the substrate within the binding cleft. This closed conformation serves to stabilize the Hsp70-substrate complex, preventing premature substrate release and protecting against aggregation. The exchange of ADP for ATP in the NBD prompts the reopening of the lid, returning the substrate-bound Hsp70 to an open conformation and facilitating substrate release (Fig. 4). The intrinsic ability of Hsp70 to hydrolyze ATP and to release ADP is low and to overcome these limitations, it requires an assistance of its cochaperones, J-domain proteins (JDPs) and nucleotide exchange factors (NEFs), respectively (Fig. 4) (Liberek *et al*, 1991; Laufen *et al*, 1999; Mayer *et al*, 2000; Mayer & Bukau, 2005; Kityk *et al*, 2012; Rohland *et al 2022*).

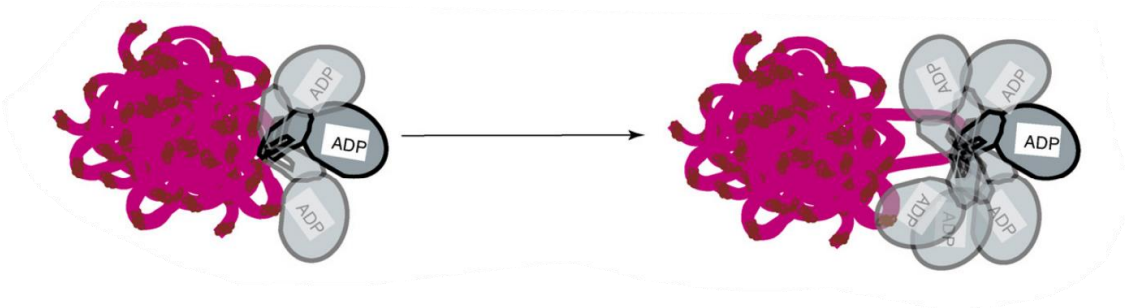

Figure 5. ***Entropic pulling-based mechanism of protein unfolding by Hsp70.*** *Hsp70, when bound to an aggregate, seeks freedom of movement, thereby facilitating the loosening of the aggregate structure through the disentanglement of polypeptides. Grey shadows represent the potential movements of Hsp70. Adapted from (Goloubinoff & De Los Rios, 2007).*

The debate surrounding how Hsp70 performs conformational work on protein substrates during their disaggregation and folding has been resolved by an entropic pulling mechanism. Tightly clustered Hsp70 molecules at the polypeptide trapped in aggregate restrict each other's movement and reduce the system's entropy. In search of freedom of movement and to increase entropy, Hsp70s generate force that pulls bound polypeptides, facilitating their disentanglement and in consequence, disaggregation (Fig. 5) (De Los Rios *et al*, 2006; Goloubinoff & De Los Rios, 2007; Rukes *et al*, 2024).

4.5 J-domain proteins

J-domain proteins (JDPs) have been organized into three distinct classes - A, B, and C, based on their structural resemblances to DnaJ from *E. coli*. Despite diversity observed among these classes, all JDPs share characteristic region of approximately 70 amino acids, named the J-domain. Within this alpha-helical structure, in a loop between two helices (II and III), there is a highly conserved HPD motif comprising histidine, proline and aspartic acid residues crucial for the interaction with Hsp70. Class A JDPs, defined by the domain architecture similar to DnaJ, are characterized by the presence of an N-terminal J-domain, followed by a region rich in glycine and phenylalanine (G/F), distinctive zinc-finger-like region (ZFLR) and two C-terminal beta-sandwich domains (CTD1 and CTD2) ending with a C-terminal dimerization domain (DD). Class B JDPs exhibit a comparable domain composition to class A, yet they are distinguished by the absence of the zinc-finger-like region. All proteins that share the J-domain, but were not classified as class A or class B, have been assigned to class C JDPs. (Fig.6) (Kampinga & Craig, 2010).

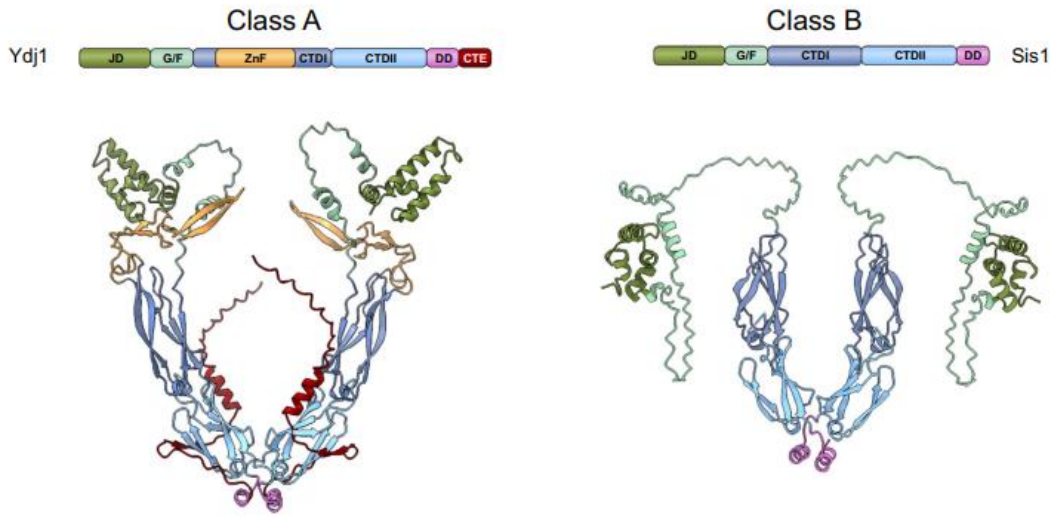

Figure 6. ***Domain organization and structure of Ydj1 and Sis1, class A and class B J-domain proteins in Saccharomyces cerevisiae, respectively.*** *Both Ydj1 and Sis1 are composed of J-domain, G/F region, CTD1, CTD2 and C-terminal dimerization domain. Additionally, Ydj1 possesses the zinc-finger-like region (ZFLR). Structural models were generated by AlphaFold2 and adapted from (Ruger-Herreros* et al*, 2024).*

J-domain proteins are essential for the Hsp70-mediated protein folding. Its regulation by JDPs involves protein substrate delivery to Hsp70 and stimulation of ATP hydrolysis (Fig. 4) (Cyr *et al*, 1992, 1994). The J-domain interacts with the NBD and establishes contact with the interdomain linker facilitating signal transmission to SBDβ, triggering ATP hydrolysis and concurrently leading to the trapping of the substrate (Kityk *et al*, 2018). Substrate preferences vary among class A and class B JDPs, which are determined by distinct composition of CTDs. It was demonstrated that DnaJ recognizes hydrophobic core of approximately 8 residues, particularly rich in aromatic residues. Similar substrate specificity is exhibited by Ydj1, whereas Sis1 differs, with a preference for aliphatic residues (Rüdiger *et al*, 2001; Fan *et al*, 2004).

Differences between class A and class B JDPs are not limited to substrate specificity, but also they exhibit disparate mechanism of interaction with Hsp70. This is due to the additional interface between the EEVD motif of Hsp70 and CTD1 of class B JDPs (yeast - Sis1, human - DNAJB1, DNAJB4), which is absent in class A. It has been established that class B JDPs utilize a regulatory mechanism that governs Hsp70 chaperone activity towards specific functions. The mechanism is based on the distinct J-domain orientation, in which the J-domain is restricted from binding to Hsp70 and requires

the CTD1 (class B JDPs) – EEVD (Hsp70) interaction to unlock the J-domain (class B JDPs) - NBD (Hsp70) interaction (Fig. 7). Presumably, this mechanism allows for unique organization of the Hsp70 system comprising class B JDPs at the aggregate surface and has been shown to be vital for the disaggregation of amyloid fibrils and amorphous aggregates (Yu *et al*, 2015; Faust *et al*, 2020; Wentink *et al*, 2020; Wyszkowski *et al*, 2021).

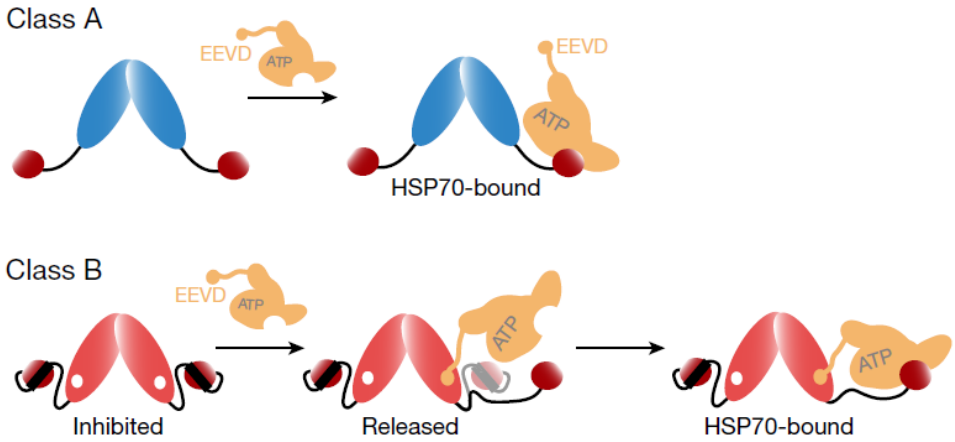

Figure 7. ***Model of mechanism of interactions between Hsp70 and class A (top) or class B (bottom) JDPs.*** *Class A JDPs interact with Hsp70 through the N-terminal J -domain. The J-domain of class B JDPs is restricted from binding to Hsp70. Consequently, class B exhibits a two-step binding mechanism, utilizing the additional interface comprising class B JDPs CTD1 and EEVD motif of Hsp70, ultimately unlocking the J-domain for Hsp70 activation. Adapted from (Faust* et al*, 2020).*

4.6 Nucleotides Exchange Factors

4.6.1 General overview

The folding activity of Hsp70 relies on the switch between ADP- and ATP-bound states, which spontaneously occurs at low rate. Therefore, nucleotide exchange factors serve to exchange ADP to ATP, by stabilizing the conformation of Hsp70 with low affinity for nucleotides. NEF activity is based on the recognition of the ADP-bound Hsp70, binding of which induces conformational changes that promote the dissociation of ADP from Hsp70. Cellular excess of ATP prompts its rebinding, which triggers the release of a protein substrate bound to Hsp70 and the dissociation of NEF (Liberek *et al*, 1991; Packschies *et al*, 1997; Dragovic *et al*, 2006; Andréasson *et al*, 2008b).

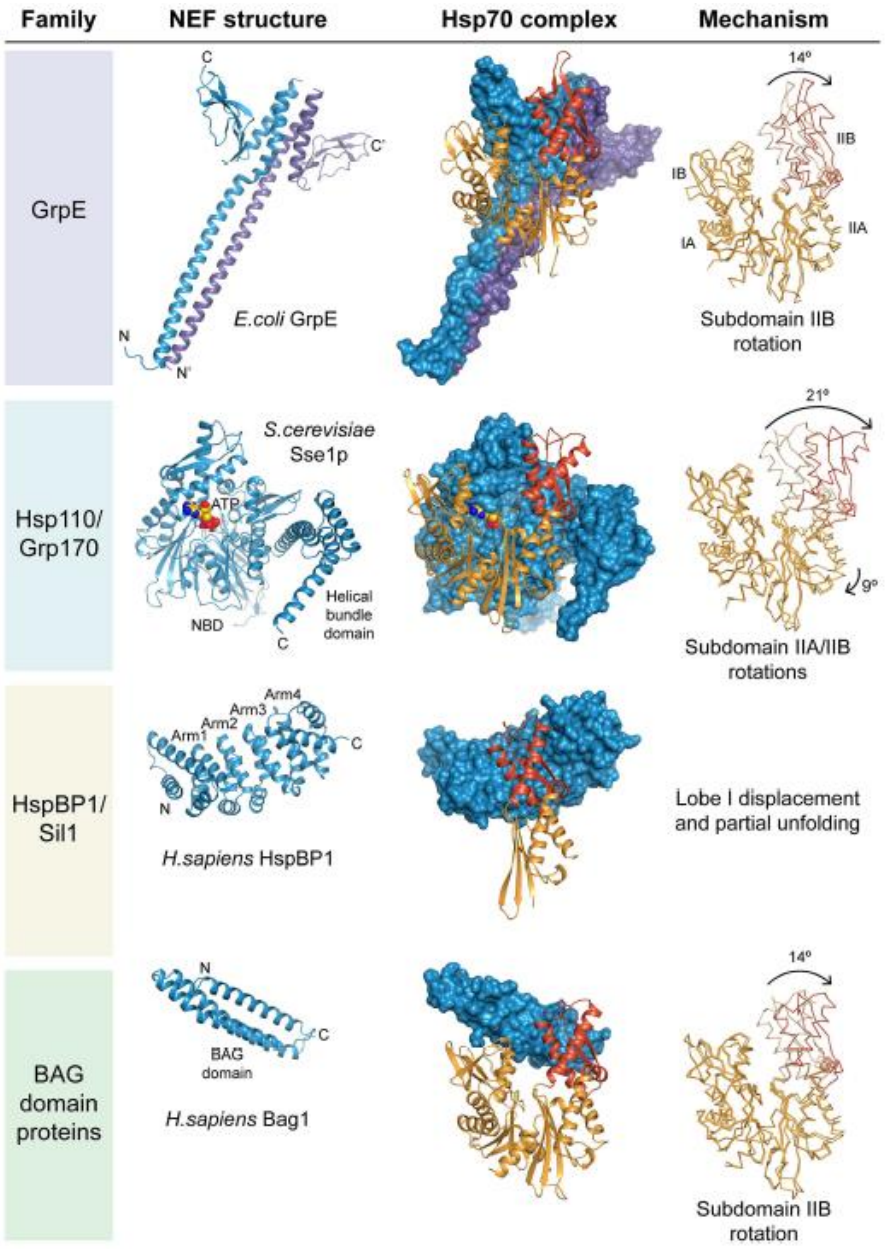

Figure 8. ***Structure and mechanism of nucleotide exchange factors.*** *Structures of four divergent families of NEFs: GrpE, Hsp110/Grp170, HspBP1/Sil1 and BAG-domain proteins alone or in the complex with NBD of Hsp70 are shown. NEF is represented in blue and NBD of Hsp70 in orange with subdomain IIb highlighted in red. On the right, the direction of the rotation of NBD of Hsp70 in the complex during nucleotide exchange is presented. Adapted from (Bracher & Verghese, 2015).*

NEFs are classified into four families, which exhibit structural diversity. Bacterial genomes exclusively encode GrpE, whereas in eucaryotic cells, three distinct families within cytosol and endoplasmic reticulum have emerged: Hsp110/Grp170, HspBP1/Sil1 and BAG-domain proteins (Fig. 8). Yeast NEFs are represented by three cytosolic forms Sse1 (Hsp110), Sse2 (Hsp110) and Fes1 (HspBP1); and ER-resident forms: Lhs1p (Hsp110), Sil1 and Snl1, the sole

representative of the BAG-domain family. Sse1 stands out as a predominant cytosolic NEF, because its level is much higher compared to other NEFs. Specifically, Sse1 is found at levels 10 times higher than Sse2, and it is 5 times more abundant than Fes1. In human cells, three homologs of Hsp110 in cytosol have been identified - Hsp105, Apg-1 and Apg-2, along with five BAG-domain proteins, one HspBP1, one form of the ER-resident Grp170 and ER-lumenal Sil1. Furthermore, eukaryotic compartments such as mitochondria and chloroplasts maintained the GrpE homologs (Abrams *et al*, 2014; Bracher & Verghese, 2015; Rosenzweig *et al*, 2019). While managing the ATPase cycle in a divergent manner, these four families share a common binding site to Hsp70 in the II lobe of the NBD (Fig. 8). Distinguished by their varying capacities to exchange nucleotides and affinities for Hsp70, they contribute uniquely to the protein quality control mechanisms within the cell (Bracher & Verghese, 2015).

4.6.2 GrpE

GrpE was identified as essential for *E. coli* growth across all temperatures, with only a few *dnaK* mutants demonstrating the capability to compensate the *grpE* deletion (Ang & Georgopoulos, 1989). Bacterial Hsp70, DnaK, is regulated by GrpE homodimer that comprises an α-helical dimerization domain terminated with a four-helix bundle at its C-terminal end, extended with a β-sheet domain that facilitates the interaction with Hsp70 (Fig. 8) (Harrison *et al*, 1997). Although the dimerization of GrpE is crucial for its activity, only one monomer interacts with DnaK (Wu *et al*, 1996). Binding to DnaK causes an extended rotation of subdomain IIB, leading to opening of the nucleotide-binding cleft, diminishing the affinity for the nucleotide 5000-fold. The largest interface is within the β-sheet domain, with additional binding sites at the elongated α-helix domain (Fig. 8) (Packschies *et al*, 1997; Rossi *et al*, 2024). In the cytosol of *E. coli*, there are two additional paralogs of Hsp70, HscA and HscC, functioning of which does not depend on GrpE. Structural analysis implies that residues within β-harpins in DnaK are pivotal for the NEF activity and those structures are shorter in these Hsp70 paralogs (Brehmer *et al*, 2001). Efficient recovery of proteins from aggregates by the bacterial Hsp70 system *in vitro* is strictly dependent on the presence of GrpE due to the limited nucleotide exchange.

4.6.3 BAG-domain proteins

The first discovered BAG-domain protein was BAG-1, named after the Bcl-2-associated athanogene, has been reported to be involved in the apoptosis regulation (Takayama *et al*, 1995). The group of proteins containing the BAG domain stands out as the most diverse among eukaryotic NEFs. The hallmark of this family lies in the presence of the BAG-domain, the helical bundle architecture of which varies among different members. The unifying feature is a common interface that interacts with the IIB subdomain of Hsp70, ensuring the NEF activity (Marzullo *et al*, 2022). BAG-domain proteins induce conformational shifts in the NBD of Hsp70 through interactions similar to those observed with GrpE (Fig. 8) (Sondermann *et al*, 2001). Specific elements in the structure of different BAG-domain proteins adapted them to regulate a spectrum of processes, including apoptosis, neuronal differentiation, tumorigenesis, stress responses and the cell cycle (Marzullo *et al*, 2022). In *S. cerevisiae, a* sole BAG-domain protein, Snl1, has been identified to be associated with endoplasmic reticulum. Biochemical data have shown that Snl1 interacts with the 60S ribosome subunit and presumably supports protein biogenesis by recruiting Hsp70 to the ribosome (Sondermann *et al*, 2002; Verghese & Morano, 2012).

4.6.4 HspBP1/Sil1

HspBP1 and Sil1 serve as cytosolic and ER-associated representatives of Armadillo type NEFs, along with their homologs Fes1 and Sil1 in *S. cerevisiae*, respectively (Kabani *et al*, 2002a, 2002b). A distinctive feature of this family are four α-helical armadillo repeats, mediating the interaction with Hsp70. The primary interface involves curved-shaped HspBP1, wherein its armadillo repeats wrap around the subdomain IIB of Hsp70 NBD (Fig. 8). Tryptophan fluorescence studies has revealed that this interaction collides with the subdomain IB, inducing the distortion of NBD of Hsp70 (Shomura *et al*, 2005; Bracher & Verghese, 2015).

Interestingly, HspBP1 and Fes1 harbor a release-domain (RD), which after the release of a substrate, interacts with the SBDβ of Hsp70, mimicking a protein substrate. Consequently, the rebinding of the true protein substrate is hindered and thus substrate release is improved. Removal of RD causes severe growth deficiency, implying a crucial role of this component in the Hsp70 cycle (Gowda *et al*, 2018). Functionally, Fes1 is essential in targeting misfolded proteins to

ubiquitin–proteasome system (UPS) and is involved in prion formation and curing (Kryndushkin & Wickner, 2007; Gowda *et al*, 2013).

4.6.5 Hsp110/Grp170

Hsp110 proteins were identified in the early 80s, however their functional properties were poorly studied despite abundant expression in most mammalian tissues and cells. In human cells, three genes encode isoforms of cytosolic Hsp110 (Hsp105, Apg1, Apg-2) and one gene of an ER-associated isoform (Grp170). In *S. cerevisiae*, Hsp110 is represented by Sse1 and its paralog Sse2, along with an ER-resident paralog, Lhs1p (Easton *et al*, 2000). Cells with *sse1Δ* display slow growth at normal temperatures and 37°C. In contrast, *sse2Δ* does not exacerbate growth defects at 30°C and 37°C. A complete loss of *sse1,2* is lethal. In the model organism *S. cerevisiae,* Sse1 has been demonstrated to be involved not only in protein refolding, but it also assists in proteasomal degradation (Kandasamy & Andréasson, 2018). Additionally, it is engaged in prion propagation and maintenance (Fan *et al*, 2007; Kryndushkin & Wickner, 2007). Sse1 also interacts with the ribosome-associated Hsp70, Ssb1/2, and was reported to participate in *de novo* protein folding (Shaner *et al*, 2005; Fan *et al*, 2007). Moreover, it has been shown to be involved in the Hsp90-based machinery (Liu *et al*, 1999; Goeckeler *et al*, 2002).

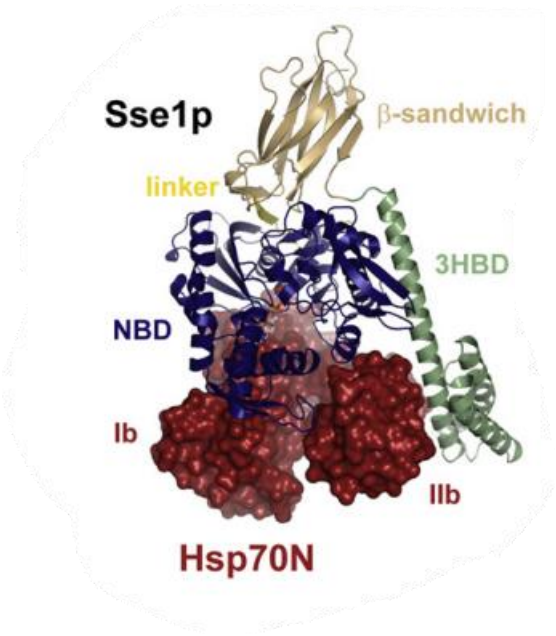

Figure 9. ***Structure of Sse1 in complex with NBD of Hsp70.*** *Ribbon representation of Sse1, where NBD is shown in blue, linker in yellow, and β-sandwich and 3HBD in brown and green, respectively. Sse1 interacts with the NBD of human Hsp70 (Hsp70N) through its NBD and 3HBD. Adapted from (Polier et al, 2008).*

4.6.5.1 Structure

Hsp110/Grp170 are members of the Hsp70 superfamily, yet they are divergent from the conserved Hsp70s due to their highly diversified C-terminal extension. The crystal structure of Sse1 has revealed the Hsp70-like domain organization comprising an N-terminal nucleotide-binding domain exhibiting ~35% similarity to

NBD of Hsp70s, followed by a β-sandwich with additional insertions and a C-terminal three helix bundle domain (3HBD) (Fig. 9) (Liu & Hendrickson, 2007). Contrary to Hsp70, the α-helical domain does not form a lid over the substrate-binding cleft, but together with the β-sandwich domain they interact with the NBD, protruding towards the opposite direction (Fig. 9) (Liu & Hendrickson, 2007). In the crystal structure of the complex between Sse1 and human Hsp70, both NBDs contact each other and the interaction is extended by the interface between the three helix bundle domain and subdomain IIB of Hsp70 (Fig. 9). In this conformation, subdomains IB and IIB of Hsp70 move away from each other, opening the nucleotide binding cleft, which results in a diminished interaction with ADP and ultimately facilitates its dissociation. Mutation in the 3HBD has demonstrated severe growth defects, emphasizing its essential role in mediating the interaction with Hsp70. The resolved structure of the complex with the NBD of human Hsp70 (Hsp70N) can be adapted for the NBD of yeast Hsp70 (Ssa1N) in terms of the mode of binding to Sse1, since the sites interacting with Hsp110 are conserved across the eucaryotic Hsp70s (Andréasson *et al*, 2008a; Polier *et al*, 2008).

Crystal structures indicate the presence of ATP in the nucleotide-binding cleft of Sse1 (Liu & Hendrickson, 2007). It has been shown that ATP binding is crucial for the complex formation with Hsp70, since it promotes structural rearrangements of Sse1 that result in the active conformation required for Hsp70 binding. In the latter step of the nucleotide exchange cycle, ATP binding to Sse1 is not mandatory for the complex integrity and its dissociation (Andréasson *et al*, 2008b). Crystals of the NBD of the human Hsp110 resembled those of Sse1 and were co-crystalized with ATP (Gozzi *et al*, 2020).

4.6.5.2 Specific features of Hsp110

While ATP binding is essential for the Hsp110 NEF activity, whether Hsp110 hydrolyses ATP is a matter of debate. Several studies indicate that ATP hydrolysis indeed occurs in Hsp110 and can be enhanced by J-domain proteins (Raviol *et al*, 2006a; Mattoo *et al*, 2013). On the other hand, human Hsp110 did not show any ATPase activity regardless the presence of a JDP (Yamagishi *et al*, 2000). Notably, a mutant lacking the intrinsic ATPase activity was incapable of facilitating protein refolding *in vitro* (Shorter, 2011). Further, studies have shown that an

ATP-hydrolysis-deficient mutant of Hsp110 supported protein refolding by the Hsp70 system and phenotype of yeast cells harboring the Sse1 mutant was unchanged (Dragovic *et al*, 2006; Goeckeler *et al*, 2008; Rampelt *et al*, 2012). Interestingly, studies on Sse1 have demonstrated that its intrinsic ATPase activity is suppressed by intramolecular interactions, since isolated NBD of Sse1 has been reported to possess high ATPase activity (Kumar *et al*, 2020).

Moreover, a distinctive feature of Hsp110 is that it binds peptides with high affinity, with specificity for aromatic residues (Oh *et al*, 1997, 1999; Goeckeler *et al*, 2008; Xu *et al*, 2012). Sse1 has been found to act as a 'holdase' defined as the ability to prevent protein aggregation by binding to a denatured protein substrate, contrary to its paralog, Sse2, which lacks this activity. Furthermore, analysis of the activity of a Sse1 variant with multiple single-residue substitutions in the SBD has revealed that although SBD is dispensable for the refolding of protein substrates by the Hsp70 system *in vitro*, the SBD mutant failed to complement the lethal phenotype of the *sse1,2Δ* (Garcia *et al*, 2017).

A recent study has revealed a second binding site within the C-terminal extension of a *Drosophila* Hsp110, an intrinsically disordered region (IDR), which is highly conserved in metazoans, but lacking in fungi. This region has been shown to be responsible for the 'holdase' activity in preventing the fibrilization of Aβ peptides and α-synuclein, which are involved in the development of the Alzheimer's and Parkinson's disease, respectively (Yakubu & Morano, 2021).

The importance of the 'holdase' activity in the Hsp110-mediated protein disaggregation remains elusive. Additionally, it is still an open question whether the primary function of Hsp110 in contributing to the Hsp70-dependent protein disaggregation lies in its NEF activity characterized as the Hsp110-driven nucleotide exchange in Hsp70. Sse1 mutants with disrupted binding to Hsp70, which exhibited substantially impaired NEF activity failed to rescue the lethal phenotype of the *sse1,2Δ* deletion, and were incapable of supporting the refolding of luciferase aggregates by Hsp70 *in vitro* (Polier *et al*, 2008). Similarly to the yeast Sse1, human Hsp110 with the diminished NEF activity did not support the disaggregation by the bichaperone system comprising Hsp70 and a J-domain protein (Rampelt *et al*, 2012).

4.6.5.3 Hsp110-based protein disaggregation

It has been reported that Hsp110 is most efficient at sub-stoichiometric amounts relatively to Hsp70, with an inhibitory effect in protein disaggregation at higher concentration (Dragovic *et al*, 2006; Polier *et al*, 2010; Rampelt *et al*, 2012; Gao *et al*, 2015; Wentink *et al*, 2020). While *in vitro,* the Hsp104-dependent protein disaggregation by the yeast chaperone system is efficient without Hsp110 (Glover & Lindquist, 1998), *in vivo* studies highlight the significance of the coordinated activities between Hsp110 and Hsp104 (Kaimal *et al*, 2017). The experiments have revealed that cells harboring a Sse1 mutant with the impaired interaction with Hsp70 were able to recruit Hsp104 to the aggregates, however subsequent solubilization of these aggregates was hampered (Kaimal *et al*, 2017).

Metazoans lack Hsp100 disaggregase, however Hsp70 and J-domain proteins are efficient in the solubilization of amorphous aggregates on account of the presence of Hsp110 (Rampelt *et al*, 2012). Apg-2 and Hsp105 play crucial role in mediating the disassembly of α-synuclein fibrils by Hsc70 and DNAJB1 (Gao *et al*, 2015; Beton *et al*, 2022).

4.6.5.4 Comparative analysis of other NEFs

The lethal phenotype of *sse1,2Δ* deletion was partially compensated by the overexpression of *fes1* (Liu *et al*, 1999; Raviol *et al*, 2006b). In the nucleotide release experiments, Sse1 was superior to Fes1 (Dragovic *et al*, 2006), yet the capacity of Fes1 to stimulate the refolding of luciferase aggregates vary across different reports (Dragovic *et al*, 2006; Raviol *et al*, 2006b; Kaimal *et al*, 2017).

In the human Hsp70-dependent protein disaggregation, BAG-1 stimulated the refolding of luciferase aggregates to the lesser extent than all human Hsp110s (Rampelt *et al*, 2012). Similarly, BAG-1 was only able to moderately stimulate the disassembly of α-synuclein fibrils by Hsc70 and DNAJB1. It has been reported that BAG-1 exhibited lower nucleotide exchange rates compared to Hsp110, however higher concentration did not improve the disaggregation activity despite similar ability to exchange nucleotide compared to Hsp110 (Gao *et al*, 2015). In *vivo* experiments in *C. elegans* have shown that knock out of Hsp110, but not BAG-1 substantially diminished the solubilization of protein aggregates and caused premature aging (Rampelt *et al*, 2012).

Despite the knowledge on how Hsp110 serves as a regulator of the ATPase cycle of Hsp70, the involvement of Hsp110 in protein disaggregation, considering the mechanism of interaction with Hsp70 with different JDP classes was not investigated. Here, I dissect an interplay between Hsp110 and Hsp70 at individual stages of protein disaggregation in the context of class of JDPs.

5. Aim of the project

In my doctoral project, I addressed the role of Hsp110 in the Hsp70-dependent disaggregation. My objective was to examine how Hsp70 activity is influenced by Hsp110, when paired with different JDP classes. Furthermore, I focused on the molecular mechanisms underlying these interactions to determine what features of Hsp110 influence the Hsp70-dependent protein disaggregation.

6. Materials

6.1 Bacterial strains

Escherichia coli BL21(DE3) codon+ F– ompT hsdS(rB – mB –) dcm+ Tetr gal endA Hte [argU ileY leuW] (CmR)

6.2 Plasmids

pCA533 used for overproduction of His6-SUMO-Ssa1 and its variants, KanR, T7 lac promoter, IPTG-induced

pCA534 vector used for overproduction of Sse1 and its variants, KanR, T7 lac promoter, IPTG-induced (Andréasson *et al*, 2008b)

pCA707 vector used for overproduction of Fes1, KanR, T7 lac promoter, IPTG-induced (Andréasson *et al*, 2008a)

pET21a vector used for overproduction of Ydj1, AmpR, T7 lac promoter, IPTG-induced

pET22b vector used for overproduction of Fluc-EGFP, AmpR, T7 lac promoter, IPTG-induced

pPROEX vector used for overproduction of His6-TEV-Sis1 and its variants, AmpR, trc (trp-lac) promoter, IPTG-induced

pPROEX vector used for overproduction of His6-TEV-Hsp105, AmpR, trc (trp-lac) promoter, IPTG – induced (Nillegoda *et al*, 2015)

6.3 Proteins

6.3.1 Chaperones

Sis1, Ydj1, Sis1 E50A, Ssa1, Ssa1 ΔEEVD, Sse1, Sse1-2, Fes1, Hsp105 – this work

Hsp104, Hsp104 D484K F508A, Hsc70, DNAJA2 and DNAJB4 - laboratory's collection (Nillegoda *et al*, 2015; Chamera *et al*, 2019)

6.3.2 Protein substrates

Luciferase (Luc) from P. pyralis, recombinant (Promega)

Luciferase-His from P. pyralis, recombinant (Chamera et al. 2019)

GFP from A. victoria, recombinant (Ziętkiewicz et al. 2004)

6.4 Antibodies

α-Ssa1 (anti-rabbit serum)

α-Sse1 (anti-rabbit serum)

Horseradish peroxidase-labeled anti-rabbit IgG secondary antibodies (Bio-Rad)

6.5 Broths

LA 1% peptone, 0,5% yeast extract, 1% NaCl, 1.5% agar

LB 1% peptone, 0,5% yeast extract, 1% NaCl

6.6 Antibiotics

Ampicillin (100 µg ml^{-1})

Kanamycin (50 µg ml^{-1})

6.7 Oligonucleotides

Name	Sequence 5' -> 3'	Description
SisForE50A	GTTTAAGGAGATATCAGCGC	Forward primer for site-specific mutagenesis for introduction E50A in Sis1
SisRevE50A	CAAAGGCCGCTGATATCTCCT	Reverse primer for site-specific mutagenesis for introduction E50A in Sis1
EEVDfor	GAGGCTGAAGCTCCATAAGTTGAAGAAGTTGATTAA	Forward primer for site-specific mutagenesis designed to introduce TAA stop codon to delete the C-terminal EEVD motif of Ssa1
EEVDrev	TTAATCAACTTCTTCAACTTATGGACCTTCAGCCTC	Reverse primer for site-specific mutagenesis designed to introduce TAA stop codon to delete the C-terminal EEVD motif of Ssa1

Sse1K69MFor	CGCCAACTTGATGAGAATTATTGG	Forward primer for site-specific mutagenesis for introduction K69M in Sse1
Sse1K69MRev	CCAATAATTCTCATCAAGTTGGCG	Reverse primer for site-specific mutagenesis for introduction K69M in Sse1
SseE572YFor	CAGAAGACCGTAAGTACACTC	Forward primer for site-specific mutagenesis for introduction E572Y in Sse1
SseE572YRev	CTCTTCAAGAGTGTACTTACGG	Reverse primer for site-specific mutagenesis for introduction E572Y in Sse1
SseE575AFor	CGTAAGAACACTCTTGCAGAGTAC	Forward primer for site-specific mutagenesis for introduction E575A in Sse1
SseE575ARev	GTGTAGATGTACTCTGCAAGAGTG	Reverse primer for site-specific mutagenesis for introduction E575A in Sse1

7. Methods

7.1 Preparation and transformation of *E. coli* competent cells

The preparation and transformation of *E. coli* competent cells were carried out using the Mix and Go! *E. coli* Transformation Kit from Zymogen. The procedure followed the provided protocol and involved utilizing a specific *E. coli* strain and buffer. The transformed cells were then plated on LA medium-containing plates supplemented with an appropriate antibiotic for selection.

7.2 Plasmid DNA isolation

Plasmid DNA from overnight *E. coli* cultures was isolated using a plasmid DNA isolation kit from A&A Biotech according to the provided protocol enclosed with the kit.

7.3 PCR-based site-directed mutagenesis

The PCR reaction mixture comprised 2.5 U of Pfu Ultra II polymerase, PFU Ultra II buffer, 50-200 ng of DNA template, 125 ng of both Forward and Reverse primers (synthesized by genomed.pl), and 1 mM dNTPs (250 µM for each nucleotide).

The PCR amplification was conducted using the Bio-Rad C1000 Thermal PCR Machine. Optimized conditions were applied for each mutagenesis, involving a hot-start at 95°C, initial denaturation for 10 minutes at 95°C, followed by 17 cycles of denaturation (95°C for 30 seconds), annealing (60 seconds), and elongation (68°C for 60 seconds per 1 kbp). The final elongation step lasted 10 minutes at 68°C. Subsequently, the PCR product was incubated with DpnI for 2 hours at 37°C to eliminate the DNA template, and ultimately utilized for the transformation of competent cells. The accuracy of mutation introduction was verified by sequencing performed by Genomed.

7.4 Protein purification

7.4.1 Ssa1 and its variants

BL21 (DE3) codon+ strain was transformed with pCA533 plasmid harboring *SSA1* gene fused with N-terminal His-tag and SUMO. 12 liters of LB broth supplemented with 50 µg/ml kanamycin were inoculated with an overnight culture of the freshly transformed cells (1 ml of overnight culture per 20 ml of LB broth) and grown at 37°C with shaking until the OD_{600} reached approximately 0.5. The expression was initiated upon addition of isopropyl β-D-1-thiogalactopyranosid (IPTG) to the final concentration of 1 mM and cells were shifted to 30°C. After 3 hours, the cells were harvested by centrifugation in 5000 rpm for 7 min using rotor JLA 10.500 (Beckman Coulter). The pellet was suspended in a lysis buffer (20 mM HEPES pH 8.0, 500 mM KCl, 5 mM imidazole, 5 mM β-mercaptoethanol, 10 % glycerol) and the lysis was carried out using a French Press at 1000 PSIG. The lysate was fractionated by centrifugation at 25000 rpm for 30 minutes and the soluble fraction containing Ssa1 was incubated with the Ni-NTA resin. After the resin was washed with the lysis buffer and buffer containing 20 mM and 50mM imidazole, the protein was eluted with the buffer containing 500 mM imidazole, while keeping the other components constant. The eluted material was dialyzed against buffer suitable for Ulp1 cleavage (50 mM HEPES-KOH pH 8.0, 150 mM KCl, 5 mM β-mercaptoethanol). After 1 hour, Ulp1 protease was added and dialyzed overnight at 4 °C. Cleaved Ssa1 was selected by incubation with Ni-NTA resin and Ssa1-containing fractions were dialyzed against buffer suitable for 5'-ATP Agarose resin (20 mM HEPES-KOH pH 8.0, 50 mM KCl, 10 mM

$Mg(OAc)_2$, 5 mM β-mercaptoethanol, 10 % glycerol). The resin was incubated with the protein preparation and washed with the same buffer prior to the elution with the buffer supplemented with 10 mM ATP. Fractions containing pure Ssa1 were pooled together, dialyzed against final buffer (50 mM HEPES-KOH pH 8.0, 100 mM KCl, 5 mM $Mg(OAc)_2$, 10 % glycerol), aliquoted and stored at -80°C.

7.4.2 Sse1 and its variants

BL21 (DE3) codon+ strain was transformed with pCA534 plasmid harboring *SSE1* gene fused with N-terminal His-tag and SUMO. Overproduction and purification of Sse1 were conducted using the same protocol utilized for Ssa1. However, following Ulp1 cleavage, Sse1 was subjected to size exclusion chromatography with buffer suitable for storage (50 mM HEPES-KOH pH 8.0, 100 mM KCl, 5 mM $Mg(OAc)_2$, 5 mM β-mercaptoethanol, 10 % glycerol). Fractions containing pure Sse1 were pooled together, aliquoted and stored at -80°C.

7.4.3 Fes1

BL21 (DE3) codon+ strain was transformed with pCA707 plasmid harboring *FES1* gene fused with N-terminal His-tag and SUMO. Overproduction and purification of Fes1 were conducted using the same protocol as for Sse1.

7.4.4 Sis1 and its variants

BL21 (DE3) codon+ strain was transformed with pPROEX plasmid harboring *SIS1* gene fused with N-terminal His-tag and a sequence recognized by TEV protease. 6 liters of LB broth supplemented with 100 µg/ml ampicillin were inoculated with an overnight culture of the freshly transformed cells (1 ml of overnight culture per 20 ml of LB broth) and grown at 37°C with shaking until the OD_{600} reached approximately 0.5. The expression was initiated upon addition of isopropyl β-D-1-thiogalactopyranosid (IPTG) to the final concentration of 1 mM and cells were shifted to 30°C. After 3 hours the cells were harvested by centrifugation at 5000 rpm for 7 min using rotor JLA 10.500 (Beckman Coulter). The pellet was suspended in a lysis buffer (50 mM HEPES-KOH pH 8.0, 750 mM KCl, 5 mM β-mercaptoethanol, 10 % glycerol) and the lysis was carried out using French Press at 1000 PSIG. The lysate was fractionated by centrifugation at 25000 rpm for 30 minutes and the soluble fraction containing

Sis1 was applied to 5 ml HisTrap™ prepacked collumn (GE Healthcare). The resin was washed with the lysis buffer and elution was carried out with a linear KCl gradient in the same buffer up to 500 mM KCl. Sis1-enriched fractions were pooled together and dialyzed against buffer suitable for TEV proteolysis (50 mM HEPES-KOH pH 8.0, 150 mM KCl). In the meantime, usually precipitation of the protein preparation occurred, followed by the addition of EDTA to the final concentration of 2 mM and centrifugation at 25000 rpm for 30 minutes to remove precipitated fraction. Afterwards TEV protease was added to the supernatant and dialyzed overnight. Protein preparation was incubated with Ni-NTA resin for selection of cleaved Sis1 and glycerol was added to final concentration of 10% to the protein solution. Subsequently, protein preparation was aliquoted and stored at -80°C.

7.4.5 Ydj1

BL21 (DE3) codon+ strain was transformed with pET21a plasmid harboring *YDJ1* gene. 6 liters of LB broth supplemented with 100 µg/ml ampicillin were inoculated with overnight culture of the freshly transformed cells (1 ml of overnight culture per 20 ml of LB broth) and grown at 37°C with shaking until the OD600 reached approximately 0.5. The expression was initiated upon addition of isopropyl β-D-1-thiogalactopyranosid (IPTG) to the final concentration of 1 mM and cells were shifted to 30°C. After 3 hours, the cells were harvested by centrifugation in 5000 rpm for 7 min using rotor JLA 10.500 (Beckman Coulter). The pellet was suspended in a lysis buffer (40 mM HEPES-KOH pH 7.5, 80 mM KCl, 5 mM β-mercaptoethanol, 10 % glycerol) and the lysis was carried out using a French Press at 1000 PSIG. The lysate was fractionated by centrifugation at 25000 rpm for 30 minutes and soluble fraction containing Ydj1 was loaded at a column packed with Q-Sepharose resin. Firstly, it was washed with the lysis buffer and elution was performed by employing the same buffer with increasing concentration of KCl up to 300 mM. Fractions containing the most concentrated Ydj1 were pooled together and dialyzed against buffer suitable for hydroxyapatite chromatography (25 mM KPi pH 7.0, 50 mM KCl, 10 % glycerol). Protein preparation was then loaded onto a column containing hydroxyapatite resin, followed by the washing with the same buffer prior to elution, which was carried out with phosphate gradient to the final concentration of 400 mM. The most

Ydj1-enriched fractions were pooled together and dialyzed against buffer suitable for purification on a Heparin resin (25 mM HEPES-KOH pH 7.5, 50 mM KCl, 10 % glycerol). Protein sample was applied to a column prepacked with Heparin resin, washed with the same buffer and the elution was performed by employing linear gradient of KCl up to 500 mM. Fractions containing pure Ydj1 were pooled together, dialyzed against final buffer (50 mM HEPES-KOH pH 7.5, 150 mM KCl, 10 % glycerol), aliquoted and stored at -80°C.

7.4.6 Hsp105

BL21 (DE3) codon+ strain was transformed with pPROEX plasmid harboring *HSP105* gene fused with N-terminal His-tag and sequence recognized by TEV protease. Overproduction and purification of Hsp105 followed the same protocol that was used for Sse1. However, cleavage was facilitated by the addition of TEV protease.

7.4.7 Fluc-EGFP

BL21 (DE3) codon+ strain was transformed with pet22b plasmid harboring *Fluc-EGFP* gene fused with N-terminal His-tag and SUMO. 6 liters of LB broth supplemented with 100 µg/ml ampicillin were inoculated with overnight culture of the freshly transformed cells (1 ml of overnight culture per 20 ml of LB broth) and grown at 37 °C with shaking until the OD_{600} reached approximately 0.5. The expression was initiated upon addition of isopropyl β-D-1-thiogalactopyranosid (IPTG) to the final concentration of 1 mM and cells were shifted to 30°C. After 3 hours, the cells were harvested by centrifugation at 5000 rpm for 7 min using rotor JLA 10.500 (Beckman Coulter). The pellet was suspended in a lysis buffer (50 mM Tris-HCl pH 8.0, 300 mM NaCl, 10 % glycerol) and the lysis was carried out using a French Press at 1000 PSIG. The lysate was fractionated by centrifugation at 25000 rpm for 30 minutes and the soluble fraction containing Fluc-EGFP was incubated with Ni-NTA resin. After the resin was washed with the lysis buffer, the protein was eluted with a linear gradient of buffer containing 300 mM imidazole, while keeping the other components constant. Fractions containing the most concentrated Fluc-EGFP were pooled together and dialyzed against buffer suitable for Q-Sepharose chromatography (50 mM Tris-HCl pH 8.0, 50 mM NaCl, 5 mM β-mercaptoethanol, 10 % glycerol). The protein preparation was incubated with Q-Sepharose resin and washed with the same buffer prior to elution, which

was carried out with a linear gradient of the same buffer containing 500 mM NaCl. Fractions containing pure Fluc-EGFP were pooled together, dialyzed against final buffer (50 mM Tris-HCl pH 7.5, 150 mM KCl, 5 mM β-mercaptoethanol, 10 % glycerol), aliquoted and stored at -80°C.

7.4.8 Determining concentration of purified proteins

Protein concentration was measured by densitometry using BSA standard curve (Sigma-Aldrich) and ImageLab software (Bio-Rad).

7.5 Biochemical assays

7.5.1 Bio-layer interferometry

Binding experiments were conducted using BLItz and Octet K2 instruments (ForteBio).

7.5.1.1 Chaperone binding to luciferase aggregates immobilized on the BLI biosensor

Firstly, the Ni-NTA biosensor (ForteBio Dip and Read) was hydrated in the HKM buffer (25 mM HEPES-KOH pH 8.0, 75 mM KCl, 15 mM $MgCl_2$) for 10 minutes. Subsequently, it was immersed in the same buffer supplemented with 6 M Urea and 8.2 μM His-tagged luciferase for 10 minutes, during which the anchoring luciferase layer reached thickness of approximately 6 nm. After washing with HKM buffer for 5 minutes, the sensor was transferred to the HKM buffer with 1.6 μM of native His-tagged luciferase and incubated at 44°C for 10 minutes. This resulted in the formation of a luciferase aggregate of the layer thickness of approximately 16 nm. Next, the biosensor was equilibrated in the HKM buffer enriched with 5 mM ATP and 2 mM DTT. Baseline, association and dissociation steps were performed in the HKM buffer supplemented with 5 mM ATP and 2 mM DTT, unless indicated otherwise. Chaperones were used at the following concentrations: 1 μM Ssa1, 1 μM Sis1, 1 μM Ydj1, 0.1 μM Sse1, 1 μM Fes1, 3 μM Hsc70, 1 μM DNAJB4, 1 μM DNAJA2 and 0.1 μM Hsp105, unless indicated otherwise.

7.5.1.2 Chaperone binding to GFP aggregates immobilized on the BLI biosensor

The Ni-NTA biosensor (ForteBio Dip and Read) was initially hydrated in the HKM buffer (25 mM HEPES-KOH pH 8.0, 75 mM KCl, 15 mM $MgCl_2$) for 10 minutes. Next, it was immersed in the HKM buffer supplemented with 9 M Urea and 12.5 μM GFP and transferred to 85°C for 15 minutes. After it was washed for 5 minutes with the HKM buffer, the sensor was incubated in the HKM buffer containing 4.2 μM GFP at 85°C for 15 minutes, which resulted in a layer of GFP aggregate ~40 nm. Finally, the biosensor was equilibrated in the HKM buffer enriched with 5 mM ATP and 2 mM DTT. All binding steps were performed in the HKM buffer supplemented with 5 mM ATP and 2 mM DTT, unless indicated otherwise. Chaperones were used at the following concentrations: 1 μM Ssa1, 1 μM Sis1, 1 μM Ydj1 and 0.1 μM Sse1.

7.5.1.3 Chaperone binding to yeast lysate aggregates immobilized on the BLI biosensor

Yeast lysate was employed from the laboratory's collection. It was prepared from W303 yeast cells cultured for 72h in the YPD medium. Following 10 minutes hydration in the HKM buffer (25 mM HEPES-KOH pH 8.0, 75 mM KCl, 15 mM $MgCl_2$), the Ni-NTA biosensor (ForteBio Dip and Read) was immersed in the same buffer containing 6 M Urea and 8.2 μM His-tagged luciferase and incubated for 10 minutes. Subsequently, the biosensor was washed in the HKM buffer, followed by the incubation at 55°C for 10 minutes in the HKM buffer containing soluble yeast proteins (5 mg/ml). Protein aggregate assembled with a layer thickness of approximately 30 nm. Finally, the biosensor was equilibrated in the HKM buffer supplemented with 5 mM ATP and 2 mM DTT. Chaperones were used at 1 μM concentration, unless specified otherwise.

7.5.1.4 BLI with fluorescently labelled protein

Ssa1 was fluorescently labelled with Alexa Fluor 488 C5-maleimide (Invitrogen). Firstly, Ssa1 was incubated with 10-molar excess of the fluorophore at 4°C for 2 hours, followed by the removal of an excess of the fluorophore with a desalting column (PD-10, GE Healthcare). Binding experiments to the luciferase aggregates immobilized on the biosensor (ForteBio Dip and Read) was performed according to the previously described method. After the final step,

samples containing dissociated proteins in the HKM buffer supplemented with 5 mM ATP were subjected to fluorescence measurement using Beckman Coulter DTX 880 Plate Reader. Chaperones were used at 1 µM concentration, except for Sse1, which was used at 0.1 µM.

7.5.1.5 BLI of direct protein-protein interactions

The Ni-NTA biosensor (ForteBio Dip and Read) was initially hydrated in the HKM buffer (25 mM HEPES-KOH pH 8.0, 75 mM KCl, 15 mM $MgCl_2$) for 10 minutes. Baseline was conducted in the HKM buffer for 30 seconds and subsequently immersed in the HKM buffer containing indicated protein (0.4 µM His-Sis1, 2.5 µM His-Sse1 and 1 µM His-Sse1-2) for 15 minutes. Binding reached saturation level, which corresponded to a layer thickness of ~15 nm for His-Sis1, ~6 nm for His-See1 and ~4 nm for His-Sse1-2. After the biosensor was washed in the HKM buffer supplemented with 5 mM ATP and 2 mM DTT, it was immersed in the same buffer containing indicated proteins at specified concentration, followed by the dissociation step in the same buffer.

7.5.2 GFP reactivation assay

GFP (2 mg/ml) was subjected to thermal aggregation at 85°C for 10 minutes in a buffer containing 40 mM Tris-HCl pH 7.5, 150 mM NaCl, 10% glycerol. The disaggregation was carried out in a buffer containing 28 mM Tris-HCl pH 7.5, 60 mM potassium glutamate, 7 mM DTT, 10 mM ATP, 7% glycerol and all chaperone proteins were used at a concentration of 1 µM, with the exception of the Hsp104 D484K F508A mutant, which was used at 0.15 µM and Sse1, which was used at 0.1 µM, if not stated otherwise. In the remodeling experiments, the preliminary incubation with Hsp70 system was arrested by the addition of 120 mM NaCl. The reactivation was initiated by the addition of the aggregated GFP to the final concentration of 0.5 µM. The fluorescent signal from the reactivated GFP was detected using Beckman Coulter DTX 880 Plate Reader. IC50 was calculated by fitting the *[Inhibitor] versus response model* to the data from three experiments using the GraphPrism Software.

7.5.3 Luciferase reactivation assay

Luciferase (Promega) at the concentration of 29.8 µM was chemically denatured in a buffer with high concentration of urea (25 mM HEPES-KOH pH 8.0, 75 mM

KCl, 15 mM MgCl2, 6M Urea) and incubated at 25 °C for 15 minutes. Next, it was transferred to 48 °C for 10 minutes incubation, subsequently diluted 25-fold into the HKM buffer (25 mM HEPES-KOH pH 8.0, 75 mM KCl, 15 mM $MgCl_2$) and incubated at 25 °C for 15 minutes. The reactivation was initiated by the addition of luciferase aggregates to the final concentration of 0.2 μM to the mixture of chaperones, which were utilized at 1 μM concentration for yeast Hsp70 system, except for Sse1 used at 0.1 μM, unless it was notated otherwise. In the case of human Hsc70 system, chaperone concentrations were used as follows: 3 μM Hsc70, 1 μM DNAJA2, 1 μM DNAJB4 and 0.1 μM Hsp105, unless stated otherwise. Reactions were performed at 25 °C. At indicated time points, aliquots of refolding reactions were diluted in Luciferase Assay Kit (Promega) and measured using Sirius Luminometer (Berthold).

7.5.4 Luminescence assay of luciferase folding

Luciferase (Promega) at concentration of 10 μM was denatured in 5 M GuHCl and 10 mM DTT 25 °C for 1 hour. Subsequently, luciferase was diluted 100-fold into the folding buffer (25 mM Hepes-KOH pH 7.5, 100 mM KCl, 10 mM $Mg(OAc)_2$, 2 mM DTT, 0.05% T20) to initiate spontaneous folding. Buffer for assisted folding contained chaperones used at 1 μM concentration, unless indicated otherwise. Reactions were performed at 25 °C. At indicated time points, aliquots of folding reactions were diluted in Luciferase Assay Kit (Promega) and measured using Sirius Luminometer (Berthold).

7.5.5 Fluorescence microscopy

Fluc-EGFP (1.3 mg/ml) was chemically denatured in a buffer with high concentration of urea (25 mM HEPES-KOH pH 8.0, 75 mM KCl, 15 mM $MgCl_2$, 6M Urea) and incubated at 25 °C for 15 minutes. Next, it was transferred to 48 °C for 10 minutes incubation, followed by the ten-fold dilution in the HKM buffer (25 mM HEPES-KOH pH 8.0, 75 mM KCl, 15 mM $MgCl_2$, 5 mM ATP, 1 mM DTT) and 15 minutes incubation at 25 °C. The reaction was initiated by the addition of the Fluc-EGFP aggregates to the final concentration of 0.3 μM. Chaperones were used at 1 μM concentration, except for Sse1, which was used at 0.1 μM. After one hour incubation, the reaction was arrested by the addition of 200 mM NaCl and transferred on ice. Specimens were imaged using a confocal laser scanning microscope Leica SP8X with a 100x oil immersion lens (Leica, Germany). Results

are shown as average from three independent experiments, where each sample within the repeat was photographed ten times. Calculations of the aggregate size were performed manually using Leica LAS X software.

7.5.6 DLS measurements

Luciferase (23.7 μM) was chemically denatured in a buffer with high concentration of urea (25 mM HEPES-KOH pH 8.0, 75 mM KCl, 15 mM $MgCl_2$, 6M Urea) and incubated at 25 °C for 15 minutes. Next, it was transferred to 48 °C for 10 minutes incubation, followed by the ten-fold dilution (25 mM HEPES-KOH pH 8.0, 75 mM KCl, 15 mM $MgCl_2$, 5 mM ATP, 1 mM DTT) and 10 minutes incubation at 25 °C. To assess the formation of the aggregates, the mixture of luciferase aggregates at 0.6 μM was subjected to Dynamic Light Scattering (DLS) measurement, confirming aggregate size ranging from 1000 to 3000 nm. The chaperone mix was then introduced at the concentration of 1 μM, except for Sse1, which was used at 0.1 μM, initiating the reaction. DLS measurements were performed using ZetaSizer NanoS instrument (Malvern) after one hour incubation. Each sample was measured three times independently at 25 °C, and particle size distributions were calculated as percentages within a range from 0.4 to 10,000 nm. The results are presented as the average diameter with the standard deviation (SD).

7.5.7 Western blot

In order to evaluate the amount of the chaperones interacting with aggregates, prior to dissociation step biosensor was immersed in the Laemmli buffer (4% SDS, 20% glycerol, 10% β-mercaptoethanol, 0.004% bromophenol blue, 125 mM Tris-HCl, pH 6.8) supplemented with 50 mM EDTA and incubated at 100 °C for 15 minutes. Samples prepared in this manner were subjected to electrophoresis under denaturing conditions using SDS-PAGE and subsequently transferred onto a membrane, following the standard protocol for Western blot analysis. Rabbit anti-sera selective for Ssa1 and Sse1, were employed as primary antibodies, diluted at ratios of 1:500 and 1:20 000 respectively. For the detection, HRP (horse radish peroxidase)-conjugated anti-rabbit antibodies were used as the secondary antibodies at dilution of 1:25 000. The visualization of the blots was achieved using SuperSignal West Pico Chemiluminescent Substrate (ThermoFisher Scientific). Subsequent scanning and imaging of the blots were conducted with ChemiDoc MP Imaging System (Bio-Rad).

8. Results

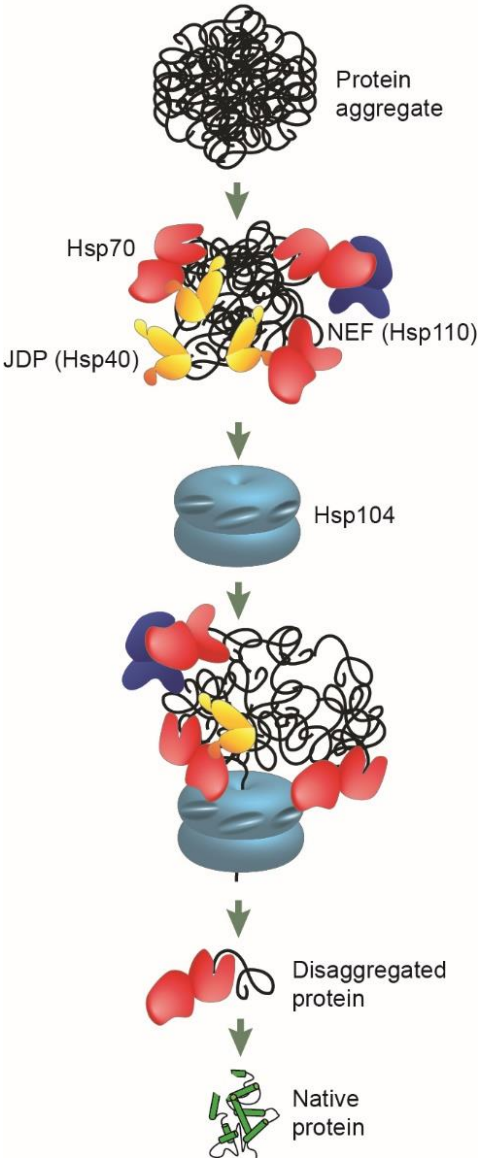

In yeast, the disaggregation machinery comprises Hsp70, J-domain protein, nucleotide exchange factor and disaggregase belonging to Hsp100 family (Fig. 10). Latest studies from our laboratory, which I took part in, showed that the yeast chaperone system exhibits a distinct mechanism regarding handling of protein aggregates by Hsp70 (Ssa1), when paired with either class A (Ydj1) or class B (Sis1) JDPs (Wyszkowski *et al*, 2021). Taking it into consideration, I wanted to shed more light on the interplay between Hsp110 (NEF), Hsp70 and JDPs in the recovery of proteins from aggregates. By using biochemical tools, I studied the role of Sse1, the major cytosolic NEF in yeast belonging to Hsp110 family, at individual stages of protein disaggregation in the context of class A or class B JDPs.

Figure 10. ***Chaperone activity in protein disaggregation.*** *Protein aggregate is first recognized and processed by the Hsp70 system comprising Hsp70 (red), JDP (yellow) and Hsp110 (blue). Hsp70 also facilitates the recruitment of Hsp104, which, in collaboration with the Hsp70 system, disentangles trapped polypeptides. Once released, the unfolded polypeptides are folded into the native state.*

Most of the data presented in this chapter was published in the reviewed preprint: "Balanced Interplay Between Hsp110, Hsp70 and Class B J-Domain Protein Improves Aggregate Disassembly" (Sztangierska W, Wyszkowski H, Pokornowska M, Rychłowski M, Liberek K, Kłosowska A. Balanced Interplay Between Hsp110, Hsp70 and Class B J-Domain Protein Improves Aggregate Disassembly. (2024). eLife doi: 10.7554/eLife.94795.1).

8.1 Sse1 differently modulates Hsp70-dependent disaggregation, when paired with different JDP classes

I started by analyzing the influence of Sse1 on the recovery of a model substrate, luciferase, from aggregates by the Hsp70 system with Ydj1 or Sis1. We previously showed that Ssa1-Sis1 exhibits delayed start of protein substrates recovery, but its disaggregation activity is more effective comparing to Ssa1-Ydj1, by which substrate recovery is fast, but the final yield is lower (Wyszkowski *et al*, 2021). When I included Sse1, luciferase recovery by Ssa1-Sis1 was significantly accelerated, however the overall output of the disaggregation was only slightly increased. Unlike with Sis1, Sse1 slightly inhibited luciferase recovery by Ssa1-Ydj1 (Fig. 11).

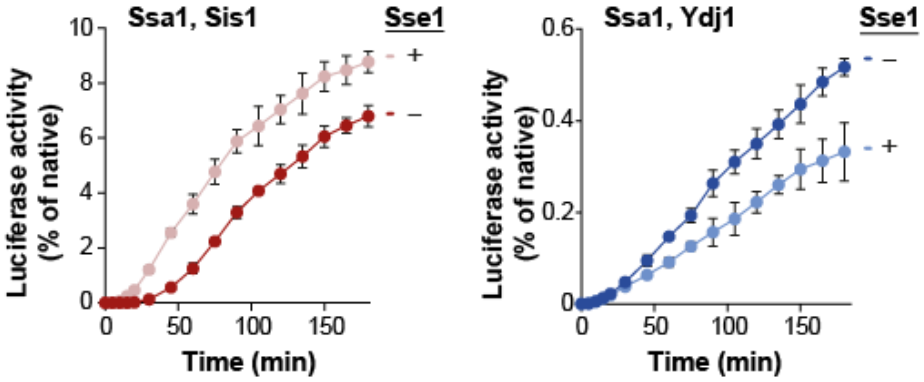

Figure 11. ***Sse1 enhances recovery of luciferase aggregates by Hsp70 system specifically with class B JDPs.*** *Recovery of aggregated luciferase by Ssa1-Sis1 +/- Sse1 (left) or Ssa1-Ydj1 +/- Sse1 (right). Luciferase activity was normalized to the native luciferase measured in the same concentration. Error bars show SD from three independent repeats. Chaperones were used at 1 μM concentration, except for Sse1, which was used at 0.1 μM.*

When I added the Hsp104 disaggregase to the previously analyzed chaperone systems, the reactivation of luciferase was even more pronounced for Ssa1-Sis1-Sse1, reaching almost 100% of the native, non-aggregated control (Fig. 12).

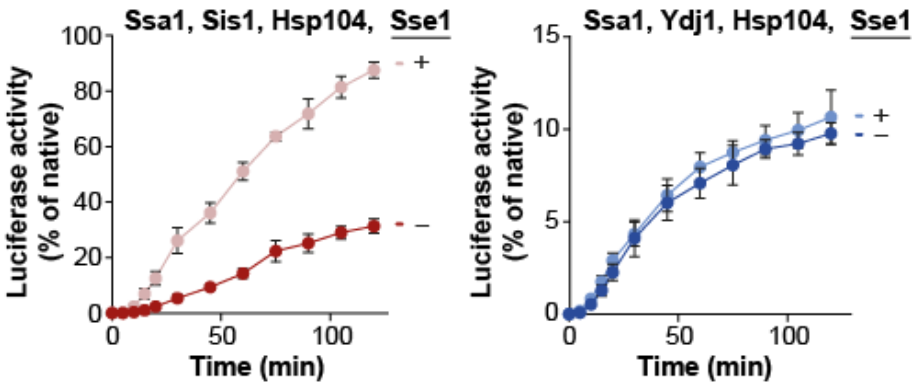

Figure 12. ***Sse1-dependent stimulation of the disaggregation activity by Hsp70-Hsp100 depends on the employed class of JDPs.*** *Recovery of aggregated luciferase by Ssa1-Sis1 +/- Sse1 (left) or Ssa1-Ydj1 +/- Sse1 (right) in the presence of Hsp104. Chaperones were used at 1 μM concentration, except for Sse1, which was used at 0.1 μM. Luciferase activity was normalized to the native luciferase measured in the same concentration. Error bars show SD from three independent repeats.*

To verify if the observed effects of Sse1 are not only specific for luciferase, I utilized a different protein substrate, aggregated green fluorescent protein (GFP).

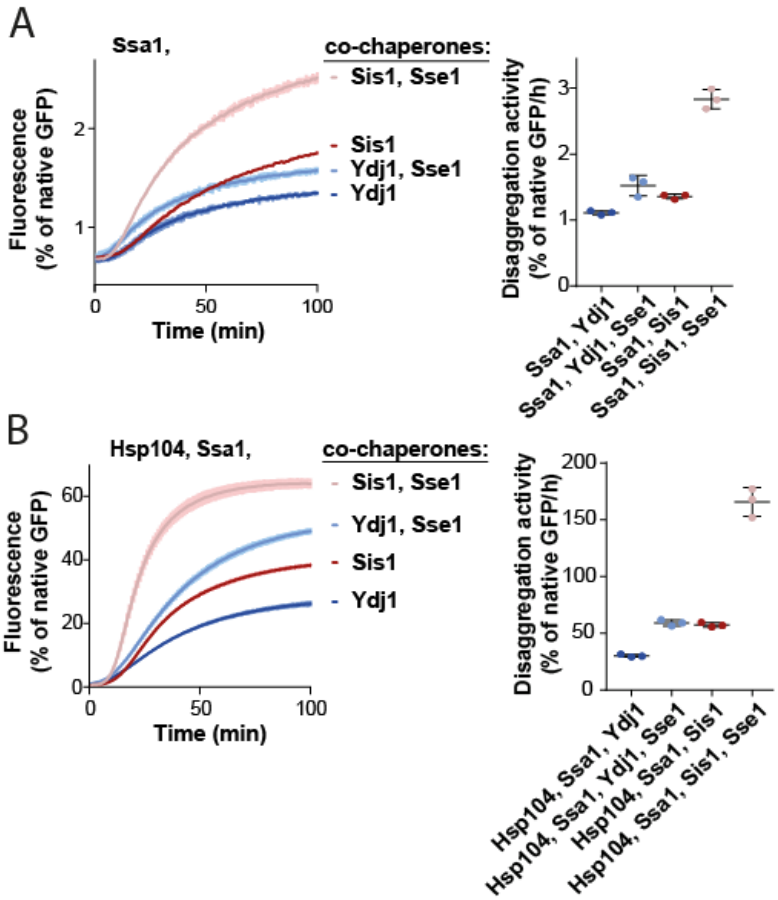

Figure 13. ***Effects of Sse1 on disaggregation by Hsp70 is not substrate-specific.*** *(A) Renaturation of heat-aggregated GFP by Ssa1-Sis1 +/- 0.1 μM Sse1 or Ssa1-Ydj1 +/- 0.1 μM Sse1 without (A) or with Hsp104 (B) GFP fluorescence was normalized to the fluorescence of native GFP in the same concentration. Bolded lines are the average of three replicates while the shades regions indicate standard deviation. Chaperones were used at 1 μM concentration, except for Sse1, which was used at 0.1 μM.*

Sse1 stimulated the disaggregation activity of both Hsp70 systems, namely Ssa1-Sis1 or Ssa1-Ydj1, nonetheless the GFP recovery rates by Ssa1-Sis1 was 2-fold higher with Sse1, whereas Ssa1-Ydj1 was only slightly stimulated (Fig. 13A). When I included Hsp104, the disaggregation rate by Ssa1-Sis1 increased 3-fold with Sse1, whereas for Ssa1-Ydj1-Sse1, the disaggregation activity was twice as high as for the Hsp70 system without the NEF (Fig. 13B).

My results indicate that the Sse1-assisted disaggregation of protein aggregates is more pronounced with class B JDP.

8.2 Positive contribution of Sse1 occurs during initial stages of protein disaggregation

Different stimulation of the recovery of proteins from aggregates by Sse1, depending on whether Hsp70 is coupled with either class A or class B JDP, could be an outcome of its divergent impact on different stages of protein recovery from aggregates, starting from the recruitment of chaperones to the aggregates, the disentanglement of polypeptides from the aggregates and ending with the final folding of the substrate. During my master thesis project, I focused on investigating the role of the bacterial NEF from *E. coli*, GrpE, in protein disaggregation, since its role, apart from stimulating the ATPase cycle of Hsp70, was a matter of a debate. My results showed that luciferase translocated by the bacterial disaggregase is incompletely folded and only the presence of GrpE mediated the folding of the released luciferase into native conformation, vital to attain its activity (unpublished results). These observations emphasize the essential role of GrpE at the latter step of protein disaggregation, namely the final folding of proteins downstream of disaggregase. Based on these results, I hypothesized that Sse1 might contribute to the folding of protein substrates similarly as bacterial GrpE. To verify this, I denatured luciferase to acquire protein substrate that would mimic the unfolded polypeptides of the latter step of protein disaggregation. According to the previous reports, it is possible to obtain misfolded, non-aggregated luciferase by incubating it at low concentration with 5 M guanidinium hydrochloride, followed by a dilution into a buffer without the denaturant (Imamoglu *et al*, 2020). In agreement with the previously published results, Ydj1-Ssa1 was superior in refolding of misfolded luciferase compared to

Sis1-Ssa1 (Lu & Cyr, 1998). Nevertheless neither Ssa1-Ydj1 nor Ssa1-Sis1 were stimulated by Sse1, indicating that the yeast Hsp110 does not contribute to the final folding (Fig. 14). My results suggest that Sse1 is not required at the last phase of protein disaggregation and rather acts at its early stages.

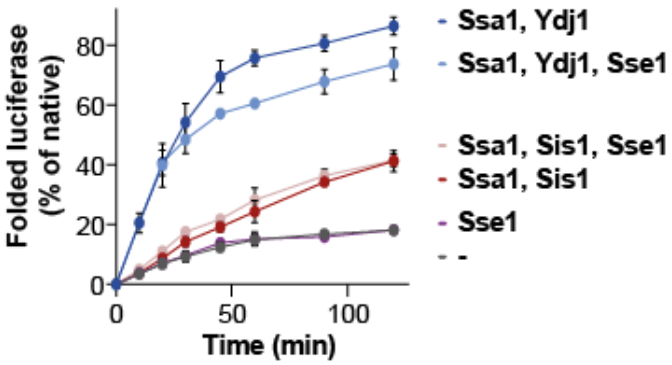

Figure 14. ***Sse1 does not contribute to the final folding of the unfolded non-aggregated luciferase.*** *Spontaneous folding of non-aggregated luciferase diluted from 5 M GuHCl alone or assisted by Hsp70 system. Chaperones were used at 1 μM concentration, except for Sse1, which was used at 0.1 μM. Luciferase activity was normalized to the native luciferase measured in the same concentration. Error bars show SD from three independent repeats.*

Knowing that, I proceeded with addressing the question of how Sse1 might impact the initial stages of protein disaggregation. Therefore, I used a real-time approach based on biolayer interferometry (BLI) to assess the impact of Sse1 on the association of chaperones to the aggregates. BLI is an optical technique based on the analysis of the interference pattern of white light reflected from two surfaces: the inner reference layer and the layer of immobilized proteins on the biosensor. Such analysis allows to determine the thickness of proteins bound to the biosensor. In my experiments, I immobilized luciferase aggregates on a Ni-NTA biosensor, which allowed me to analyze the assembly of the chaperone complex at the aggregate (Chamera *et al*, 2019). Consistent with our previously published results, Ssa1-Sis1 showed delayed binding reaching approximately 3-fold higher level of binding (~6 nm) in comparison to Ssa1-Ydj1, whose binding was rapid, albeit less efficient (~2 nm) (Fig. 15) (Wyszkowski *et al*, 2021). In the case of Ssa1-Sis1, the presence of Sse1 significantly accelerated the initial association and generated biolayer thickness of approximately 9 nm. This is in contrast to Ssa1-Ydj1, binding of which was unaffected by Sse1, albeit the initial phase was marginally improved. Binding of the Hsp70 systems (Ssa1-Sis1 and

Ssa1-Ydj1) to the aggregates required ATP, which is in accordance with the ATP-dependance of Hsp70 (Szabo *et al*, 1994) (Fig. 15).

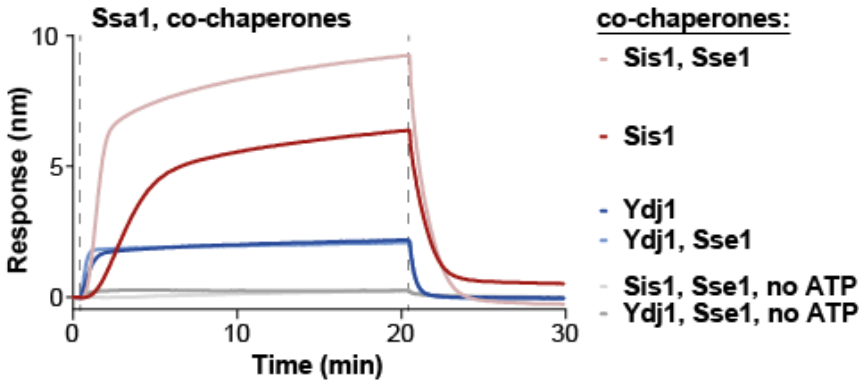

Figure 15. ***Impact of Sse1 on binding of Hsp70 system to luciferase aggregates.*** *Luciferase aggregates immobilized on the biosensor were incubated with Ssa1-Sis1 +/- Sse1 or Ssa1-Ydj1 +/- Sse1, with or without ATP. First dashed line indicates the moment, when chaperones were introduced. Second dashed line indicates the start of the dissociation step. Chaperones were used at 1 µM concentration, except for Sse1, which was used at 0.1 µM.*

To exclude the possibility that the observed effects of Sse1 on the assembly of disaggregation complexes to luciferase aggregates are substrate-specific, I additionally performed binding experiments with immobilized GFP aggregates and aggregated yeast lysate proteins on biosensors. The presence of Sse1 substantially accelerated the binding of Ssa1-Sis1 to the aggregated surface of both protein substrates. These results indicate that the observed effects of Sse1 on the binding of the Hsp70 system to aggregates are not limited to luciferase (Fig. 16A,B).

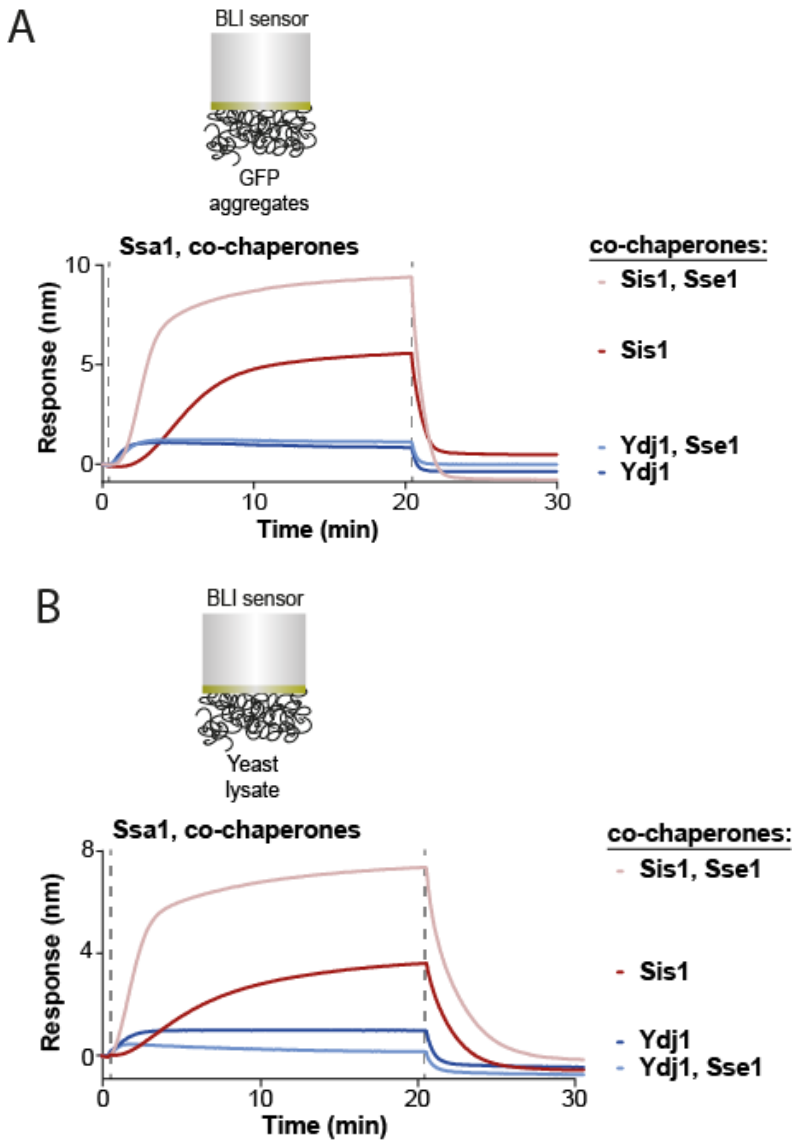

Figure 16. ***Effects of Sse1 on assembly of Hsp70 system with aggregate is not limited to luciferase.*** *(A) Sensor-bound GFP aggregates or (B) heat-aggregated yeast lysate proteins were incubated with Ssa1-Sis1 +/- Sse1 or Ssa1-Ydj1 +/- Sse1. Chaperones were used at 1 μM concentration, except for Sse1, which was used at 0.1 μM.*

Taken together, my results suggest that Sse1 plays a major role at the initial stages of protein disaggregation, exerting beneficial impact on Hsp70 binding to the aggregates, particularly when a JDP from class B is involved.

8.3 Hsp110 is required for more pronounced recruitment of Hsp70

Differential biolayer thicknesses might vary in the composition of the chaperones within the disaggregation complex. Since Sse1 is a 110-kDa protein, the significantly enhanced level of binding in the case of Ssa1-Sis1-Sse1, despite the low concentration of the applied Sse1, might be associated with the bulkiness of

this protein. To assess this, I used Western Blot to analyze the interacting Ssa1 and Sse1 with the sensor-bound luciferase aggregates. After the association of the chaperones, I removed the sensor and proceeded with the Western blot analysis. The results showed that the amount of Sse1 is minor in comparison to Ssa1, whose amount diverge between Hsp70 system comprising Sis1 or Ydj1 (Fig. 17).

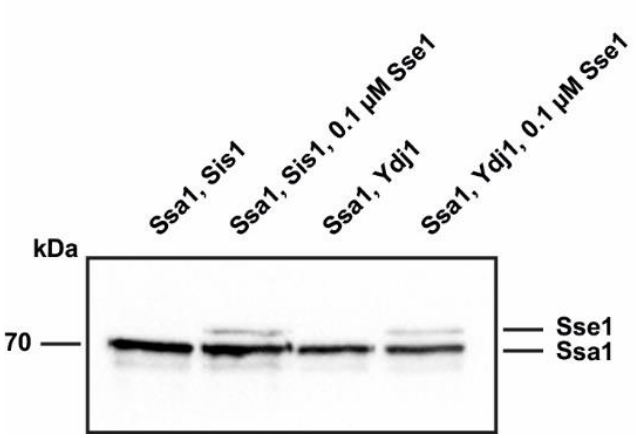

Figure 17. ***Contribution of Sse1 to the chaperon layer on the aggregated surface is minimal.*** *Western blot analysis of the amount of Sse1 and Ssa1 bound to the immobilized luciferase aggregates on the BLI sensor incubated with Ssa1-Sis1 +/- Sse1 or Ssa1-Ydj1 +/- Sse1. Chaperones were used at 1 µM concentration, except for Sse1, which was used at 0.1 µM.*

Since Western Blot analysis showed limitations in precisely quantifying the amount of interacting Ssa1 with luciferase aggregates immobilized on the biosensor, I employed fluorescently labelled Hsp70 in order to evaluate whether higher level of binding in the case of Ssa1-Sis1 with Sse1 might be associated with more abundant binding of Ssa1 to the aggregated surface. To address this, I performed BLI experiments in the same manner as previously described (Fig. 15), yet I utilized fluorescent Ssa1(Ssa1*A488) (Fig. 18A). Following the dissociation of the proteins from luciferase aggregates immobilized on the biosensor, I measured fluorescence of the released Ssa1*A488 (Fig. 18B). The beneficial impact of Sse1 was limited to class B JDP and resulted in 50% higher fluorescence signal corresponding to the amount of Ssa1*A488, comparing to Ssa1*A488 when only Sis1 was present. The amount Ssa1*A488 interacting with luciferase aggregates was lower in the case of Ydj1 and remained unchanged in the presence of Sse1 (Fig. 18B).

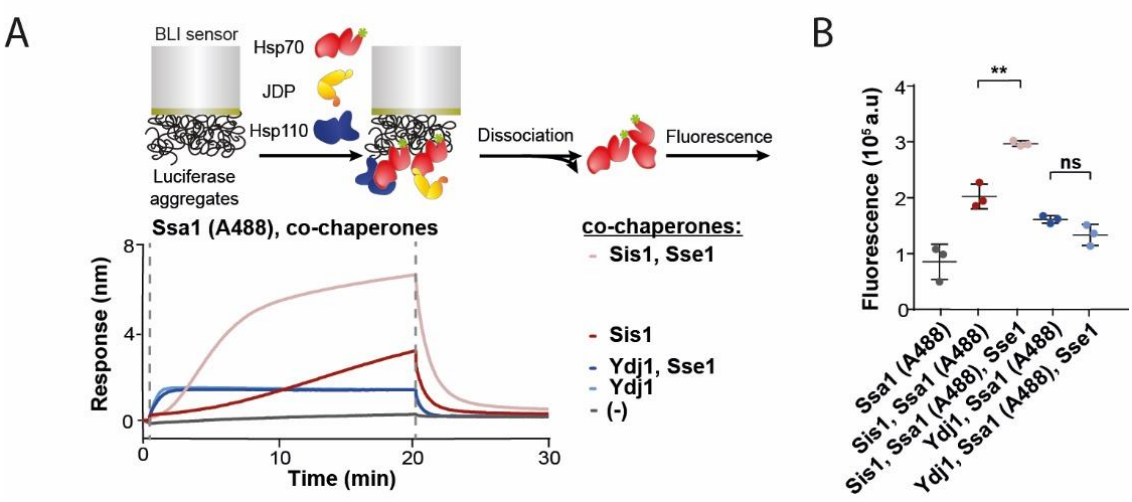

Figure 18. ***Sse1 promotes more abundant binding of Hsp70 to the aggregated surface, when paired with class B JDP.*** *(A) Upper panel shows the scheme of the BLI experiment. Sensor covered with luciferase aggregates was incubated with Ssa1 labelled with Alexa 488 fluorophore (A488*) coupled with either Sis1 or Ydj1 in the presence or absence of Sse1. Chaperones were used at 1 μM concentration, except for Sse1, which was used at 0.1 μM. (B) Fluorescence signal of the released Ssa1 (A488*), measured after the dissociation step.*

My results show that the improved disaggregation efficacy by Sse1 in the case of the Hsp70 system comprising Ssa1-Sis1 is accomplished by augmented loading of Hsp70 on aggregate.

Presumably, in the case of Ssa1-Sis1 alone, 1 μM of Ssa1 might be insufficient in processing the aggregates and reaching high level of binding. Assuming that Ssa1 is a limiting factor, I was curious whether it is possible to obtain similar effect as for Ssa1-Sis1-Sse1 only by increasing the pool of available Ssa1. However, even the saturating concentration of Ssa1 of 5 μM was not enough to observe comparable binding to the one prompted by Sse1 (Fig. 19).

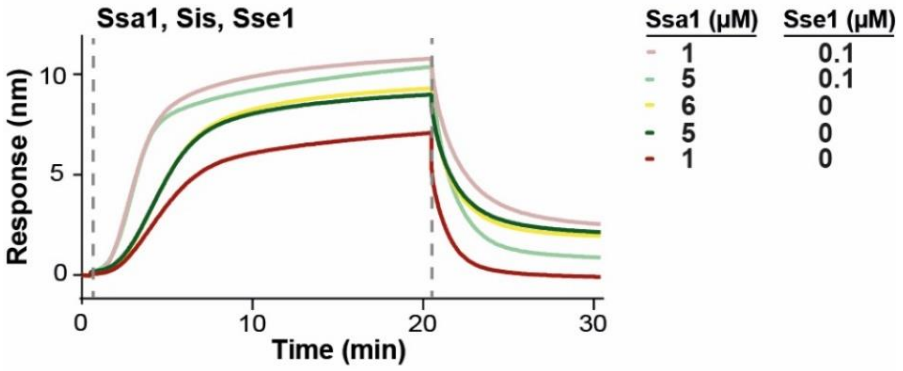

Figure 19. ***Increasing Hsp70 level is not sufficient to reach the same binding level of Hsp70 system as with Sse1.*** *Sensor-bound luciferase aggregates incubated with constant concentration of Sis1 and different concentrations of Ssa1 +/- Sse1. Sis1 was used at 1 μM, and Ssa1 and Sse1 were used at the indicated concentrations.*

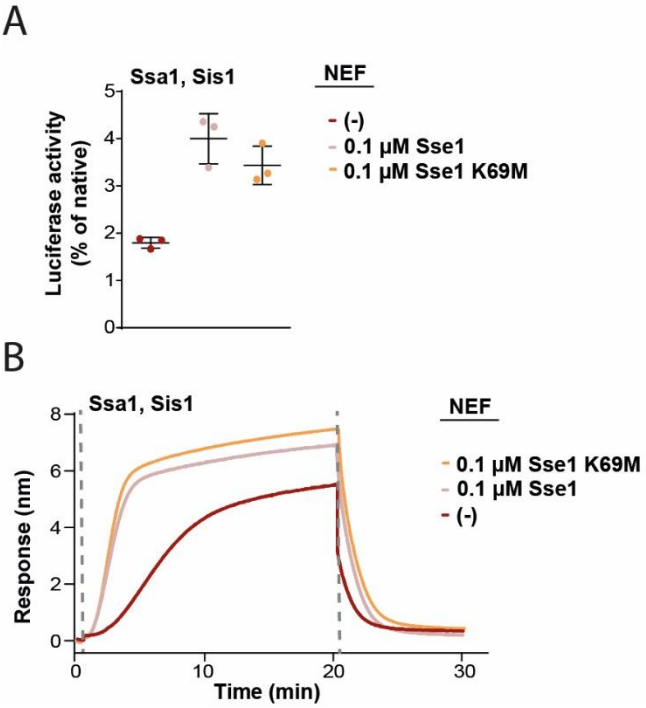

Figure 20. ***ATPase activity of Sse1 is dispensable for stimulating disaggregation activity by Hsp70 system.*** *(A) Refolding of luciferase aggregates measured after 1h incubation with Ssa1-Sis1 +/- Sse1 or Sse1 variant with the point mutation in the ATPase domain (K69M) (B) Binding of Ssa1-Sis1 +/- Sse1 or Sse1 variant to the luciferase aggregates immobilized on the biosensor. Chaperones were used at 1 μM concentration, except for Sse1 and its variant, which were used at indicated concentrations.*

It seems that the stimulation by Sse1 follows a more complex mechanism than increasing the pool of Hsp70 molecules capable of aggregate binding, yet the question is whether this mechanism of action is driven by the specific features of Sse1? Previously published reports addressed the question, whether Sse1 can hydrolyze ATP, which was proposed to be facilitated by specific J-domain proteins (Raviol *et al*, 2006a; Mattoo *et al*, 2013). This aspect is still unclear and it cannot be excluded that Hsp110 might improve refolding of protein substrates by serving independently of Hsp70 via its intrinsic ATPase activity. In order to investigate if the intrinsic ability of Sse1 to hydrolyze ATP is crucial in stimulating the binding of the Hsp70 system to an aggregate, I introduced the well-established ATP-hydrolysis defective variant of Sse1 K69M (Shaner *et al*, 2004). Both the disaggregation activity and the level of binding to luciferase aggregates exhibited by Ssa1-Sis1 were stimulated in the same manner as by the wild type Sse1 (Fig. 20A,B).

My results indicate that the intrinsic ATPase activity is dispensable for positive contribution of Sse1 to the disaggregation activity of the Hsp70 system.

Another distinctive trait of Sse1, which should be taken into consideration, is its capability of substrate binding. I decided to utilize NEF from another family, Fes1, belonging to the Armadillo type, which lacks the ability to interact with protein substrates. Fes1 possesses four armadillo repeats and a release-domain, though it regulates the ATPase cycle of Hsp70 differently than Hsp110 (Gowda *et al*, 2018). I performed disaggregation of luciferase aggregates as well as a BLI

experiment with luciferase aggregates and observed that Fes1 improved both disaggregation and Ssa1-Sis1 binding to the aggregates similarly as Sse1, however 1 μM concentration was necessary to observe the stimulation (Fig. 21A,B). These results suggest that the substrate-binding activity specific for Sse1 is not critical for the stimulation of binding and disassembly of protein aggregates by the Hsp70 system. At this point, a question arises, why higher concentration of Fes1 is required to achieve similar effects to Sse1. Since it was reported that Fes1 has lower ability to exchange nucleotide in comparison to Sse1, higher concentration might be necessary to attain similar outcome (Dragovic *et al*, 2006).

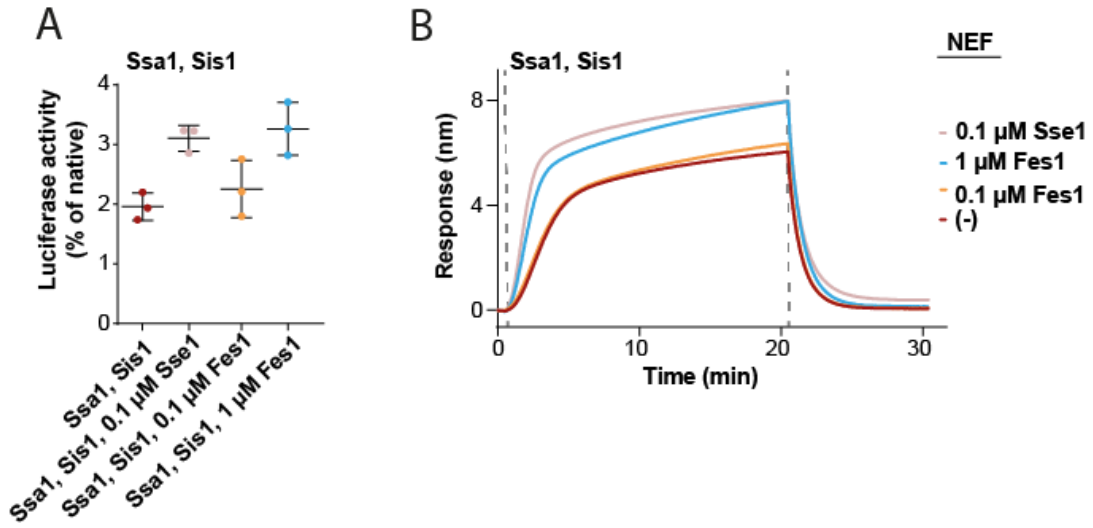

Figure 21. ***Fes1 stimulates refolding of proteins from aggregates by Hsp70 system.*** *(A) Recovery of luciferase aggregates by Ssa1-Sis1 in the presence of Sse1 or Fes1. Luciferase activity was measured after 1h incubation. (B) Binding of Ssa1-Sis1 in the presence of indicated NEF with luciferase aggregates immobilized on the biosensor. Chaperones were used at 1 μM concentration, except for Sse1 and Fes1, which were used at indicated concentrations.*

To evaluate the contribution of Fes1 to the extra chaperone layer in terms of the amount of Ssa1 bound to the aggregate, I employed previously described BLI experiment, based on the fluorescence measurement of the dissociated Ssa1 labelled with Alexa488. I observed that 1 μM concentration of Fes1 increased the amount of Ssa1*A488 present at the aggregate surface in a similar compared to Sse1 present at 0.1 μM concentration (Fig. 22).

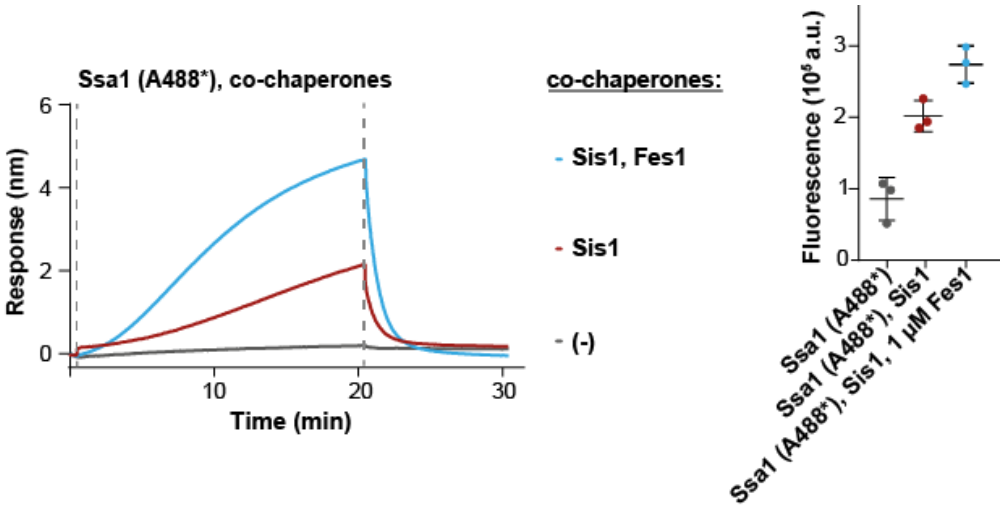

Figure 22. ***Fes1 increases the amount of Hsp70 interacting with an aggregate.*** *The sensor-covered luciferase aggregates were incubated with Ssa1 labelled with Alexa488 and Sis1 in the presence of Fes1, followed by fluorescence measurement after the dissociation step. Binding kinetics together with fluorescence of Ssa1 (A488*) and Sis-Ssa1 (A488*) was adapted from Fig. 18. Chaperones were used at 1 μM concentration.*

Summarizing, ATP hydrolysis and substrate-binding ability unique for Sse1 is not required for the stimulation of the Hsp70-dependent disaggregation, since Fes1 enhances disaggregation by the Hsp70 system, despite the lack of the ability to bind substrates.

8.4 Sse1 promotes modification of aggregates by Hsp70

In our previously published paper, we showed that Sis1 promoted more abundant loading of Hsp70 onto an aggregated substrate, leading to a modification of the aggregate, which we refer to as aggregate remodeling, ultimately resulting in enhanced disaggregation efficacy (Wyszkowski *et al*, 2021). To explore whether Sse1 stimulates remodeling activity of Hsp70 system, I used Hsp104 variant (Hsp104 D484K F508A) as a tool to probe for extra binding sites that can be used by the variant to recognize, disentangle and refold aggregated polypeptide in an Hsp70-independent manner.

Both mutations of the Hsp104 variant are located in the M-domain of the Hsp104 variant, where D484K disrupts an internal interaction, making the protein derepressed and hyperactive, without the need of activation by Hsp70 (Lipińska *et al*, 2013) and F508A restricts Hsp104 from binding to Hsp70 (Chamera *et al*, 2019). Combined mutations generate a hyperactive Hsp104 variant, whose activity is independent of Hsp70. The idea was that if the preliminary processing

of aggregates by Hsp70 system with Sse1 would favor aggregate remodeling activity, it would elevate the disaggregation capacity of the Hsp104 D484K F508A variant.

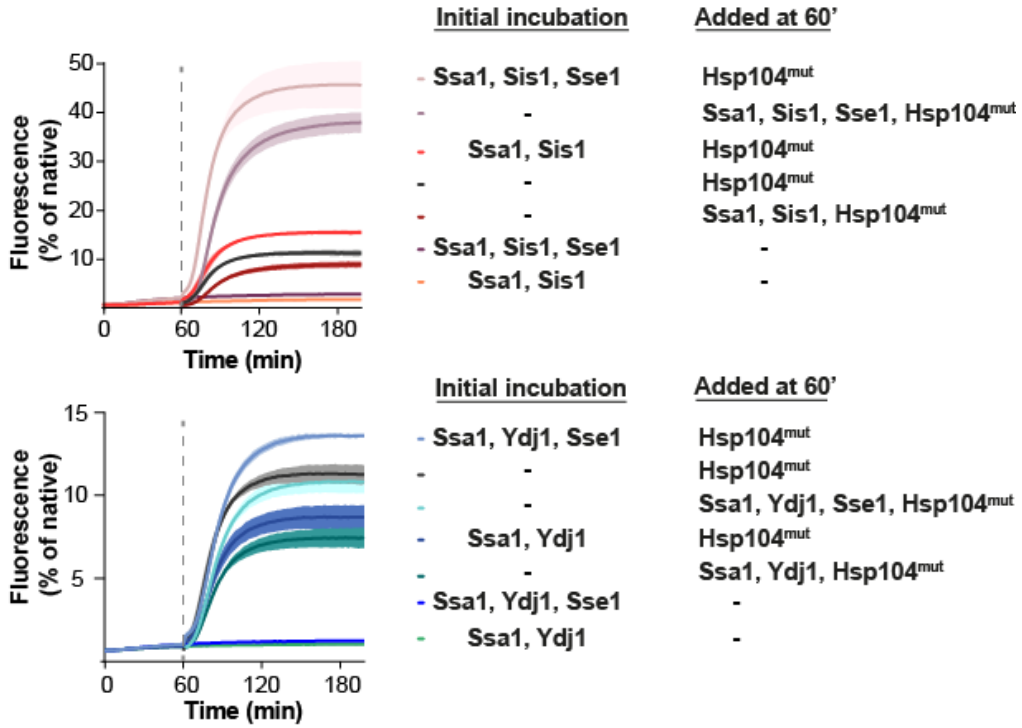

Figure 23. ***Initial incubation of aggregates with Hsp70 system improves disaggregation by Hsp104 D484K F508A.*** *GFP aggregates were initially incubated with Hsp70 system comprising the indicated chaperones, followed by the addition of the hyperactive Hsp104 variant (indicated with Hsp104^{mut}). Dashed lines present the end of the initial incubation and the addition of the Hsp104 D484K F508A variant. Chaperones were used at 1 μM concentration, except for Sse1 and Hsp104 variant, which were used at 0.1 μM and 0.15 μM, respectively. The experiment was performed by dr Agnieszka Kłosowska.*

Firstly, GFP aggregates were incubated with the Hsp70 system for 60' and subsequently the Hsp104 variant was added, with continuous fluorescence measurement. When GFP aggregates were incubated with Ssa1-Sis1, the yield of GFP recovery was minor, but it increased in the presence of the Hsp104 variant up to ~ 10% of the native GFP (Fig. 23). An even higher reactivation level was observed, when the initial incubation with Ssa1-Sis1 was included prior to the addition of the Hsp104 variant, reaching ~ 15% of the native GFP. Addition of Sse1 generated higher level of GFP recovery compared to Ssa1-Sis1 alone. Particularly, when GFP aggregates were subjected to an initial incubation with Ssa1-Sis1-Sse1, the addition of the Hsp104 variant yielded reactivation to ~ 50% of native GFP. This level of recovery was not attainable when Ssa1-Sis1-Sse1 were simultaneously added with the Hsp104 variant, yielding ~ 40% of native

GFP (Fig. 23). In the case of Ydj1, reactivation of GFP both alone and with the Hsp104 variant moderately increased in the presence of Sse1, regardless the initial incubation with Ssa1-Ydj1 or Ssa1-Ydj1-Sse1 (Fig. 23).

The Sse1-induced aggregate remodeling could have many positive consequences, such as disentanglement of polypeptides or global rearrangements, which might change properties of the aggregated substrates. Thus, I aimed to explore whether the enhanced remodeling activity by Sse1 might be manifested in the change of the size of the aggregates.

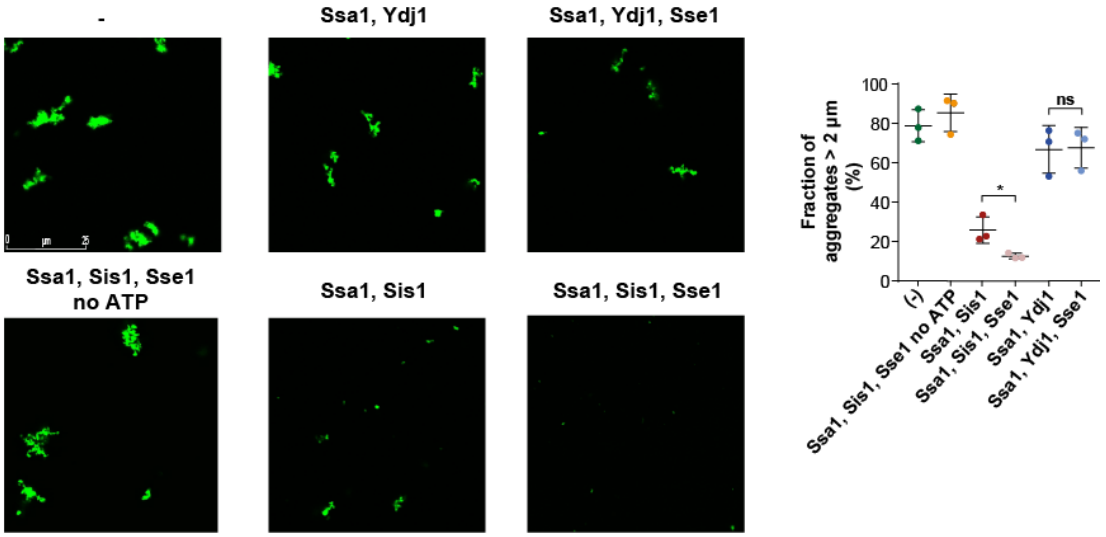

Figure 24. ***Sse1 causes major reduction in the size of the aggregates specifically with class B JDPs.*** *Images captured by fluorescence microscopy illustrate heat-aggregated luciferase fused with GFP, incubated with Hsp70 system in the presence of Sse1. Left panels shows the control of the luciferase-GFP aggregates alone and incubated with the Hsp70 system in the absence of ATP. Chaperones were used at 1 µM concentration, except for Sse1, which was used at 0.1 µM. Quantification of the fraction of aggregates > 2 µm is from three independent replicates. Two-tailed t test was performed: *p < 0.05, ns: not significant.*

To examine this, I used luciferase C-terminally fused with GFP, which I thermally denatured. Due to the high thermal stability of GFP, I was able to visualize luciferase aggregates on account of GFP fluorescence. I observed differences in the size of the aggregates upon incubation with the Hsp70 system comprising class A or class B JDP using confocal microscopy. Quantification showed that after thermal inactivation, approximately 80% of aggregates were larger than 2 µm. Incubation with Ssa1-Sis1 declined fraction of aggregates > 2 µm to 25.8%, whereas Sse1 substantially enhanced the observed effect, resulting in only 12.5% of aggregates > 2 µm (Fig. 24). The presence of ATP was essential for the decrease in the aggregate size. Incubation of Luc-GFP aggregates with

Ydj1-Ssa1 only slightly affected the aggregates, regardless the presence of Sse1, with nearly 70% of aggregates remaining larger than 2 μm after the incubation with the chaperones (Fig. 24).

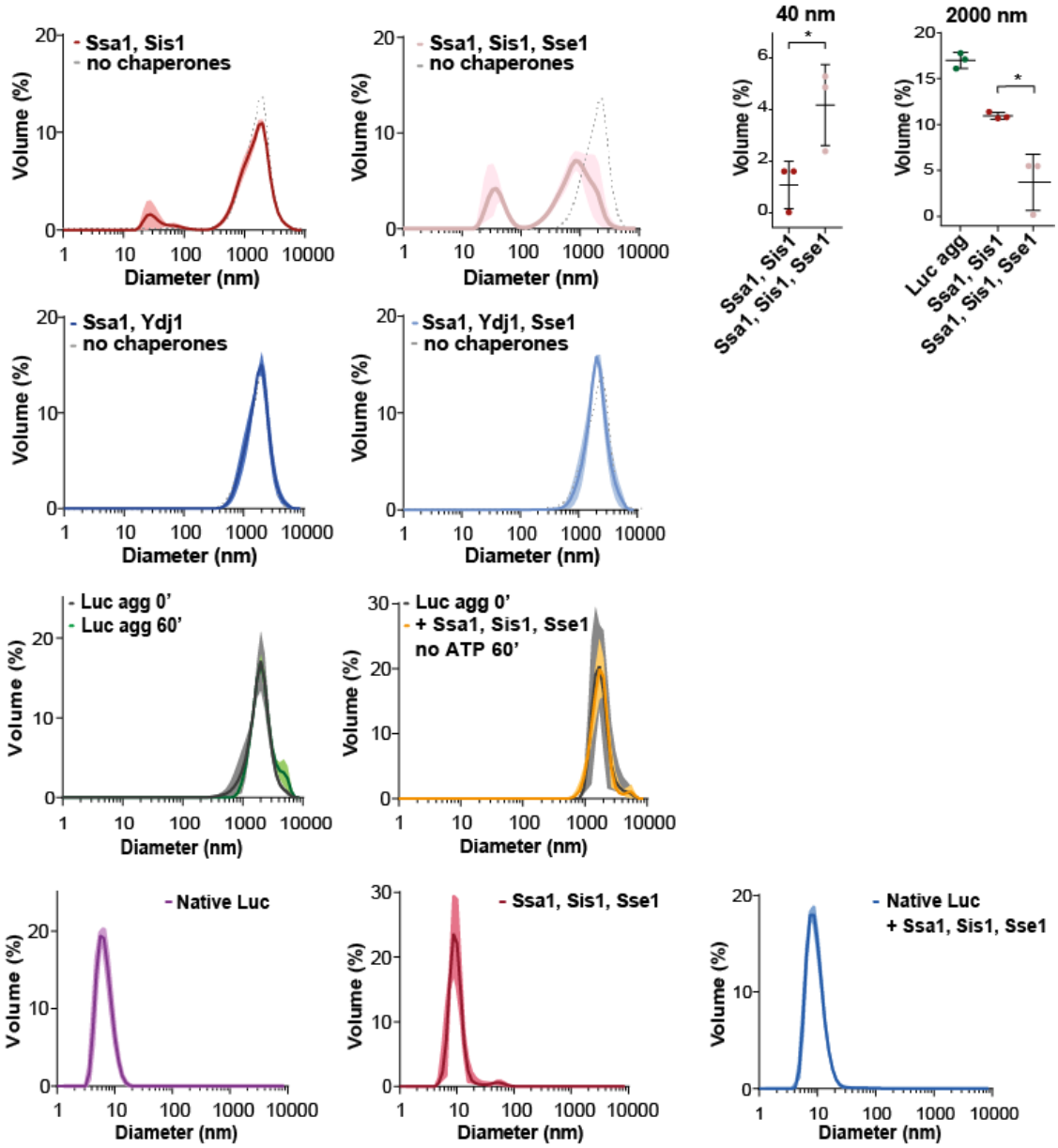

Figure25. ***Modification of aggregates mediated by Sse1 occurs, when paired with class B JDP.*** *The size distribution of luciferase aggregates was analyzed using dynamic light scattering. This included luciferase aggregates alone or incubated with Ssa1-Sis1 or Ssa1-Ydj1, with or without the addition of Sse1, as detailed in the figure. The measurements were taken after an incubation period of 1 hour and in the presence of ATP, unless otherwise specified. Additional experiments assessed the diameter of native luciferase, chaperones alone, and chaperones with native luciferase, as shown in the lower sections of the figure.* Chaperones were used at 1 μM concentration, except for Sse1, which was used at 0.1 μM. *Bolded lines are the average of three replicates while the shades indicate standard deviation. Dashed lines designate the size distribution of the samples prior to the incubations. Bottom panel shows the height of the peak at 40 nm or 2000 nm for Ssa1-Sis1 with or without Sse1, analyzed with the two-tailed t test: *p < 0,05, **p < 0,01 using the GraphPrism Software*.

I also used another experimental technique, dynamic light scattering (DLS) to analyze changes in the size of the aggregates induced by the Hsp70 system. This method is used to measure the hydrodynamic diameter of the dispersed particles based on their velocity due to Brownian motions. Peak of approximately 2000 nm corresponded to aggregated luciferase, while the DLS signal of approximately 10 nm was generated by native luciferase and chaperones alone, as well as both mixed together (Fig. 25). Incubation with Ssa1-Sis1 diminished the peak at 2000 nm and an additional peak appeared corresponding to the aggregates, whose diameter ranges between 30 and 100 nm (Fig. 25). The presence of Sse1 significantly reduced the dominant peak at 2000 nm and increased the amount of small aggregates 2-fold (Fig. 25). With regard to Ssa1-Ydj1, luciferase aggregates did not encounter any size changes irrespective of Sse1. Similarly to the previous experiment, changes in the size of the aggregates upon the addition of chaperones were not observed unless ATP was present (Fig. 25).

To sum up, my results show that Sse1 augments the remodeling activity of the Hsp70 system specifically with class B JDPs, causing major changes in the morphology of the aggregates and emergence of small aggregate species.

8.5 The interaction between C-terminal domain of Sis1 and EEVD motif of Hsp70 is essential for stimulation by Sse1

The major question arising from my results is what determines the disparate impact of Sse1 on the Hsp70-dependent disaggregation with either class A or class B JDPs? Each of the class of JDPs display divergent binding with Hsp70. The EEVD motif of Hsp70, which is dispensable for class A JDPs, is obligatory for the collaboration with class B (Yu *et al*, 2015; Faust *et al*, 2020). However, when the interaction between a class B JDP and Hsp70 is abolished through the deletion of the EEVD motif in Hsp70, it can be partially restored by perturbing the interactions that restrain the J-domain from NBD binding e.g. through the E50A mutation in Sis1 (Yu *et al*, 2015). In agreement with our previously published results, the binding pattern of Sis1 E50A-Ssa1 ΔEEVD to luciferase aggregates resembled the one of Ssa1-Ydj1 (Wyszkowski *et al*, 2021). An addition of Sse1

decreased both the level of binding and the disaggregation activity of Sis1 E50A-Ssa1 ΔEEVD (Fig. 26A,B).

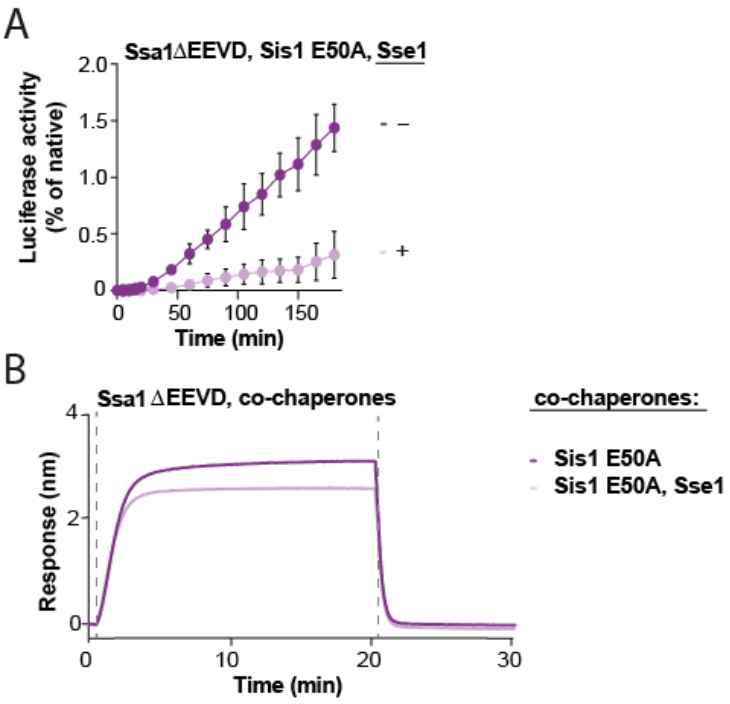

Figure 26. ***The additional interface between Sis1 (CTD1) – Ssa1 (EEVD) is essential for Sse1-based stimulation.*** *(A) The recovery of the luciferase aggregates and BLI experiments (B) were carried out with the indicated variants of Hsp70/JDP in the presence of Sse1. Chaperones were used at 1 μM concentration, except for Sse1, which was used at 0.1 μM.*

Thus, the auxiliary, class B-specific binding of Sis1 CTD1 with the EEVD motif of Ssa1 is a key feature in the Sse1-dependent stimulation.

8.6 Susceptibility of Hsp70 system to high concentrations of Sse1 depends on JDP class

My results show that the degree of stimulation by Sse1 is determined by the class of JDP. It is known from the literature that the impact of Sse1 is concentration-dependent, with optimal efficacy at sub-stoichiometric ratio relative to Hsp70 (Dragovic *et al*, 2006; Polier *et al*, 2008). In the context of my results, I wanted to know, to what extent the optimal concentration of Sse1 differs when class A or class B JDPs are involved. I employed several biochemical assays to explore the contribution of Sse1 at individual stages of protein disaggregation across its different concentrations.

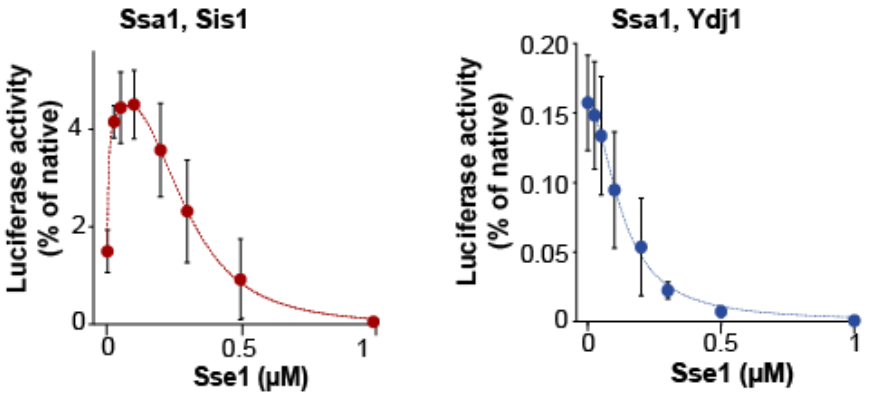

Figure 27. ***Distinct susceptibility of the Hsp70 system to the excess of Sse1, when paired with either class A or class B JDPs.*** *Titration of Sse1 in the recovery of the luciferase aggregates by the Hsp70 system. Luciferase activity was measured after 1h of incubation and normalized to the activity of native luciferase. Chaperones were used at 1 μM concentration, except for Sse1, which was used at the indicated concentrations.*

Firstly, I titrated Sse1 in the reactivation of luciferase aggregates and observed that Ssa1-Sis1 was still stimulated by Sse1 at 0.3 μM concentration (1 : 0.3; Ssa1 : Sse1 molar ratio), however no positive effect was observed for Ssa1-Ydj1, even at molar ratio of Ssa1 : Sse1 more permissive than 1 : 0.1 (Fig. 27).

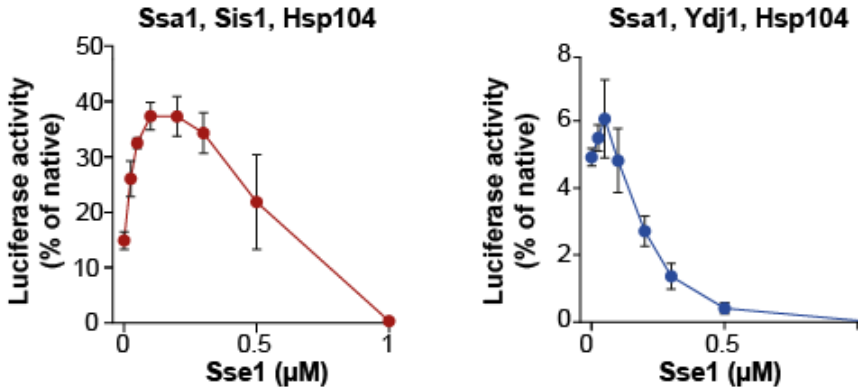

Figure 28. ***Presence of Hsp104 shifts the optimum of Sse1 in protein disaggregation by the Hsp70 system.*** *The titration of Sse1 in the disaggregation of the luciferase aggregates experiment was performed in the presence of Hsp104. Luciferase activity was measured after 1h incubation and normalized to the activity of native luciferase. Chaperones were used at 1 μM concentration, except for Sse1, which was used at the indicated concentrations.*

The dose-response relationship was also observed when I added Hsp104 to the Hsp70 system, however the optimal concentration of Sse1 for the disaggregation activity was shifted, with no inhibition at 0.5 μM concentration (1 : 0.5; Ssa1 : Sse1 molar ratio) for Hsp104-Ssa1-Sis1 and slight stimulation for Hsp104-Ssa1-Ydj1 at low Ssa1 : Sse1 molar ratio, with highest efficacy at 0.05 μM Sse1 concentration (Fig. 28).

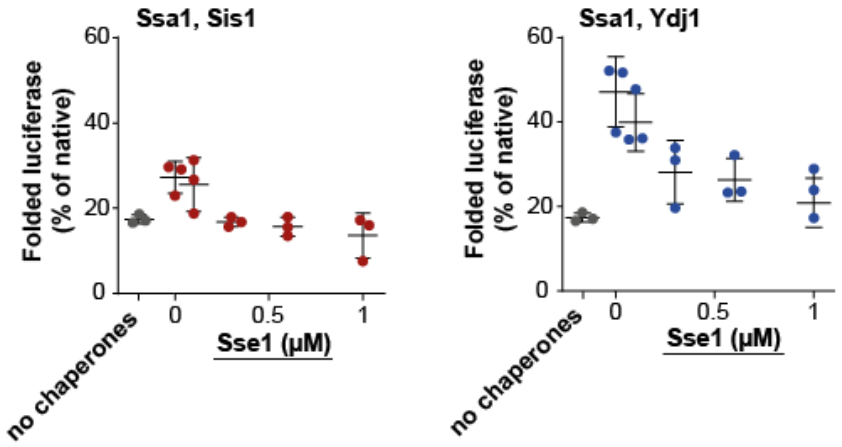

Figure 29. ***Excess of Sse1 negatively influences the folding of non-aggregated luciferase.*** *Spontaneous folding of luciferase incubated in 5 M GuHCl was measured after 3 h incubation upon the addition of the indicated chaperones with increasing concentration of Sse1. Chaperones were used at 1 μM concentration, except for Sse1, which was used at indicated concentrations.*

Knowing from the previous experiments that the relevance of Sse1 at individual stages of protein disaggregation might vary, I performed folding experiments with non-aggregated luciferase by the Hsp70 system across different Sse1 concentrations. In contrast to the reactivation of aggregated luciferase, Sse1 hampered the folding activity of Ssa1-Sis1 and Ydj1-Ssa1 across a full range of investigated concentrations (Fig. 29).

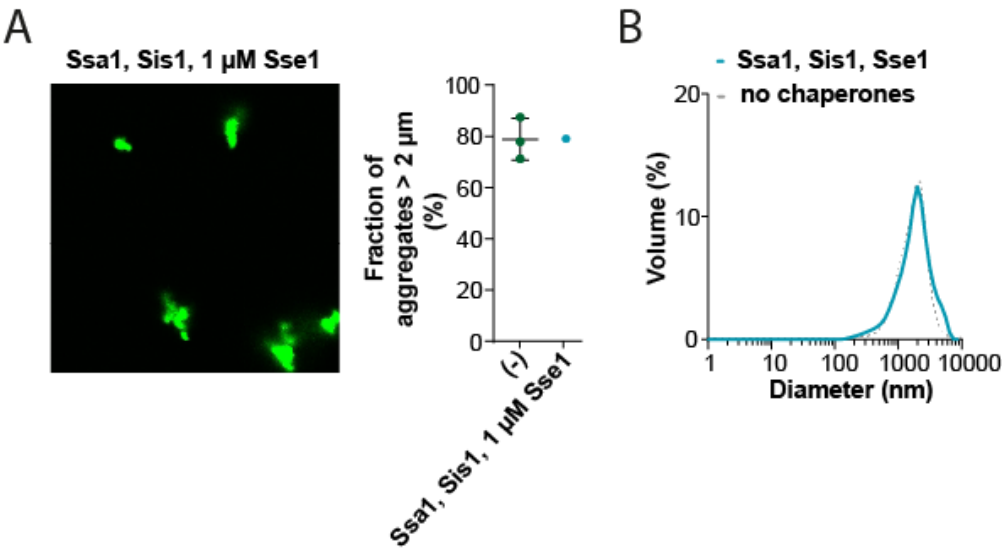

Figure 30. ***Equimolar concentration of Sse1 to Hsp70 does not induce aggregate remodeling.*** *Changes in the size of Luc-GFP aggregates incubated for 1h with Ssa1-Sis1 in the presence of 1 μM Sse1 monitored by fluorescence microscopy and DLS. Chaperones were used at 1 μM concentration.*

I was wondering whether it is possible that the inhibitory impact of 1 μM Sse1 on the final folding resulting in hardly any disaggregation activity displayed by

Ssa1-Sis1, could mask the positive effect on the aggregate remodeling activity. I employed DLS together with fluorescence microscopy to analyze, whether any changes in the size of the aggregates are induced by 1 μM Sse1, despite no apparent disaggregation activity.

I observed no alterations in the size of the aggregates after the incubation with Ssa1-Sis1 in the presence of 1 μM Sse1 (Fig. 30 A,B).

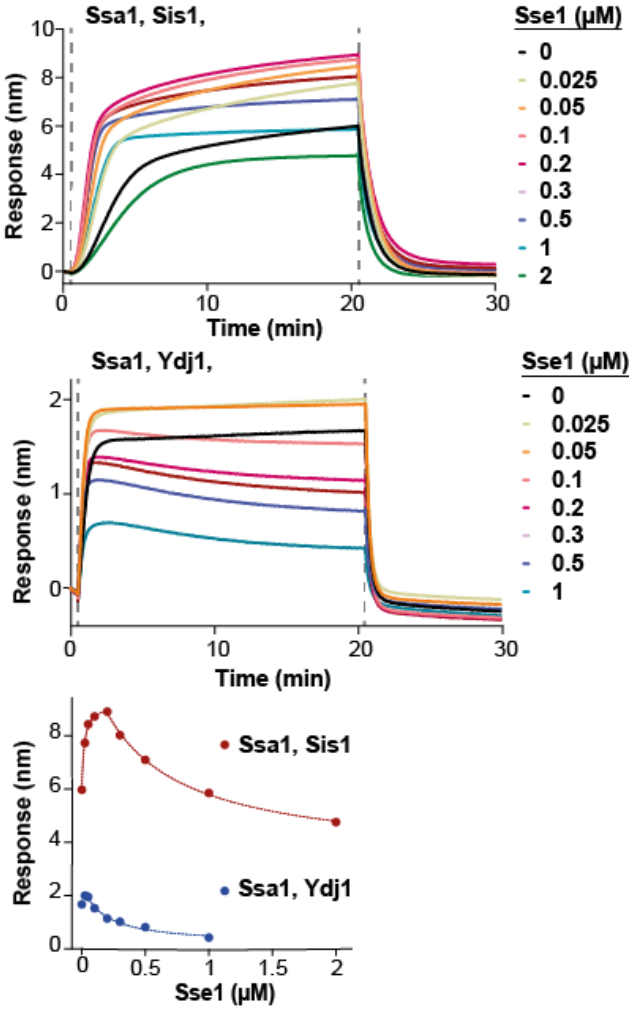

Figure 31. ***Different optimum for Sse1 in the binding of Hsp70 system to aggregate in case of class A or class B JDPs.*** *Binding of Ssa1-Sis1 or Ssa1-Ydj1 to luciferase aggregates immobilized on the BLI sensor across a range of Sse1 concentrations. Bottom panel shows a plot of the binding signal prior to the dissociation step of Ssa1-Sis1 (red) or Ssa1-Ydj1 (blue), at increasing concentrations of Sse1. Chaperones were used at 1 μM concentration, except for Sse1, which was used at the indicated concentrations.*

Consistently, negative effect of 1 μM Sse1 on the remodeling activity of the Hsp70 system comprising Sis1 was reflected in its limited positive impact on the association of the Hsp70 system to the aggregate (Fig. 31).

Binding of the Hsp70 systems with Sis1 and Ydj1 to luciferase aggregates immobilized on the BLI sensor was differently affected by increasing level of Sse1, where maximum level of binding was observed at 0.2 μM and 0.05 μM Sse1 concentrations for Ssa1-Sis1 and Ydj1-Ssa1, respectively (Fig. 31).

To conclude, Sse1 demonstrates a biphasic impact on the Hsp70 disaggregation activity, where its contribution depends not only on the class of JDP, but also vary at different stages of protein disaggregation, where optimal concentration of Sse1 is shifted to higher levels during the initial phase (aggregate binding) and when Hsp104 is present.

8.7 Affinity of Sse1 to Ssa1 determines the efficacy of Hsp70-dependent disaggregation

I wanted to focus more on the mechanism behind the biphasic effect of Sse1. The inhibition by excessive Sse1 might occur through binding to the substrate in a way it restricts it from binding to Ssa1 or it could be directly associated with Sse1 binding to Ssa1. To investigate the second possibility, I introduced a well-described Sse1-2 variant (N575Y N575A) with abolished interaction with the A300 residue of Ssa1. The Sse1 variant exhibits reduced Hsp70 binding to 20% and is almost inactive in exchanging the nucleotide (Polier *et al*, 2008).

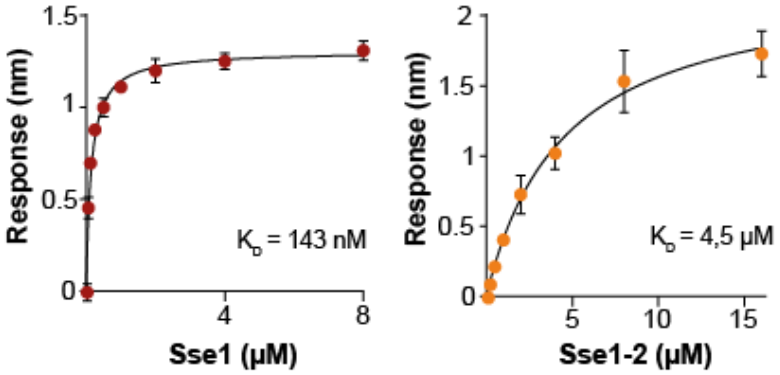

Figure 32. ***Sse1-2 variant exhibits decreased affinity for Ssa1.*** *Dissociation constant is determined based on the level of Ssa1 binding to Sse1 or Sse1-2. Sse1 was immobilized on the BLI sensor through His6-SUMO tag and Ssa1 was used at concentrations: 16, 8, 4, 2, 1, 0.5, 0.25, 0.125, 0.063 and 0.032 μM. Points indicate mean with SD from three independent experiments. The One site – specific binding model was fitted to the data with the GraphPrism software.*

I wanted to characterize the association between Ssa1 and Sse1 or Sse1-2 variant. In order to determine the affinity between these proteins, I employed BLI technique, in which I immobilized Sse1 or Sse1-2 directly to the biosensor through the His-tag and titrated Ssa1 to further calculate the KD. The limited Sse1-2 binding to Ssa1 diminished the affinity for Ssa1 approximately 30-fold compared to Sse1 wild type (Fig. 32).

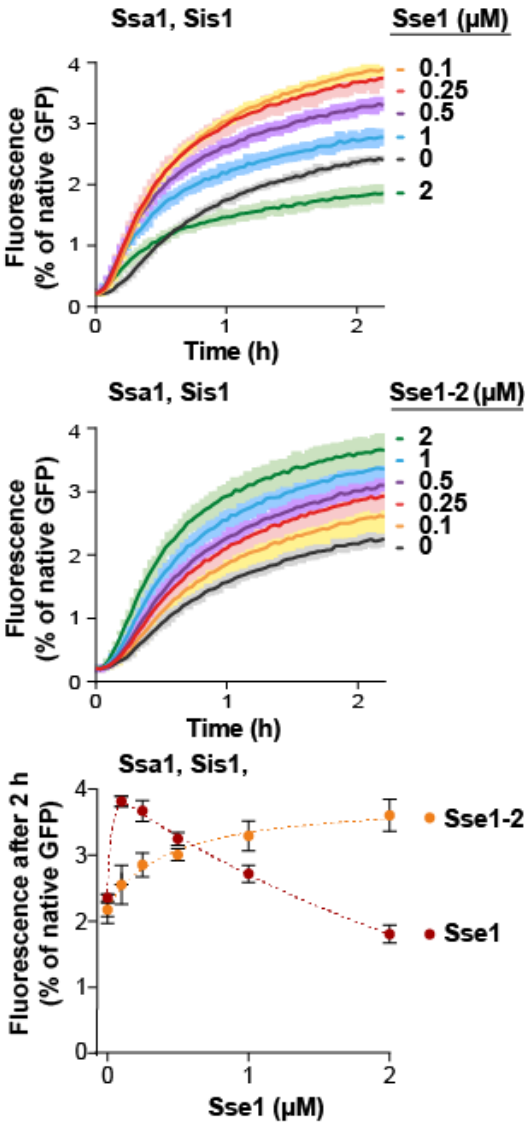

Figure 33. ***Susceptibility of Hsp70 to Sse1 is inversely correlated with strength of Sse1-Hsp70 interaction.*** *Renaturation of heat-aggregated GFP by Ssa1-Sis1 in the presence of increasing concentration of Sse1 or Sse1-2 variant. Bottom panel demonstrates the comparison of the disaggregation activity of Ssa1-Sis1 after 2 h incubation with Sse1 (red) or Sse1-2 (orange). Chaperones were used at 1 μM concentration, except for Sse1 and Sse1-2, which were used at the indicated concentrations. Dashed lines show fitting of the [Agonist] versus response model to the data from three experiments using the GraphPrism Software. The experiment was performed by dr Agnieszka Kłosowska.*

In consistence with the lower Sse1-2 binding affinity for Ssa1, when I incubated GFP aggregates, the most effective recovery level by Ssa1-Sis1 with 0.1 μM Sse1 could be achieved only when 2 μM of Sse1-2 was present (Fig. 33). When luciferase aggregates were used as a substrate, the beneficial influence of Sse1-2 on the disaggregation by Ssa1-Sis1 was moderate, where 10-fold higher concentration of Sse1-2 was most efficient, nevertheless the efficacy did not reach the level supported in the presence of Sse1 wild type (Fig. 34A). At the same time, 1 μM concentration of Sse1-2 accelerated the initial kinetics of Ssa1-Sis1 binding to the luciferase aggregates and reached the same level of binding compared, as when paired with 0.1 μM Sse1 (Fig. 34B).

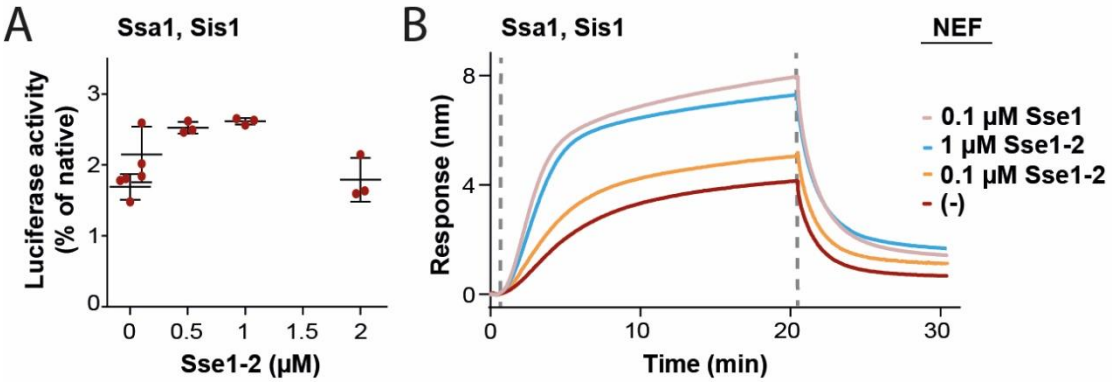

Figure 34. ***Impact of Sse1-2 variant on disaggregation activity and binding capacity by Hsp70 system.*** *(A) Luciferase reactivation upon addition of Ssa1-Sis1 with Sse1-2 at indicated concentrations measured after 1h incubation. (B) BLI sensor with immobilized luciferase aggregates was incubated with Ssa1-Sis1 in the presence of varying concentrations of Sse1 or Sse1-2. Chaperones were used at 1 μM concentration, except for Sse1 and Sse1-2, which were used at the indicated concentrations.*

This suggest that the high affinity of Sse1 for Ssa1 enables strong stimulation of Hsp70-dependant disaggregation at very low concentrations of Sse1, however by exceeding the optimal concentrations, Sse1 negatively affects the recovery of the aggregated substrates, emphasizing the crucial role of Sse1 affinity for Ssa1 in regulating Hsp70 activity.

8.8 Competition between Sse1 and Sis1 for binding to Ssa1

It seems that the most apparent explanation for the inhibitory effect of the excessive amount of Sse1 hinges on the elevated dissociation of Ssa1 from a substrate, which hinders protein disaggregation. However, no noticeable inhibition of GFP recovery by Ssa1-Sis1 was observed in the presence of 2 μM Sse1-2, even though it was reported that at this concentration, Sse1-2 exhibits the ability to exchange nucleotide in Hsp70 similar as the wild type (Polier *et al*, 2008). I suspected that an additional inhibitory mechanism might occur specifically with class B JDPs. Knowing that Ssa1 forms complex with Sis1 prior to the assembly to the aggregated substrate (Wyszkowski *et al*, 2021), I reasoned that Sse1 could have an influence on it.

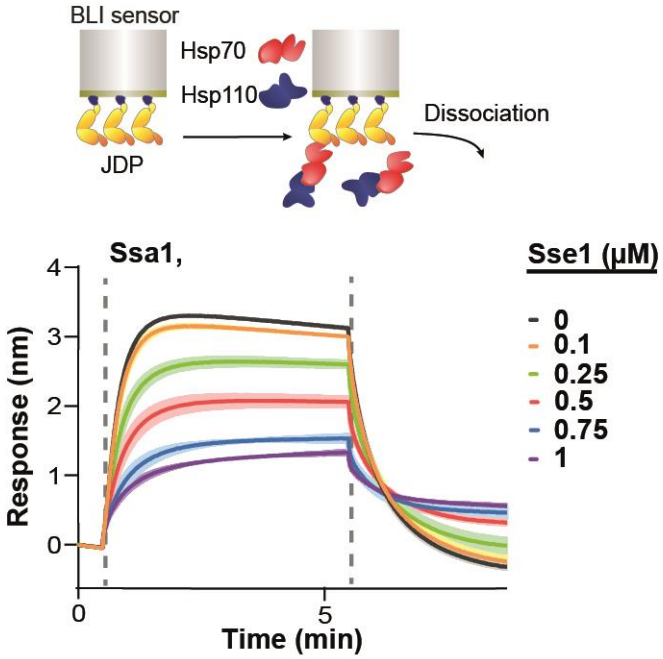

Figure 35. ***Sse1 prevents Ssa1 from binding to Sis1.*** *Upper panel shows the scheme of the BLI experiment. Sis1 was immobilized through the His6–SUMO tag and incubated with 1 μM Ssa1 in the presence of increasing concentration of Sse1. Lines are the average of three replicates and the shades designate standard deviation. Dashed lines indicate addition of chaperones to sensor-bound Sis1 and dissociation step.*

In order to investigate that, I immobilized N-terminally His_6-tagged Sis1 on the biosensor and analyzed binding of Ssa1 under increasing concentrations of Sse1. The binding of Ssa1 gradually decreased across concentration range of Sse1, reaching 40% of Ssa1 binding alone in the presence of 1 μM Sse1 (Fig. 35).

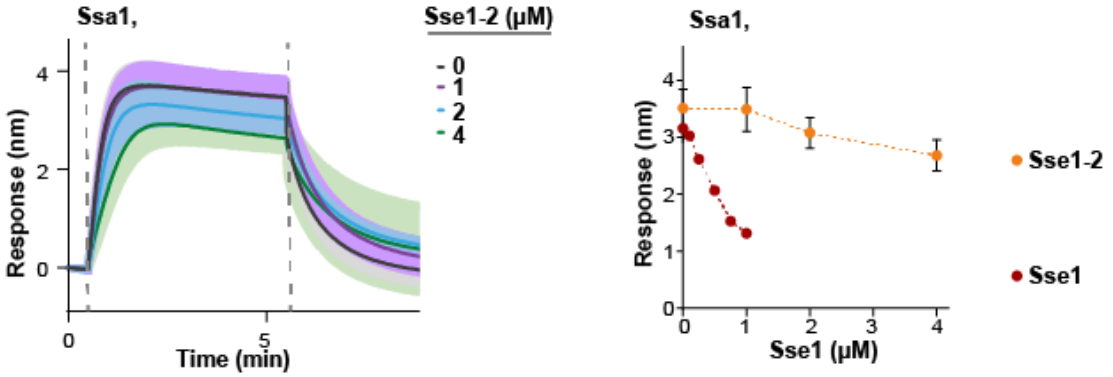

Figure 36. ***Reduced affinity of Sse1-2 generates milder effect on Ssa1 binding to Sis1****. Binding of 1 μM Ssa1 to the immobilized Sis1 on the BLI sensor in the presence of changing concentration of Sse1-2. Right panel: a comparison of the binding signal prior to the dissociation step in the presence of the indicated concentrations of Sse1 or Sse1-2 is presented. The binding signal of Ssa1-Sse1 WT was adapted from Fig. 35.*

When I performed an analogous experiment, but instead used Sse1-2, the binding between Ssa1 and Sis1 was moderately diminished under the elevated level of Sse1-2, in agreement with the reduced affinity of Sse1-2 for Ssa1. Even 4 μM Sse1-2 disrupted the Ssa1-Sis1 complex formation to a lesser extent in comparison to the 1 μM of wild type Sse1 (Fig. 36).

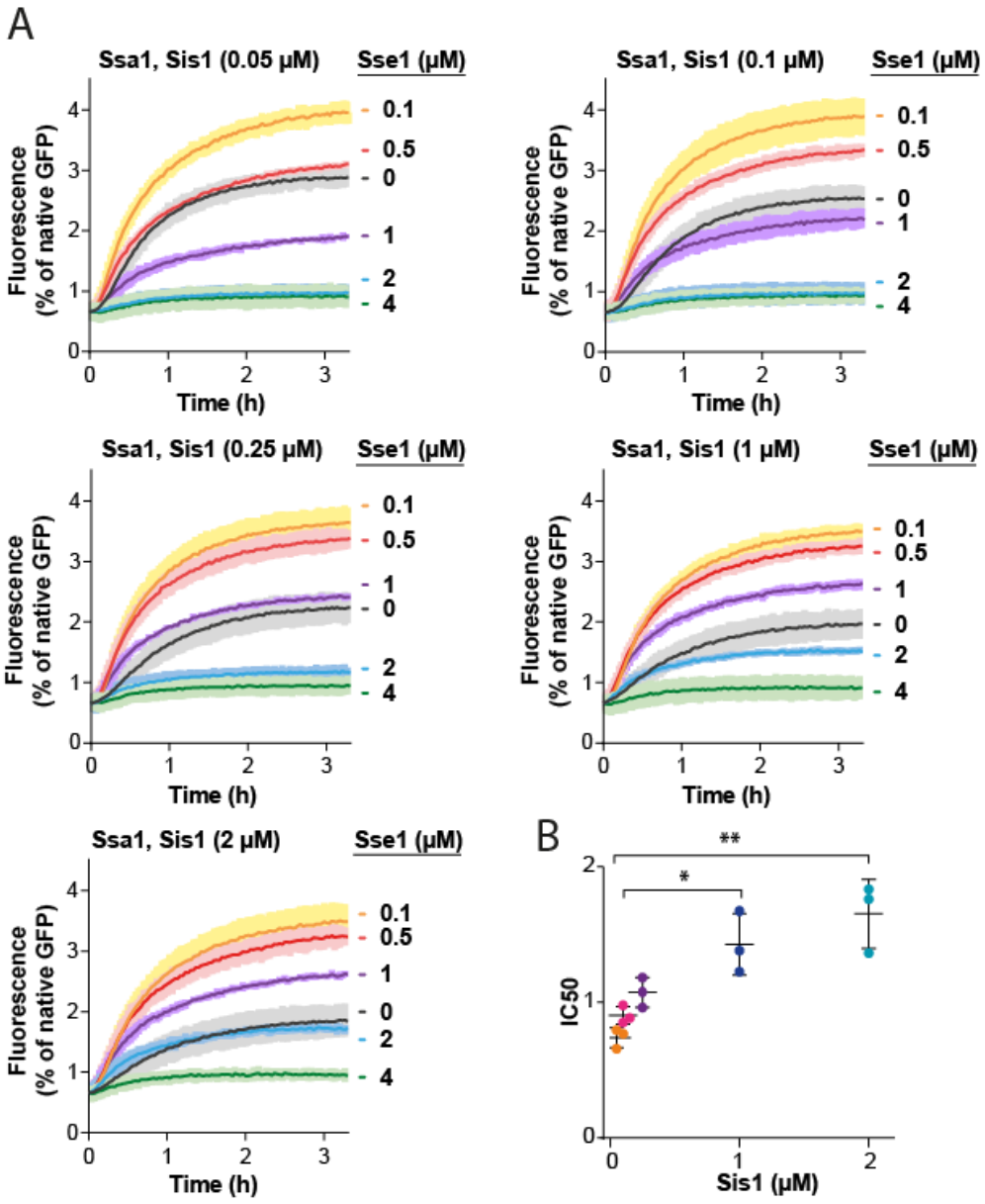

Figure 37. ***Apparent competition between Sse1 and Sis1 for Ssa1 binding.*** *Disaggregation activity of Hsp70 system comprising 1 μM Ssa1, Sis1 at the indicated concentrations and increasing concentration of Sse1 in the GFP renaturation assay. IC50 of Sse1 was determined by fitting the [Inhibitor] versus response model to the data from three experiments using the GraphPrism Software (dashed lines). Two-tailed t test: *p < 0.05, **p < 0.01. The experiment was performed by dr Agnieszka Kłosowska.*

The observed limitation of the Ssa1 availability for binding to Sis1 might be manifested by the competition between class B JDP and Hsp110. If that is the case, I would observe a correlation between concentrations of these proteins and the disaggregation rate. To verify that, GFP aggregates were incubated with Ssa1-Sis1 comprising various Sis1 and Sse1 concentrations. Results from GFP reactivation assay showed that susceptibility of Ssa1-Sis1 to the elevated Sse1 level decreases, when higher level of Sis1 was used, as 2 μM Sse1 still stimulated the disaggregation by Ssa1-Sis1 when 2 μM Sis1 was present (Fig. 37A,B).

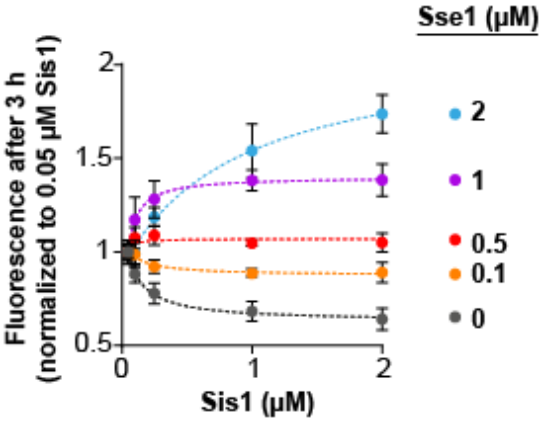

Figure 38. ***Inhibition of disaggregation by Sse1 depends on Sis1 concentration.*** *Comparison of the GFP recovery yielded by Ssa1-Sis1-Sse1 with indicated concentrations of Sis1 and Sse1, measured after 3 h. The values are adapted from Fig. 38. Dashed lines show fitting of the [Agonist] versus response model to the data from three experiments using the GraphPrism Software.*

Notably, increasing concentration of Sis1 generated lowered disaggregation rate, however when Sse1 was included, this phenomenon was reversed and disaggregation capacity still increased at very high Sse1 concentrations compared to those in the presence of 0.05 μM Sis1 (Fig. 38).

To conclude, Sse1 restricts Ssa1 from binding to Sis1, which highlights the significance of maintaining a delicate equilibrium between Sis1 and Sse1 for the efficient Hsp70-dependent disaggregation.

8.9 Human Hsp110 follows similar trends in regulation of Hsp70-dependet disaggregation

Being able to ground the role of yeast Sse1 in the disaggregation of protein aggregates by the Hsp70 system with regards to class of JDPs, I further wanted to dissect whether human ortholog, Hsp105, would similarly affect the recovery of the proteins from aggregates by the human Hsp70 system.

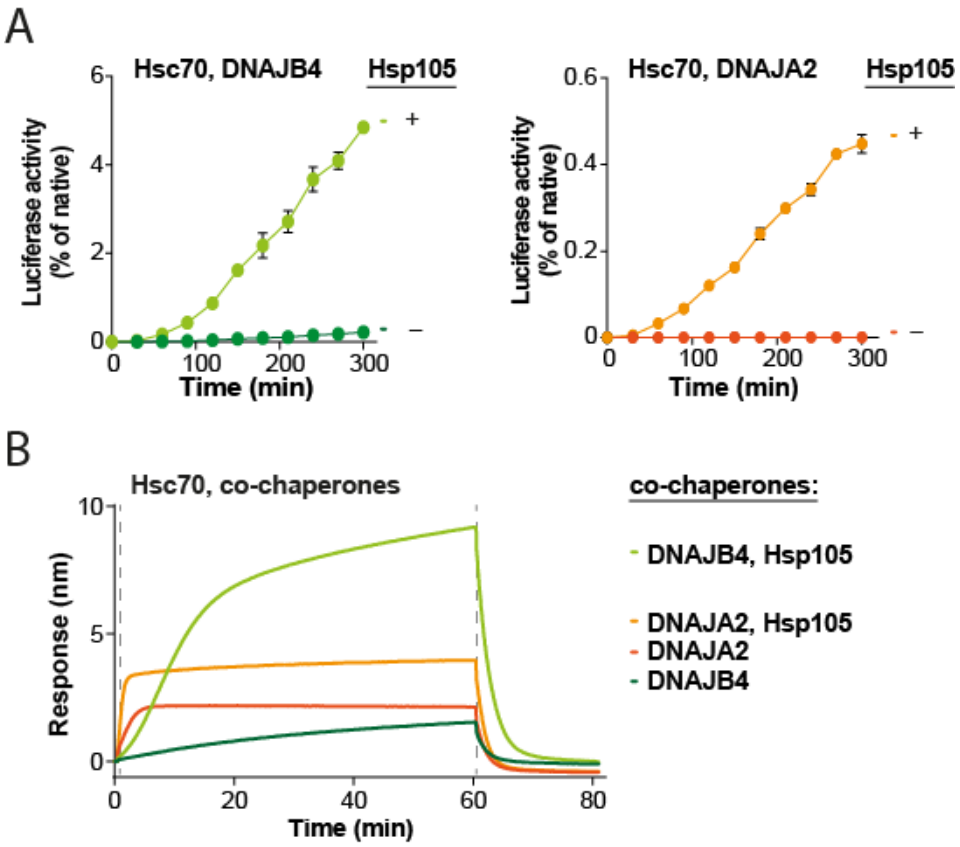

Figure 39. ***Human Hsp110 shows similar trends in protein disaggregation compared to yeast.*** *(A) Recovery of luciferase aggregates upon incubation with Hsc70-DNAJB4 +/- Hsp105 (left) or Hsc70-DNAJA2 +/- Hsp105 (right). (B) Binding of Hsc70-DNAJB4 or Hsc70-DNAJA2 with or without Hsp105 to heat-aggregated luciferase immobilized on the BLI biosensor. Chaperones were used at the following concentrations: 3 μM Hsc70, 1 μM DNAJB4, 1 μM DNAJA2 and 0.1 μM Hsp105. The experiments were performed by dr Hubert Wyszkowski.*

The Hsc70-DNAJB4 showed a delayed binding to luciferase aggregates reaching approximately 2 nm biolayer thickness, whereas Hsp105 accelerated the assembly of the Hsp70 system and resulted in 5-fold higher level of binding. The ortholog of Ydj1, DNAJA2, behaved identically to Ssa1-Ydj1 and its binding was stimulated upon the addition of Hsp105 (Fig. 39A). Both Hsc70-DNAJA2 and Hsc70-DNAJB4 yielded higher disaggregation efficacy upon the addition of Hsp105, nonetheless, stimulated to the higher level for DNAJB4 compared to DNAJA2 (Fig. 39B).

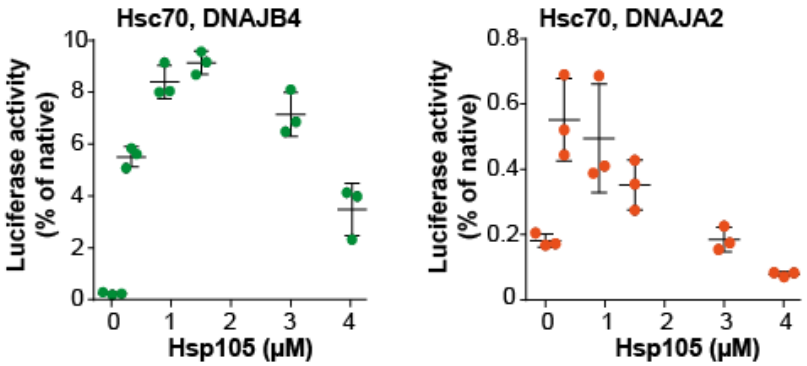

Figure 40. ***Human Hsp70 system exhibits higher tolerance for elevated levels of Hsp105.*** *Titration of Hsp105 in the recovery of aggregated luciferase by Hsc70-DNAJB4 or Hsc70-DNAJA2. Luciferase activity was measured after 4 h and normalized to the activity of native protein. Chaperones were used at the following concentrations: 3 μM Hsc70, 1 μM DNAJB4 and 1 μM DNAJA2, except for Hsp105, which was used at the indicated concentrations. The experiment was performed by dr Hubert Wyszkowski.*

Given that Hsp105 has a positive impact on the disaggregation efficacy mediated by Hsc70-DNAJA2, the resilience of the human Hsp70 system to excessive quantities of Hsp105 seems to be shifted in comparison to the yeast system. In the reactivation of luciferase, as Hsp105 was titrated across a range of concentrations, Hsc70-DNAJB4 exhibited stimulation by Hsp105 in a molar ratio slightly above 1:1, contrary to the inhibition, although not complete in the case of DNAJA2 (Fig. 40).

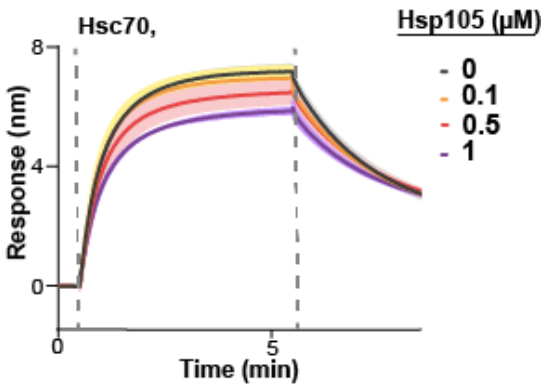

Figure 41. ***Negative impact of Hsp105 on complex formation between human Hsp70 and class B JDP.*** *BLI sensor with immobilized His6-SUMO-DNAJB4 was incubated with 1 μM Hsc70 and increasing concentration of Hsp105. Lines are the average of three replicates and the shades designate standard deviation. Dashed lines indicate addition of chaperones to sensor-bound DNAJB4 and dissociation step.*

In an analogous way to the yeast system, I analyzed the binding of Hsc70 to DNAJB4 at the increasing concentrations of Hsp105. The presence of 1 μM Hsp105 diminished the binding by 15% compared to Hsc70 alone, implying that the Hsp110-induced restriction of Hsp70 binding to class B JDPs is present in the human Hsp70 system, yet the inhibition is milder comparing to the yeast Hsp70 chaperone system (Fig. 41). Taken together, the human Hsp70 system displays similar behavior in the Hsp110-dependent disaggregation, where the degree of stimulation by Hsp110 is determined by the class of JDPs.

9. Discussion

9.1 Degree of stimulation of Hsp70-dependent disaggregation by Sse1 is determined by class of JDPs

My findings provide insight into the understanding of the contribution of yeast Hsp110 to the disaggregation of protein aggregates by the Hsp70 system, when paired with either class A or class B JDPs. While the Hsp70-dependent disaggregation is prompted by Sse1 regardless of the class of JDP, the enhancement is particularly noticeable for Sis1 (Figs. 12, 13, 14A,B). The interplay between Hsp110 and Hsp70 not only relies on the class of a JDP, but also varies across different stages of protein disaggregation (Figs. 12, 13, 15, 16).

The higher degree of stimulation of the Hsp70 activity by Sse1 in the presence of Sis1 is reflected in a more rapid and efficient formation of chaperone complexes at the aggregate surface, yielding higher disaggregation rate (Figs. 12, 13, 16). The fundamental feature of Sis1, which determines the more pronounced disaggregation activity with Sse1, is its auxiliary binding through CTD1 to the EEVD motif of Ssa1. When I perturbed this interaction, both disaggregation activity and binding to aggregates were limited by Sse1, likewise Ssa1-Ydj1 (Fig. 27A,B). Considering binding sites between Hsp70 and JDP, it is assumed that due to the single interface of Ydj1 with Hsp70 via the J-domain, one homodimer of Ydj1 can bind two molecules of Hsp70, while Sis1, featuring the additional binding site with Hsp70 can bind 4 molecules of Hsp70 per homodimer. I presumed that such expanded network od interactions might play role in Sse1-dependent stimulation. Accordingly, for the system comprising Ssa1 ΔEEVD and Sis1 E50A, with an unlocked J-domain, both the mode of binding to the aggregate and the influence of Sse1 resembled the one for Ssa1-Ydj1. The binding through J-domain is unstable and additional interface with EEVD motif introduce stability to the chaperone complex. Therefore, my results indicate that stable complex formation between Ssa1 and Sis1 is vital for the stimulation by the Sse1.

9.2 Mechanism behind the Sse1-based disaggregation activity

Interestingly, Sse1 is engaged at early stages of protein disaggregation by mediating the assembly of the chaperone complex at the aggregate rather than the final folding of the polypeptides (Figs. 14, 15). My results showed that the presence of Sse1 did not promote the folding of non-aggregated luciferase by the Hsp70 system, irrespective of the class of the JDP (Fig. 14). Taken into consideration unpublished results from my master's thesis, where bacterial NEF, GrpE was crucial to restore the native state of luciferase at latter step of disaggregation process, it can be speculated that different NEFs may have different functions in Hsp70 activity, with the yeast Hsp110 dedicated to perform a role in aggregate processing at early stages of protein disaggregation.

9.2.1 Aggregate modification by Sse1

Positive impact of Sse1 is manifested by global rearrangements of aggregates that involve their fragmentation into smaller species (Fig. 42), a phenomenon detected by fluorescence microscopy and DLS as the emergence, upon processing by Ssa1-Sis1-Sse1, of distinguishable in size aggregates (Figs. 24, 25). Likewise, it was also observed for α-synuclein fibrils that they were disassembled through fragmentation by the human Hsc70 system with the human Hsp110, Apg2 (Beton *et al*, 2022). The question is what determines the Sse1-induced modification of the aggregates? The BLI experiments showed that Sse1 impacts the chaperone complex formation at the aggregate in a manner that significantly enhances both the initial kinetics and the level of Ssa1-Sis1 binding to aggregates (Figs. 15, 16A,B). The thicker protein layer corresponds to the substantially improved loading of Hsp70 onto the aggregate, as verified using fluorescently labelled Ssa1 (Fig. 18 A,B). In line with that, in a previously published report, the authors have proposed a mechanism behind the disaggregation activity of the human Hsc70 system, based on the clustering of Hsc70 that generated entropic pulling, enabling the disaggregation of amyloid fibrils by DNAJB1 in collaboration with Hsp110. It was suggested that human Hsp110-induced disaggregation is a result of selective reshuffling of Hsc70 to enhance its abundant crowding at high density positions at the aggregate surface

(Goloubinoff & De Los Rios, 2007; Wentink *et al*, 2020). This would imply that a pool of available yeast Hsp70, Ssa1, could be a limiting factor for higher level of binding in the case of Ssa1-Sis1. Nevertheless, when I increased the concentration of Ssa1 5-fold, which I determined to be saturated, it was still incapable of accelerating binding of the Hsp70 system to the same extent as in the presence of Sse1 (Fig. 19). It suggests that the mechanism behind the stimulation by Sse1 is more complex than increasing the proportion of Hsp70 molecules capable of aggregate binding. To test how the Sse1-mediated formation of densely packed Hsp70 contribute to the higher efficacy of protein disaggregation, I utilized the Hsp104 variant (D484K F508A), which refolds proteins from aggregates independently of Hsp70. Initial incubation of GFP aggregates with Ssa1-Sis1 and Sse1 improved the disaggregation capacity of the Hsp104 variant (Fig. 23). This suggests that Sse1 facilitates the remodeling of aggregates and despite being not fully refolded, the disentangled polypeptides are more amenable to processing by Hsp104, resulting in more efficient protein disaggregation.

The Sse1-induced disentanglement of polypeptides might result in creating new binding sites, which may be limited to the extracted polypeptide chains, but could also be localized within deeper layers of the aggregate, allowing for aggregate penetration by Hsp70 system (Fig. 42). To verify the second scenario, a following experiment could be performed: I would immobilize thermally aggregated GFP on the BLI sensor, followed by the incubation with thermally aggregated luciferase. This way, the created aggregate would be characterized by having GFP in the inner layer and luciferase on the outer surface. Next, I would perform a BLI-based binding experiment with Ssa1-Sis1-Sse1 and analyze the dissociated proteins with Western blot using primary antibodies specific for GFP. If I would detect a signal corresponding to GFP, that would indicate that the Hsp70 system with Sse1 reaches beneath the luciferase layer and allows to extract GFP. Such aggregate infiltration could potentially lead to aggregate fragmentation into smaller species, which I observed with microscope and DLS.

It is known that Sse1 disrupts the interaction between a substrate and Hsp70, however my results indicate that Sse1 additionally prevents Hsp70 from complex formation with class B JDP (Fig. 35). One might assume that this effect may have

only negative outcome on the disaggregation efficacy. However, despite the slight inhibition of Ssa1 binding to Sis1 in the presence of 0.1 μM concentration of Sse1, the Hsp70-dependent protein disaggregation is the most effective at such condition. It can be speculated that sub-stoichiometric amount of Sse1 does not disrupt the complex completely, but it rather releases Ssa1 from non-productive binding to Sis1. The released Ssa1 might be transmitted to a different position, thereby regrouping nonoptimal chaperones arrangements at the aggregate surface. Thus, Hsp110 might contribute to the plasticity of the chaperone machinery, potentially allowing for deep penetration of aggregate surface to reach otherwise buried sites (Fig. 42). A similar mechanism, involving limited dissociation of the Hsp70-substrate complex, has been proposed for the human Hsp110 in the disaggregation of amyloid fibrils by the Hsc70 system (Wentink *et al*, 2020).

9.2.2 Involvement of Sse1 in Hsp104-dependent disaggregation

My previous considerations concerned the chaperone system comprising Hsp70 and JDP. When the wild type Hsp104 was involved, the stimulation of the protein disaggregation by Sse1 was even more pronounced (Figs. 12, 13B). What facilitates higher performance of Hsp104-Hsp70 in the presence of Sse1? Sse1 mediates the more abundant binding of Hsp70 to the aggregate. Since the cooperation of Hsp70 with Hsp104 requires multiple Hsp70 interacting with one hexamer of Hsp104 (Chamera *et al*, 2019), the Sse1-induced higher local concentration of Hsp70 might mediate docking of more Hsp104. Alternatively, it is possible that the more dense arrangement of Hsp70 at the aggregate surface facilitated by Sse1 limits the substrate availability for the Hsp104 disaggregase. To examine this, I would perform a BLI binding experiment with Ssa1-Sis1-Sse1 and include an additional binding step, where I would introduce Hsp104. The increase in the level of binding after the addition of Hsp104 would correspond to the Hsp104 interacting with the aggregate. In our previous work, we successfully evaluated the recruitment of the Hsp104 to the aggregate in the context of different JDP classes (Wyszkowski *et al*, 2021). But how to explain the stimulation of the Hsp104-dependent protein disaggregation by Sse1 in case the BLI experiment would reveal the level of Hsp104 binding to the aggregate unaffected? Considering the remodeling activity of Sse1 that hinges on the

fragmentation of the aggregates, it leads to creating new possible binding sites. Finally, the aggregate-remodeling activity governed by Sse1 explains its importance in the clearance of luciferase-GFP aggregates *in vivo*, where the removal of the foci were observed only under *SSE1* induced expression in thermosensitive phenotype of *sse1-200 sse2Δ* (Kaimal *et al*, 2017), showing that the activity of the Hsp70-JDP system without NEF is not sufficient to support the Hsp104-dependent protein disaggregation.

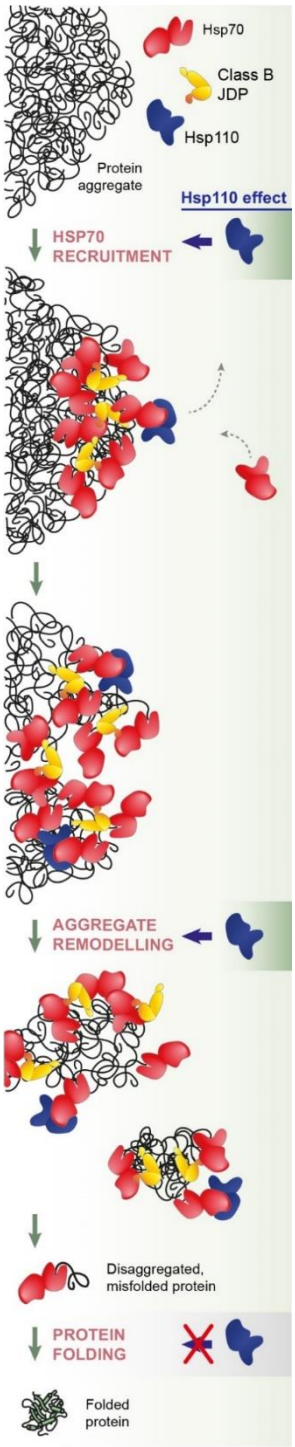

Figure 42. ***Influence of Hsp110 on Hsp70-dependent disaggregation.*** *Hsp110 acts at early stages of protein disaggregation, but not during final folding. The potentiation of the Hsp110-mediated disaggregation occurs through ample loading of Hsp70 on the aggregate leading to the disentanglement of polypeptides and aggregate remodeling into smaller species (dark green shades). Alternatively, Hsp110 disrupts the interaction between Hsp70 and class B JDPs, thereby uncovering new binding sites within the aggregate that could be infiltrated (grey dashed lines).*

9.2.3 Human Hsp110-dependent disaggregation

The trends with yeast proteins for the Hsp110-mediated protein disaggregation regarding class A and class B JDPs are also observed in the human chaperone system. Both refolding of proteins from aggregates and aggregate binding by the human Hsc70 system were improved by Hsp105, however the stimulation was more pronounced when coupled with class B JDP (Fig. 39A, B). The previously observed sigmoidal shape of binding of Ssa1-Sis1 was also observed for human Hsc70-DNAJB4, suggesting that the class B-specific mode of Hsp70 association is evolutionary conserved. However without Hsp110 the binding level with DNAJB4 was lower than with DNAJA2 and it required the presence of Hsp105 to reach a much higher level. The binding of Hsc70-DNAJA2, like in the case of Ssa1-Ydj1, was rapid, reaching 2 nm. Yet, in comparison to the yeast Ssa1-Ydj system, the binding of the human system with class A JDP was stimulated by Hsp110, however less compared to that with DNAJB4 (Fig. 39B). The observed minimal disaggregation activity and weak binding of the Hsc70 system alone to the luciferase aggregates, highlights the importance of Hsp110 in the recovery of proteins from aggregates by the human Hsc70 system (Fig. 39A, B). Presumably, on account of the loss of Hsp100 during evolution, metazoan Hsp70 system were forced to gain stress-related functions empowering the disaggregation of protein aggregates. Presumably, a stricter dependence on the NEF was inherent element of such adaptation. In order to investigate, which component of the Hsp70 system from yeast and human determines the different dependance on Hsp110 in the Hsp70-dependent protein disaggregation, I would perform the following experiment: I would exchange each component of the human Hsc70 system with the corresponding one from yeast and measure their activity in the disaggregation of the luciferase aggregates. The human and yeast Hsp70, JDP and Hsp110 collaborate with heterogeneous proteins, as has been demonstrated in numerous studies, in which Ssa1 was replaced with Hsc70 (Garcia *et al*, 2017). Such analysis of mixed system could help pinpointing divergent sites responsible for species-specific traits of the disaggregation machinery.

9.3 Features of Hsp110 contributing to protein disaggregation

Sse1 possesses features that may contribute to the improved Hsp70-dependent protein disaggregation. I analyzed the contribution of the intrinsic ATPase activity and the NEF activity to the Hsp110-based protein disaggregation. The ATPase inactive mutant (K69M) of Sse1 was effective in stimulating both the disaggregation activity and binding of Hsp70 system similarly to the wild type Sse1, indicating that the intrinsic ATPase activity is not required for the stimulation of Hsp70-dependent disaggregation by Sse1 (Fig. 20A,B). This is in accordance with *in vivo* experiments, where Sse1 K69M variant did not impair the reactivation of firefly luciferase aggregates in cytosol and nucleus (Kaimal *et al*, 2017).

Further, I analyzed the importance of the NEF activity of Sse1 by introducing the well-described Sse1-2 variant with decreased nucleotide exchange activity due to the partially abolished interaction with Hsp70 (Polier *et al*, 2008). Neither chaperone complex assembly nor recovery of proteins from aggregates were stimulated by sub-stoichiometric level of Sse1-2 (Figs. 33, 34A,B). Due to the reduced affinity for Hsp70 that limited the NEF activity, the Sse1-2 variant required 10 times higher concentration to enhance protein disaggregation by Hsp70 to the level characteristic for the wild type Sse1 (Figs. 32, 33, 34A,B). My results imply that the NEF activity is vital in the potentiation of the Hsp70-dependent disaggregation by Sse1.

The third feature of Hsp110 is the ability to bind substrates. The fact that Sse1-2 had intact SBD and yet the stimulation of disaggregation was affected suggests that the interaction of Hsp110 with a substrate is not sufficient for the stimulation of disaggregation.

To further elaborate on the significance of the NEF activity, I introduced another yeast NEF, Fes1, which lacks substrate-binding domain. My results showed that Fes1 stimulated both binding of Ssa1-Sis1 to the aggregate and recovery of proteins from aggregates equally to the wild type Sse1, albeit likewise Sse1-2 variant, it required 10-fold higher concentration (Fig. 21A,B). It seems that certain aspects regarding Fes1 still lack clarity, for instance, in *in vitro* experiments Fes1 demonstrates the ability to enhance the disaggregation activity of the Hsp70

system similarly to Sse1, yet its overexpression *in vivo* can only partially restore the refolding of heat-aggregated luciferase in cells and support growth of cells with the deletion of *sse1,sse2* (Kaimal *et al*, 2017). Nevertheless, considering that the level of Fes1 in a cell is at one-fifth of the Sse1 level, the reported 8.4-fold overexpression of *FES1* was 6 times too low to reach the level necessary for the increased disaggregation efficacy that I observed *in vitro* (Kaimal *et al*, 2017). It should be also considered that both of these NEFs differently approach misfolded substrates, with Sse1 managing the refolding pathway, whereas Fes1 directs them to degradation (Gowda *et al*, 2013, 2018).

Nevertheless, such high degree of stimulation of protein disaggregation by the 35-kDa Fes1 was unexpected, since it was proposed for the human Hsc70 system that the bulkiness of human Hsp110, with its molecular mass of 100 kDa, is critical for the potentiation of amyloid disaggregation by the human Hsc70 system with DNAJB1(Wentink *et al*, 2020). Accordingly, another NEF from BAG family (35 kDa) was not nearly as effective as Hsp110, even when its concentration was adjusted to compensate for its lower affinity Hsp70 (Wentink *et al*, 2020). Although, the proposed dependance between the molecular mass of a NEF and potentiation of amyloid disaggregation might be limited to the human system or it might not apply to amorphous aggregate. Another explanation can be that in the case of the stimulation of Hsp70-dependent protein disaggregation by Fes1, presumably structural orientation of its four alpha-helical armadillo repeats mimics the bulky Hsp110. Taken together, the open question is whether the human Hsp110 family is unique in terms of being superior to other human NEFs in potentiating the Hsp70-dependent disaggregation and whether the importance of NEF's bulkiness is limited to the amyloid substrate? To estimate the differences in regulating the disaggregation activity by human Hsp110 and BAG, disaggregation of luciferase aggregates and α-synuclein amyloid should be compared. The experiments should also involve the human Fes1 homolog, HspBP1, which would provide a broader picture of the impact of yeast and human NEFs on protein disaggregation. Furthermore, taken into consideration my results on the negative impact of Sse1 on the final folding of a polypeptide, it would be interesting to elucidate the activity of BAG family in terms of its impact on the latter step of protein disaggregation, since its negative effect could obscure

the beneficial influence at early stages of protein disaggregation. All of these aspects should be investigated to uncover to what extent the yeast and human NEFs' mechanisms are conserved.

9.4 Concentration-dependent effects of Sse1 on disaggregation by Hsp70 system

It was previously reported that the effect of Hsp110 on Hsp70 activity is concentration-dependent, however the mechanism behind the inhibitory effect remains poorly understood (Dragovic *et al*, 2006; Polier *et al*, 2008). The optimal concentration of Sse1 is sub-stoichiometric to the amount of Hsp70 and above a certain level, the Hsp70-dependent protein disaggregation is inhibited (Figs. 27, 28, 33). The ratio of Ssa1 : Sis1 : Sse1 that reached highest efficacy in the recovery of GFP aggregates was 1 : 0.1 : 0.1, which resembles the physiological conditions (Fig. 33) (Brownridge *et al*, 2013).

The Hsp70 system, when coupled with class A JDP is more vulnerable to excessive amounts of Sse1 (Figs. 27, 28, 31). I hypothesize that it is due to the high potency of Hsp110 to release nucleotides, triggering the dissociation of the chaperone complex from the protein substrate. Presumably, due to the singular interface of Ydj1 with Ssa1, the chaperone complex does not form clusters at the aggregate surface and exhibits less stable association with the aggregate, which might lead to accelerated dissociation of Ssa1 by the Sse1.

In the case of Sis1, the mechanism behind the lesser inhibition by Sse1 might be associated with the two-step binding of class B JDPs with Hsp70, which activates protein disaggregation (Faust *et al*, 2020). This mechanism drives the more abundant loading of chaperones at the aggregate surface and leads to the formation of multiple complex assemblies of the chaperones, allowing for stronger interaction of the chaperone complex with the substrate. This could make the system with Sis1 more resilient to the inhibition by Sse1.

My results indicate that there is an additional inhibitory mechanism by Sse1 that prevents Ssa1 from binding to Sis1 (Fig. 35). In favor of the apparent competition between Sse1 and Sis1 for binding to Ssa1 is that increasing concentrations of Sis1 overcome the detrimental influence of elevated Sse1 on the recovery of GFP

aggregates by the Hsp70 system (Fig. 37A). Interestingly, the recovery by Ssa1-Sis1 yielded the highest disaggregation rate at low, sub-stoichiometric concentrations of Sis1, whereas Ydj1 was reported to stimulate Hsp70 still at 1 μM concentration (Figs. 37A, 38) (Wyszkowski *et al*, 2021). It raises a question of what dictates such differences in JDP concentration demand and whether it is accomplished through the interaction with a substrate or Ssa1. This should be also investigated in terms of Sse1, 1 μM concentration of which is detrimental to Ssa1 with 0.1 μM Sis1, yet still stimulates disaggregation with 1 μM Sis1. Summarizing, it is significant to maintain a subtle balance between Hsp70 and its co-chaperones for their effective interplay.

My results indicate that the optimal concentration of Sse1 varies not only when Ssa1 is paired with different JDPs classes, but also at different stages of protein disaggregation, with folding of an unfolded, non-aggregated protein substrate being most susceptible (Figs. 27, 29, 31). The inhibition of the folding of non-aggregated luciferase by Sse1 might be a result of aggregation of the newly unfolded polypeptides because of the limited prevention of aggregation by Hsp70 due to the disrupted interaction with the substrate by the NEF (Fig. 29). This could be verified with a DLS experiment, where I would add non-aggregated luciferase to the mix of the chaperones. The emergence of aggregate species over time in the presence of high concentration of Sse1 would mean that Ssa1 is incapable of protecting unfolded luciferase from aggregation.

In the presence of Hsp104, the optimal concentration of Sse1 was shifted to lower Sse1 : Ssa1 ratio (Figs. 27, 28). Presumably, the high efficacy of protein disaggregation was not overshadowed by the negative impact of Sse1 on its latter step due to contribution of Hsp104 to the final folding. Overall, my results might explain, why optimal concentration of Hsp110 vary across different scientific reports (Raviol *et al*, 2006b; Polier *et al*, 2008; Shorter, 2011; Garcia *et al*, 2017).

In the case of the human Hsp70 system, the optimal concentration of Hsp105 facilitating the most efficient recovery of luciferase aggregates was shifted in comparison to the yeast chaperone system. In the presence of Hsp110 at slightly higher ratio to Hsp70 than 1 : 1, the protein disaggregation was still stimulated in the case of DNAJB4 and marginally inhibited with DNAJA2 (Fig. 40). These

results indicate that the human Hsp70 system is less vulnerable to the excessive amounts of Hsp110 in comparison to the yeast Hsp70 system, in line with high relevance of the human Hsp110 in protein disaggregation. Differences between the yeast and human Hsp110 activity might be a result of a diverse affinity of Hsp110 to Hsp70. This could be evaluated by employing microscale thermophoresis (MST) with fluorescently labelled Hsc70. However, if the affinity were to resemble that between Sse1 and Ssa1, the difference might lie in the different affinities of human and yeast Hsp70s for the JDPs, as the complex formation between Hsp70 and their JDP and NEF co-chaperones are strongly interconnected. Taken together, further study is required to fully understand the complexity of the human Hsp70 system and its NEF fine-tuned interplay with co-chaperones in the disaggregation of amorphous and fibrillar aggregates.

10. References

Abrams JL, Verghese J, Gibney PA & Morano KA (2014) Hierarchical Functional Specificity of Cytosolic Heat Shock Protein 70 (Hsp70) Nucleotide Exchange Factors in Yeast. *J Biol Chem* 289: 13155–13167

Andréasson C, Fiaux J, Rampelt H, Druffel-Augustin S & Bukau B (2008a) Insights into the structural dynamics of the Hsp110–Hsp70 interaction reveal the mechanism for nucleotide exchange activity. *Proc Natl Acad Sci U S A* 105: 16519–16524

Andréasson C, Fiaux J, Rampelt H, Mayer MP & Bukau B (2008b) Hsp110 is a nucleotide-activated exchange factor for Hsp70. *J Biol Chem* 283: 8877–8884

Ang D & Georgopoulos C (1989) The heat-shock-regulated grpE gene of Escherichia coli is required for bacterial growth at all temperatures but is dispensable in certain mutant backgrounds. *J Bacteriol* 171: 2748–2755

Ben-Zvi AP & Goloubinoff P (2001) Review: Mechanisms of Disaggregation and Refolding of Stable Protein Aggregates by Molecular Chaperones. *Journal of Structural Biology* 135: 84–93

Beton JG, Monistrol J, Wentink A, Johnston EC, Roberts AJ, Bukau BG, Hoogenboom BW & Saibil HR (2022) Cooperative amyloid fibre binding and disassembly by the Hsp70 disaggregase. *The EMBO Journal* 41: e110410

Bracher A & Verghese J (2015) The nucleotide exchange factors of Hsp70 molecular chaperones. *Front Mol Biosci* 2: 10

Brehmer D, Rüdiger S, Gässler CS, Klostermeier D, Packschies L, Reinstein J, Mayer MP & Bukau B (2001) Tuning of chaperone activity of Hsp70 proteins by modulation of nucleotide exchange. *Nat Struct Biol* 8: 427–432

Brownridge P, Lawless C, Payapilly AB, Lanthaler K, Holman SW, Harman VM, Grant CM, Beynon RJ & Hubbard SJ (2013) Quantitative analysis of chaperone network throughput in budding yeast. *Proteomics* 13: 1276–1291

Bukau B, Deuerling E, Pfund C & Craig EA (2000) Getting Newly Synthesized Proteins into Shape. *Cell* 101: 119–122

Chamera T, Kłosowska A, Janta A, Wyszkowski H, Obuchowski I, Gumowski K & Liberek K (2019) Selective Hsp70-Dependent Docking of Hsp104 to Protein Aggregates Protects the Cell from the Toxicity of the Disaggregase. *Journal of Molecular Biology* 431: 2180–2196

Cyr DM, Langer T & Douglas MG (1994) DnaJ-like proteins: molecular chaperones and specific regulators of Hsp70. *Trends in Biochemical Sciences* 19: 176–181

Cyr DM, Lu X & Douglas MG (1992) Regulation of Hsp70 function by a eukaryotic DnaJ homolog. *J Biol Chem* 267: 20927–20931

De Los Rios P, Ben-Zvi A, Slutsky O, Azem A & Goloubinoff P (2006) Hsp70 chaperones accelerate protein translocation and the unfolding of stable protein aggregates by entropic pulling. *Proc Natl Acad Sci U S A* 103: 6166–6171

Deville C, Franke K, Mogk A, Bukau B & Saibil HR (2019) Two-Step Activation Mechanism of the ClpB Disaggregase for Sequential Substrate Threading by the Main ATPase Motor. *Cell Rep* 27: 3433-3446.e4

Dragovic Z, Broadley SA, Shomura Y, Bracher A & Hartl FU (2006) Molecular chaperones of the Hsp110 family act as nucleotide exchange factors of Hsp70s. *EMBO J* 25: 2519–2528

Easton DP, Kaneko Y & Subjeck JR (2000) The Hsp110 and Grp170 stress proteins: newly recognized relatives of the Hsp70s. *Cell Stress Chaperones* 5: 276–290

Ellis RJ & Minton AP (2006) Protein aggregation in crowded environments. *Biol Chem* 387: 485–497

Fan C-Y, Lee S, Ren H-Y & Cyr DM (2004) Exchangeable Chaperone Modules Contribute to Specification of Type I and Type II Hsp40 Cellular Function. *Mol Biol Cell* 15: 761–773

Fan Q, Park K-W, Du Z, Morano KA & Li L (2007) The Role of Sse1 in the de Novo Formation and Variant Determination of the [PSI+] Prion. *Genetics* 177: 1583–1593

Faust O, Abayev-Avraham M, Wentink AS, Maurer M, Nillegoda NB, London N, Bukau B & Rosenzweig R (2020) HSP40 proteins use class-specific regulation to drive HSP70 functional diversity. *Nature* 587: 489–494

Flaherty KM, DeLuca-Flaherty C & McKay DB (1990) Three-dimensional structure of the ATPase fragment of a 70K heat-shock cognate protein. *Nature* 346: 623–628

Gao X, Carroni M, Nussbaum-Krammer C, Mogk A, Nillegoda NB, Szlachcic A, Guilbride DL, Saibil HR, Mayer MP & Bukau B (2015) Human Hsp70 Disaggregase Reverses Parkinson's-Linked α-Synuclein Amyloid Fibrils. *Mol Cell* 59: 781–793

Garcia VM, Nillegoda NB, Bukau B & Morano KA (2017) Substrate binding by the yeast Hsp110 nucleotide exchange factor and molecular chaperone Sse1 is not obligate for its biological activities. *Mol Biol Cell* 28: 2066–2075

Glover JR & Lindquist S (1998) Hsp104, Hsp70, and Hsp40: A Novel Chaperone System that Rescues Previously Aggregated Proteins. *Cell* 94: 73–82

Goeckeler JL, Petruso AP, Aguirre J, Clement CC, Chiosis G & Brodsky JL (2008) The Yeast Hsp110, Sse1p, Exhibits High Affinity Peptide Binding. *FEBS Lett* 582: 2393–2396

Goeckeler JL, Stephens A, Lee P, Caplan AJ & Brodsky JL (2002) Overexpression of yeast Hsp110 homolog Sse1p suppresses ydj1-151 thermosensitivity and restores Hsp90-dependent activity. *Mol Biol Cell* 13: 2760–2770

Goloubinoff P & De Los Rios P (2007) The mechanism of Hsp70 chaperones: (entropic) pulling the models together. *Trends Biochem Sci* 32: 372–380

Goloubinoff P, Mogk A, Zvi APB, Tomoyasu T & Bukau B (1999) Sequential mechanism of solubilization and refolding of stable protein aggregates by a bichaperone network. *Proc Natl Acad Sci U S A* 96: 13732–13737

Gowda NKC, Kaimal JM, Kityk R, Daniel C, Liebau J, Öhman M, Mayer MP & Andréasson C (2018) Nucleotide exchange factors Fes1 and HspBP1 mimic substrate to release misfolded proteins from Hsp70. *Nat Struct Mol Biol* 25: 83–89

Gowda NKC, Kandasamy G, Froehlich MS, Dohmen RJ & Andréasson C (2013) Hsp70 nucleotide exchange factor Fes1 is essential for ubiquitin-dependent degradation of misfolded cytosolic proteins. *Proceedings of the National Academy of Sciences* 110: 5975–5980

Gozzi GJ, Gonzalez D, Boudesco C, Dias AMM, Gotthard G, Uyanik B, Dondaine L, Marcion G, Hermetet F, Denis C, *et al* (2020) Selecting the first chemical molecule inhibitor of HSP110 for colorectal cancer therapy. *Cell Death Differ* 27: 117–129

Harrison CJ, Hayer-Hartl M, Liberto MD, Hartl F-U & Kuriyan J (1997) Crystal Structure of the Nucleotide Exchange Factor GrpE Bound to the ATPase Domain of the Molecular Chaperone DnaK. *Science* 276: 431–435

Haslberger T, Weibezahn J, Zahn R, Lee S, Tsai FTF, Bukau B & Mogk A (2007) M domains couple the ClpB threading motor with the DnaK chaperone activity. *Mol Cell* 25: 247–260

Hipp MS, Kasturi P & Hartl FU (2019) The proteostasis network and its decline in ageing. *Nat Rev Mol Cell Biol* 20: 421–435

Imamoglu R, Balchin D, Hayer-Hartl M & Hartl FU (2020) Bacterial Hsp70 resolves misfolded states and accelerates productive folding of a multi-domain protein. *Nat Commun* 11: 365

Jiang J, Prasad K, Lafer EM & Sousa R (2005) Structural Basis of Interdomain Communication in the Hsc70 Chaperone. *Mol Cell* 20: 513–524

Kabani M, Beckerich J-M & Brodsky JL (2002a) Nucleotide exchange factor for the yeast Hsp70 molecular chaperone Ssa1p. *Mol Cell Biol* 22: 4677–4689

Kabani M, McLellan C, Raynes DA, Guerriero V & Brodsky JL (2002b) HspBP1, a homologue of the yeast Fes1 and Sls1 proteins, is an Hsc70 nucleotide exchange factor. *FEBS Lett* 531: 339–342

Kaimal JM, Kandasamy G, Gasser F & Andréasson C (2017) Coordinated Hsp110 and Hsp104 Activities Power Protein Disaggregation in Saccharomyces cerevisiae. *Mol Cell Biol* 37: e00027-17

Kampinga HH & Craig EA (2010) The HSP70 chaperone machinery: J proteins as drivers of functional specificity. *Nat Rev Mol Cell Biol* 11: 579–592

Kandasamy G & Andréasson C (2018) Hsp70-Hsp110 chaperones deliver ubiquitin-dependent and -independent substrates to the 26S proteasome for proteolysis in yeast. *J Cell Sci* 131: jcs210948

Kityk R, Kopp J & Mayer MP (2018) Molecular Mechanism of J-Domain-Triggered ATP Hydrolysis by Hsp70 Chaperones. *Molecular Cell* 69: 227-237.e4

Kityk R, Kopp J, Sinning I & Mayer MP (2012) Structure and Dynamics of the ATP-Bound Open Conformation of Hsp70 Chaperones. *Molecular Cell* 48: 863–874

Klaips CL, Jayaraj GG & Hartl FU (2018) Pathways of cellular proteostasis in aging and disease. *J Cell Biol* 217: 51–63

Kryndushkin D & Wickner RB (2007) Nucleotide exchange factors for Hsp70s are required for [URE3] prion propagation in Saccharomyces cerevisiae. *Mol Biol Cell* 18: 2149–2154

Kumar V, Peter JJ, Sagar A, Ray A, Jha MP, Rebeaud ME, Tiwari S, Goloubinoff P, Ashish F & Mapa K (2020) Interdomain communication suppressing high intrinsic ATPase activity of Sse1 is essential for its co-disaggregase activity with Ssa1. *The FEBS Journal* 287: 671–694

Landreh M, Sawaya MR, Hipp MS, Eisenberg DS, Wüthrich K & Hartl FU (2016) The formation, function and regulation of amyloids: insights from structural biology. *Journal of Internal Medicine* 280: 164–176

Laufen T, Mayer MP, Beisel C, Klostermeier D, Mogk A, Reinstein J & Bukau B (1999) Mechanism of regulation of Hsp70 chaperones by DnaJ cochaperones. *Proceedings of the National Academy of Sciences* 96: 5452–5457

Lee J, Kim J-H, Biter AB, Sielaff B, Lee S & Tsai FTF (2013) Heat shock protein (Hsp) 70 is an activator of the Hsp104 motor. *Proceedings of the National Academy of Sciences* 110: 8513–8518

Lee S, Sowa ME, Watanabe Y, Sigler PB, Chiu W, Yoshida M & Tsai FTF (2003) The Structure of ClpB: A Molecular Chaperone that Rescues Proteins from an Aggregated State. *Cell* 115: 229–240

Li J, Wu Y, Qian X & Sha B (2006) Crystal structure of yeast Sis1 peptide-binding fragment and Hsp70 Ssa1 C-terminal complex. *Biochem J* 398: 353–360

Liberek K, Georgopoulos C & Zylicz M (1988) Role of the Escherichia coli DnaK and DnaJ heat shock proteins in the initiation of bacteriophage lambda DNA replication. *Proc Natl Acad Sci U S A* 85: 6632–6636

Liberek K, Marszalek J, Ang D, Georgopoulos C & Zylicz M (1991) Escherichia coli DnaJ and GrpE heat shock proteins jointly stimulate ATPase activity of DnaK. *Proc Natl Acad Sci U S A* 88: 2874–2878

Lipińska N, Ziętkiewicz S, Sobczak A, Jurczyk A, Potocki W, Morawiec E, Wawrzycka A, Gumowski K, Ślusarz M, Rodziewicz-Motowidło S, *et al* (2013) Disruption of Ionic Interactions between the Nucleotide Binding Domain 1 (NBD1) and Middle (M) Domain in Hsp100 Disaggregase Unleashes Toxic Hyperactivity and Partial Independence from Hsp70 *. *Journal of Biological Chemistry* 288: 2857–2869

Liu Q & Hendrickson WA (2007) Insights into Hsp70 Chaperone Activity from a Crystal Structure of the Yeast Hsp110 Sse1. *Cell* 131: 106–120

Liu X-D, Morano KA & Thiele DJ (1999) The Yeast Hsp110 Family Member, Sse1, Is an Hsp90 Cochaperone *. *Journal of Biological Chemistry* 274: 26654–26660

Lu Z & Cyr DM (1998) Protein folding activity of Hsp70 is modified differentially by the hsp40 co-chaperones Sis1 and Ydj1. *J Biol Chem* 273: 27824–27830

Marzullo L, Turco MC & Uversky VN (2022) What's in the BAGs? Intrinsic disorder angle of the multifunctionality of the members of a family of chaperone regulators. *J Cell Biochem* 123: 22–42

Mattoo RUH, Sharma SK, Priya S, Finka A & Goloubinoff P (2013) Hsp110 Is a Bona Fide Chaperone Using ATP to Unfold Stable Misfolded Polypeptides and Reciprocally Collaborate with Hsp70 to Solubilize Protein Aggregates. *J Biol Chem* 288: 21399–21411

Mayer MP & Bukau B (2005) Hsp70 chaperones: Cellular functions and molecular mechanism. *Cell Mol Life Sci* 62: 670–684

Mayer MP, Schröder H, Rüdiger S, Paal K, Laufen T & Bukau B (2000) Multistep mechanism of substrate binding determines chaperone activity of Hsp70. *Nat Struct Mol Biol* 7: 586–593

Mogk A, Kummer E & Bukau B (2015) Cooperation of Hsp70 and Hsp100 chaperone machines in protein disaggregation. *Frontiers in Molecular Biosciences* 2

Mogk A, Schlieker C, Strub C, Rist W, Weibezahn J & Bukau B (2003) Roles of Individual Domains and Conserved Motifs of the AAA+ Chaperone ClpB in Oligomerization, ATP Hydrolysis, and Chaperone Activity *. *Journal of Biological Chemistry* 278: 17615–17624

Morimoto RI (2011) The Heat Shock Response: Systems Biology of Proteotoxic Stress in Aging and Disease. *Cold Spring Harb Symp Quant Biol* 76: 91–99

Morshauser RC, Wang H, Flynn GC & Zuiderweg ER (1995) The peptide-binding domain of the chaperone protein Hsc70 has an unusual secondary structure topology. *Biochemistry* 34: 6261–6266

Munson M, Balasubramanian S, Fleming KG, Nagi AD, O'Brien R, Sturtevant JM & Regan L (1996) What makes a protein a protein? Hydrophobic core designs that specify stability and structural properties. *Protein Science* 5: 1584–1593

Nillegoda NB & Bukau B (2015) Metazoan Hsp70-based protein disaggregases: emergence and mechanisms. *Front Mol Biosci* 2: 57

Nillegoda NB, Kirstein J, Szlachcic A, Berynskyy M, Stank A, Stengel F, Arnsburg K, Gao X, Scior A, Aebersold R, *et al* (2015) Crucial HSP70 co-chaperone complex unlocks metazoan protein disaggregation. *Nature* 524: 247–251

Oguchi Y, Kummer E, Seyffer F, Berynskyy M, Anstett B, Zahn R, Wade RC, Mogk A & Bukau B (2012) A tightly regulated molecular toggle controls AAA+ disaggregase. *Nat Struct Mol Biol* 19: 1338–1346

Oh HJ, Chen X & Subjeck JR (1997) Hsp110 protects heat-denatured proteins and confers cellular thermoresistance. *J Biol Chem* 272: 31636–31640

Oh HJ, Easton D, Murawski M, Kaneko Y & Subjeck JR (1999) The Chaperoning Activity of hsp110: IDENTIFICATION OF FUNCTIONAL DOMAINS BY USE OF TARGETED DELETIONS*. *Journal of Biological Chemistry* 274: 15712–15718

Packschies L, Theyssen H, Buchberger A, Bukau B, Goody RS & Reinstein J (1997) GrpE accelerates nucleotide exchange of the molecular chaperone DnaK with an associative displacement mechanism. *Biochemistry* 36: 3417–3422

Polier S, Dragovic Z, Hartl FU & Bracher A (2008) Structural Basis for the Cooperation of Hsp70 and Hsp110 Chaperones in Protein Folding. *Cell* 133: 1068–1079

Polier S, Hartl FU & Bracher A (2010) Interaction of the Hsp110 Molecular Chaperones from S. cerevisiae with Substrate Protein. *Journal of Molecular Biology* 401: 696–707

Rampelt H, Kirstein-Miles J, Nillegoda NB, Chi K, Scholz SR, Morimoto RI & Bukau B (2012) Metazoan Hsp70 machines use Hsp110 to power protein disaggregation. *EMBO J* 31: 4221–4235

Raviol H, Bukau B & Mayer MP (2006a) Human and yeast Hsp110 chaperones exhibit functional differences. *FEBS Lett* 580: 168–174

Raviol H, Sadlish H, Rodriguez F, Mayer MP & Bukau B (2006b) Chaperone network in the yeast cytosol: Hsp110 is revealed as an Hsp70 nucleotide exchange factor. *The EMBO Journal* 25: 2510–2518

Rohland L, Kityk R, Smalinskaitė L & Mayer MP Conformational dynamics of the Hsp70 chaperone throughout key steps of its ATPase cycle. *Proc Natl Acad Sci U S A* 119: e2123238119

Rosenzweig R, Moradi S, Zarrine-Afsar A, Glover JR & Kay LE (2013) Unraveling the Mechanism of Protein Disaggregation Through a ClpB-DnaK Interaction. *Science* 339: 1080–1083

Rosenzweig R, Nillegoda NB, Mayer MP & Bukau B (2019) The Hsp70 chaperone network. *Nat Rev Mol Cell Biol* 20: 665–680

Rossi M-A, Pozhidaeva AK, Clerico EM, Petridis C & Gierasch LM (2024) New insights into the structure and function of the complex between the Escherichia coli Hsp70, DnaK, and its nucleotide-exchange factor, GrpE. *Journal of Biological Chemistry* 300: 105574

Rüdiger S, Buchberger A & Bukau B (1997) Interaction of Hsp70 chaperones with substrates. *Nat Struct Mol Biol* 4: 342–349

Rüdiger S, Schneider-Mergener J & Bukau B (2001) Its substrate specificity characterizes the DnaJ co-chaperone as a scanning factor for the DnaK chaperone. *EMBO J* 20: 1042–1050

Ruger-Herreros C, Svoboda L, Mogk A & Bukau B (2024) Role of J-domain Proteins in Yeast Physiology and Protein Quality Control. *Journal of Molecular Biology*: 168484

Rukes V, Rebeaud ME, Perrin L, Rios PDL & Cao C (2024) Single-molecule evidence of Entropic Pulling by Hsp70 chaperones. 2024.02.06.579217 doi:10.1101/2024.02.06.579217 [PREPRINT]

Saibil H (2013) Chaperone machines for protein folding, unfolding and disaggregation. *Nat Rev Mol Cell Biol* 14: 630–642

Schatz G & Dobberstein B (1996) Common Principles of Protein Translocation Across Membranes. *Science* 271: 1519–1526

Schirmer EC, Glover JR, Singer MA & Lindquist S (1996) HSP100/Clp proteins: a common mechanism explains diverse functions. *Trends Biochem Sci* 21: 289–296

Schlieker C, Weibezahn J, Patzelt H, Tessarz P, Strub C, Zeth K, Erbse A, Schneider-Mergener J, Chin JW, Schultz PG, *et al* (2004) Substrate recognition by the AAA+ chaperone ClpB. *Nat Struct Mol Biol* 11: 607–615

Shaner L, Trott A, Goeckeler JL, Brodsky JL & Morano KA (2004) The function of the yeast molecular chaperone Sse1 is mechanistically distinct from the closely related hsp70 family. *J Biol Chem* 279: 21992–22001

Shaner L, Wegele H, Buchner J & Morano KA (2005) The Yeast Hsp110 Sse1 Functionally Interacts with the Hsp70 Chaperones Ssa and Ssb*. *Journal of Biological Chemistry* 280: 41262–41269

Shiber A & Ravid T (2014) Chaperoning Proteins for Destruction: Diverse Roles of Hsp70 Chaperones and their Co-Chaperones in Targeting Misfolded Proteins to the Proteasome. *Biomolecules* 4: 704–724

Shomura Y, Dragovic Z, Chang H-C, Tzvetkov N, Young JC, Brodsky JL, Guerriero V, Hartl FU & Bracher A (2005) Regulation of Hsp70 function by HspBP1: structural analysis reveals an alternate mechanism for Hsp70 nucleotide exchange. *Mol Cell* 17: 367–379

Shorter J (2011) The Mammalian Disaggregase Machinery: Hsp110 Synergizes with Hsp70 and Hsp40 to Catalyze Protein Disaggregation and Reactivation in a Cell-Free System. *PLOS ONE* 6: e26319

Sondermann H, Ho AK, Listenberger LL, Siegers K, Moarefi I, Wente SR, Hartl F-U & Young JC (2002) Prediction of Novel Bag-1 Homologs Based on Structure/Function Analysis Identifies Snl1p as an Hsp70 Co-chaperone in Saccharomyces cerevisiae*. *Journal of Biological Chemistry* 277: 33220–33227

Sondermann H, Scheufler C, Schneider C, Hohfeld J, Hartl FU & Moarefi I (2001) Structure of a Bag/Hsc70 complex: convergent functional evolution of Hsp70 nucleotide exchange factors. *Science* 291: 1553–1557

Szabo A, Langer T, Schröder H, Flanagan J, Bukau B & Hartl FU (1994) The ATP hydrolysis-dependent reaction cycle of the Escherichia coli Hsp70 system DnaK, DnaJ, and GrpE. *Proc Natl Acad Sci U S A* 91: 10345–10349

Takayama S, Sato T, Krajewski S, Kochel K, Irie S, Millan JA & Reed JC (1995) Cloning and functional analysis of BAG-1: a novel Bcl-2-binding protein with anti-cell death activity. *Cell* 80: 279–284

Verghese J & Morano KA (2012) A Lysine-Rich Region within Fungal BAG Domain-Containing Proteins Mediates a Novel Association with Ribosomes. *Eukaryot Cell* 11: 1003–1011

Wentink AS, Nillegoda NB, Feufel J, Ubartaitė G, Schneider CP, De Los Rios P, Hennig J, Barducci A & Bukau B (2020) Molecular dissection of amyloid disaggregation by human HSP70. *Nature* 587: 483–488

Wu B, Wawrzynow A, Zylicz M & Georgopoulos C (1996) Structure-function analysis of the Escherichia coli GrpE heat shock protein. *The EMBO Journal* 15: 4806–4816

Wyszkowski H, Janta A, Sztangierska W, Obuchowski I, Chamera T, Kłosowska A & Liberek K (2021) Class-specific interactions between Sis1 J-domain protein and Hsp70 chaperone potentiate disaggregation of misfolded proteins. *Proc Natl Acad Sci U S A* 118: e2108163118

Xu X, Sarbeng EB, Vorvis C, Kumar DP, Zhou L & Liu Q (2012) Unique peptide substrate binding properties of 110-kDa heat-shock protein (Hsp110) determine its distinct chaperone activity. *J Biol Chem* 287: 5661–5672

Yakubu UM & Morano KA (2021) Suppression of aggregate and amyloid formation by a novel intrinsically disordered region in metazoan Hsp110 chaperones. *Journal of Biological Chemistry* 296: 100567

Yamagishi N, Nishihori H, Ishihara K, Ohtsuka K & Hatayama T (2000) Modulation of the Chaperone Activities of Hsc70/Hsp40 by Hsp105α and Hsp105β. *Biochemical and Biophysical Research Communications* 272: 850–855

Yu HY, Ziegelhoffer T, Osipiuk J, Ciesielski SJ, Baranowski M, Zhou M, Joachimiak A & Craig EA (2015) Roles of intramolecular and intermolecular interactions in functional regulation of the Hsp70 J-protein co-chaperone Sis1. *J Mol Biol* 427: 1632–1643

Zeymer C, Fischer S & Reinstein J (2014) trans-Acting Arginine Residues in the AAA+ Chaperone ClpB Allosterically Regulate the Activity through Inter- and Intradomain Communication. *J Biol Chem* 289: 32965–32976

Zhu X, Zhao X, Burkholder WF, Gragerov A, Ogata CM, Gottesman ME & Hendrickson WA (1996) Structural Analysis of Substrate Binding by the Molecular Chaperone DnaK. *Science* 272: 1606–1614

Ziętkiewicz S, Krzewska J & Liberek K (2004) Successive and Synergistic Action of the Hsp70 and Hsp100 Chaperones in Protein Disaggregation*. *Journal of Biological Chemistry* 279: 44376–44383